International Science Group
ISG-KONF.COM

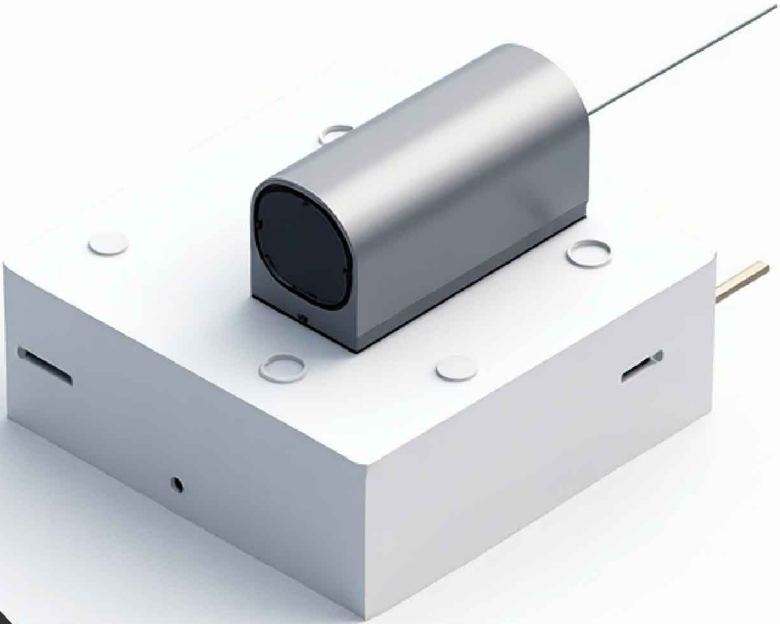

OPTICAL DEVICE FOR MONITORING CARBON DIOXIDE CONCENTRATION IN AGGRESSIVE GASEOUS ENVIRONMENTS

ISBN 979-8-89940-592-1
DOI 10.46299/979-8-89940-592-1

Dudatiev Ihor, Ovchynnykov Kostyantyn, Pinaiev Bohdan

OPTICAL DEVICE FOR MONITORING CARBON DIOXIDE CONCENTRATION IN AGGRESSIVE GASEOUS ENVIRONMENTS

Monograph

2025

UDC 535.6

Reviewers:

Oleksandr Vasilevskyi, Doctor of Engineering Science, Professor, The University of Texas at Austin, (USA)

Vyacheslav Kovtun, Doctor of Engineering Science, Professor, Vinnytsia National Technical University (Ukraine)

Authors:

Dudatiev I., Ph.D., Associate Professor of department of information radioelectronic technologies and systems, Vinnytsia National Technical University (Ukraine)

Ovchynnykov K., Ph.D., Associate Professor of department of Automation and Intelligent Information Technologies, Vinnytsia National Technical University (Ukraine)

Pinaiev B., Ph.D., Senior Lecturer of the department of information radioelectronic technologies and systems, Vinnytsia National Technical University (Ukraine)

Optical device for monitoring carbon dioxide concentration in aggressive gaseous environments: monograph / Dudatiev I., Ovchynnykov K., Pinaiev B. – Primedia eLaunch, Boston, USA, 2025. – 113 p.

Library of Congress Cataloging-in-Publication Data

ISBN – 979-8-89940-592-1
DOI – 10.46299/979-8-89940-592-1

The monograph presents the development of a device for monitoring carbon dioxide concentration in aggressive gaseous environments based on the optical absorption method with improved metrological characteristics.

The research conducted in the monograph has led to new, scientifically substantiated theoretical and practical results that are crucial for enhancing accuracy while ensuring the required response speed in the process of carbon dioxide concentration monitoring in aggressive gaseous environments. This is achieved through the optical absorption method with compensation for influencing factors affecting the optical transducer.

UDC 535.6

ISBN – 979-8-89940-592-1

INTRODUCTION

Accurate determination of the concentration of components in flue gases is a critically important aspect for ensuring the efficiency and safety of industrial processes. In today's world, with increasing demands for environmental safety and energy efficiency, the control of harmful gas emissions is becoming increasingly significant. In particular, the accuracy of measurements of flue gas component concentrations, such as carbon dioxide (CO_2), nitrogen oxides (NO_x), and other pollutants, not only helps to reduce the negative impact on the environment but also ensures optimal conditions for the functioning of technological processes.

Thanks to the development of cutting-edge technologies in the field of measurement instruments and the improvement of control methods, there is a growing need for more accurate and reliable methods of gas concentration determination. This enables the achievement of high measurement accuracy, which, in turn, allows for effective management of combustion processes, ensures precise environmental monitoring, and compliance with the regulations and standards set for atmospheric emissions.

Modern methods of measuring the concentration of flue gas components are based on various principles, including optical absorption methods, electrochemical sensors, and physico-chemical technologies. In this context, it is important to consider both traditional methods and the latest achievements in the field, which allow for more accurate, faster, and cost-effective solutions for controlling the concentration of flue gas components.

The topic of this work focuses on the analysis of methods and tools for controlling the concentration of flue gas components, the development of mathematical models, and the determination of the metrological characteristics of these systems, which enable achieving maximum accuracy and reliability in measurements.

Approved for publication by the Academic Council of Vinnytsia National Technical University (protocol No. 88/25 dated 28.04.2025)

TABLE OF CONTENTS

CHAPTER 1

ANALYSIS OF MODERN METHODS AND MEANS OF MONITORING THE CONCENTRATION OF FLUE GAS COMPONENTS

An **aggressive environment** is a term used to describe any physical, chemical, or biological setting that poses a threat to the integrity and durability of materials, components, and structures. These environments are known for containing substances or conditions that can lead to accelerated deterioration processes such as corrosion, oxidation, chemical attack, or physical degradation. Materials exposed to such environments often require enhanced protection and specialized engineering solutions to ensure their long-term performance and safety.

Aggressive environments are commonly encountered in industrial sectors such as petrochemicals, power generation, marine transportation, wastewater treatment, and construction. The damage caused by these environments can result in significant economic losses, safety hazards, and environmental issues. Therefore, understanding the specific characteristics of such environments and selecting appropriate materials and protection methods are crucial steps in the design and maintenance of infrastructure and equipment.

Another important factor is the presence of corrosive substances, such as chlorides, sulfides, and ammonia. Chlorides, in particular, are notorious for penetrating protective coatings and triggering localized forms of corrosion like pitting or crevice corrosion, especially in stainless steel and reinforced concrete. Sulfides and ammonia are frequently found in industrial emissions and chemical waste, where they can combine with moisture to form aggressive compounds that damage metals and other construction materials.

Temperature extremes also play a significant role in making an environment aggressive. High temperatures can accelerate chemical reactions, increasing the rate at which corrosion or material degradation occurs. In environments with thermal cycling, materials may also experience expansion and contraction, leading to cracking or mechanical failure. Conversely, extremely low temperatures can make certain materials brittle, reducing their load-bearing capacity and increasing the risk of sudden failure.

Humidity and the presence of water or water vapor further intensify the aggressiveness of an environment. Moisture acts as a medium for transporting corrosive agents to material surfaces. In particular, when water combines with salts such as sodium chloride, it forms an electrolyte that facilitates electrochemical reactions leading to rust and corrosion. This is especially problematic in marine environments, coastal regions, and areas with high humidity levels.

Moreover, the presence of toxic or reactive gases, such as hydrogen sulfide (H_2S), carbon dioxide (CO_2), and ammonia (NH_3), adds another layer of complexity. These gases can not only corrode materials but also pose serious health and safety risks to workers. Hydrogen sulfide, for instance, can form metal sulfides that degrade structural integrity, while ammonia can stress certain plastics and metals, leading to stress corrosion cracking.

In response to these challenges, engineers and material scientists employ various strategies to combat aggressive environments. These include the use of corrosion-resistant alloys, composite materials, surface treatments such as galvanizing and anodizing, protective coatings like epoxies and polyurethanes, and even cathodic protection systems. Environmental monitoring and regular maintenance schedules also play critical roles in identifying early signs of material failure and preventing catastrophic outcomes.

The systematization of methods for controlling gas concentration in aggressive environments is presented in the form of a table 1.1.

Table 1.1

Systematization of gas concentration control methods

Method category	Basic methods	Principle of operation
Physical methods	Absorption spectroscopy	Measurement of light absorption by gases
	Raman spectroscopy	Analysis of light scattering by gas molecules
	Optical-acoustic spectroscopy	Measuring pressure changes from light absorption
Chemical methods	Volumetric method	Measuring the volume of the reacting gas
	Titrimetric method	Titration of gas with reagent
	Colorimetry	Analysis of the color change of the reagent after the reaction
Electrochemical methods	Potentiometric method	Electrode potential measurement
	Amperometry	Current measurement during reaction
	Conductometry	Analysis of electrical conductivity changes
Thermochemical methods	Catalytic oxidation detection	Oxidation of gas on a catalyst with heat release
	Pyrolysis method	Decomposition of gases at high temperatures
Chromatographic methods	Gas chromatography	Separation of gas mixture and analysis of components
	Gas-liquid chromatography	Liquid phase chromatography
Biosensor methods	Enzymatic sensors	Using biological reactions to detect gases
	Microorganism sensors	Using bacteria sensitive to certain gases

Let's consider and analyze each of the presented methods in more detail. Physical methods for determining the concentration of gases in the atmosphere use a variety of physical principles to measure the concentrations of gas components without using chemical reactions. These methods allow the determination of gases with high accuracy and sensitivity and are often used for monitoring atmospheric pollution and research in the fields of ecology and industry.

Basic physical methods for determining gas concentrations.

Absorption and spectroscopy method (UV, visible, IR, X-ray radiation). Principle: A gas molecule absorbs light in certain parts of the spectrum, which makes it possible to measure the concentration of the gas by changing the intensity of radiation passing through the gas mixture. This is the basis of absorption spectroscopy (UV, IR, visible light, X-ray radiation).

Infrared spectroscopy (IR). Many gas molecules absorb infrared radiation at specific wavelengths that are characteristic of their vibrational transitions. By measuring the absorption of IR light, the concentration of gases such as CO_2, CO, methane (CH_2), ozone (O_2), and others can be determined. Applications: Monitoring greenhouse gas emissions, measuring pollutant gases in the atmosphere, studying atmospheric processes.

Ultraviolet spectroscopy (UV). Principle: Ultraviolet spectra are used to detect gases such as ozone (O_2) and nitrogen oxides (NO_x). The gas absorbs light in the UV range, and its concentration can be estimated from the change in absorption. Application: Determination of concentrations of ozone, nitrogen oxides and other harmful gases in the atmosphere.

X-ray spectroscopy. Principle: X-rays can be used to study elements and their isotopes in gases. The gas absorbs X-rays depending on its composition, which allows analysis of its concentration. Applications: Specialized studies, detection of traces of heavy elements in gases.

Thermal conductivity method. Principle: The gas passed through the detector has a certain thermal conductivity, which depends on its composition. A gas mixture containing components with different thermal conductivities changes the overall thermal conductivity of the mixture, and this change is measured by a sensitive sensor. Application: The thermal conductivity detector is often used to measure the concentrations of gases such as hydrogen (H_2), methane (CH_2), nitrogen oxides (NO_x), oxygen (O_2), and other gases that have noticeable differences in thermal conductivity compared to other gases. Instrument: Thermal conductivity detector (TCD), which is often used in gas chromatography.

Radioactive emission method (ionization-based gas detectors). Principle: This method is based on measuring the change in ionization of a gas that occurs as a result of its interaction with radioactive radiation. The gas is ionized and the number of ions formed is proportional to the concentration of the gas. Application: This can be used to detect and quantify gases such as radon, nitrogen dioxide (NO_2), carbon monoxide (CO) and others.

Laser spectroscopy method (laser absorption spectroscopy). Principle: Laser radiation can be used for highly sensitive determination of gases in the atmosphere. Lasers with a specific wavelength can be absorbed by gas molecules, which allows for precise analysis of gas components using absorption or fluorescence spectroscopy. Application: Determination of concentrations of gases such as CO_2, CO, NO_2, methane (CH_2), and for measuring greenhouse gases, especially in atmospheric research.

Acoustic spectroscopy method. Principle: The change in the speed of sound in a gas depends on its composition. Spectroscopy of sound waves allows you to measure changes in the speed of sound in a gas mixture, which correlates with the concentration of gases. Application: Determination of gases such as CO_2, ammonia (NH_2), methane (CH_2), hydrogen (H_2) and others.

Diffusion method. Principle: Diffusion of gases is the process by which gas molecules move towards an area of lower pressure. By measuring the rate of diffusion of gases, information can be obtained about their concentration in a mixture. Application: Used for the analysis of miscible gases such as air, nitrogen, oxygen, and for the detection of toxic gases.

Fluorescence method. Principle: When absorbing light of a certain wavelength, some gases or their molecules can emit light of a different wavelength, which can be detected and measured. This makes it possible to determine the concentration of the gas in the atmosphere. Application: Determination of gases such as ozone (O_2), hydrogen sulfide (H_2S), ammonia (NH_2) and others.

Advantages of physical methods. Speed and non-contact: Most physical methods allow for results to be obtained without the need for contact with the gas, which reduces the risk of contamination and ensures speed of measurements. Sensitivity and accuracy: Physical methods are generally very sensitive and can detect even the smallest changes in gas concentrations. Wide application: Physical methods can be used for a wide range of gases, including toxic, organic and inorganic gases.

Disadvantages: Need for expensive equipment: Some methods require specialized and expensive equipment, such as laser systems, spectrometers, and detectors. Sensitivity to external conditions: Measurement results can be affected by temperature and humidity fluctuations, as well as the presence of other gases in the mixture.

Physical methods for determining the concentration of gases in the atmosphere are very effective, accurate and rapid tools for monitoring air quality, detecting toxic gases and studying atmospheric processes. They allow measurements to be made without the use of chemical reagents and with high sensitivity.

Chemical analysis methods are a set of methods used to study the composition and properties of various materials by conducting chemical reactions. They allow you to determine the quantity, quality and nature of components in samples, as well as their interaction. Chemical analysis methods are widely used in various fields of science and industry, such as chemistry, biochemistry, pharmacy, ecology, food industry, etc.

The main types of chemical analysis methods: Qualitative analysis methods: used to detect the presence of certain components in a sample without determining their quantity; Quantitative analysis methods: used to accurately determine the concentration or amount of a component in a sample.

Qualitative methods. Qualitative methods allow you to detect certain elements or compounds in a sample, that is, determine their presence or absence.

Precipitation reactions: These reactions are based on the formation of sparingly soluble precipitates when a sample solution reacts with additional reagents. For example, to detect chlorides in water, a solution of silver nitrate ($AgNO_2$) can be added, which will result in the formation of a white precipitate of silver chloride ($AgCl$).

Gas-producing reactions: Used to detect gaseous products produced during chemical reactions. For example, carbonates can be reacted with acids to detect carbon dioxide.

Color reactions: Some chemical compounds change color when they react with certain reagents. These reactions can be used for qualitative analysis, for example, the reaction with phenolphthalein, where bases are detected by a color change of the indicator.

Test strips: To determine the presence of certain ions or compounds, test strips can be used that change color depending on the presence or concentration of the compound being analyzed.

Quantitative methods. Quantitative methods allow for the precise determination of the amount or concentration of a component in a sample. Such methods include titration, gravimetry, spectroscopy, and others.

Titration: This is a method in which a sample is added to a titrant (a standard solution of known concentration) until it reaches the equivalence point. Based on the volume of the titrant, the concentration of the component in the sample can be calculated. Titration can be acid-base, redox, complexometric, etc.

Gravimetry: A method in which the components of a sample to be analyzed are converted into sparingly soluble compounds (precipitates), which are weighed after filtration and drying. The mass of the precipitate can be used to determine the amount of substance in the sample.

Spectroscopy: This method uses the interaction of light with a material to determine its composition. Various types of spectroscopy are used for quantitative analysis, such as atomic absorption, infrared, ultraviolet spectroscopy. Based on the measurement of the absorption or emission of light, the concentration of elements or compounds can be determined.

Chromatography: This is a method of separating components in a mixture by using the difference in their interactions with two phases: mobile (liquid or gaseous) and stationary (liquid or solid). Chromatography allows not only to separate components, but also to determine their amount.

Electrochemical methods: These are based on measuring electrical parameters (e.g. potential or current) that change during a chemical reaction. The most common method is potentiometry, which measures the electrical potential between electrodes in the presence of a sample.

Principles of chemical methods. Chemical reaction: Chemical analysis methods are usually based on specific chemical reactions between the sample being analyzed and additional reagents, resulting in changes from which conclusions can be drawn about the amount or presence of components in the sample.

Selectivity: Chemical methods must be selective enough to react only with the compound to be determined, minimizing the influence of other components of the sample.

Interpretation of results: To correctly interpret the results, it is necessary to know the exact conditions of the reaction (temperature, reagent concentrations, etc.) and to use appropriate indicators or measurement methods.

Advantages of chemical methods: High accuracy and sensitivity; Ability to analyze a wide range of components; They can be relatively simple to perform if the appropriate method is correctly selected.

Disadvantages: May require special chemicals and equipment; Some methods may be sensitive to external factors such as temperature or humidity; Importance of correct interpretation of results, as the same reactions may give different results depending on the conditions.

Electrochemical analysis methods use the interaction of electrical parameters (such as electric potential, current, voltage) with chemical processes to investigate the composition of materials, determine ion concentrations in solutions, and study reactions occurring at phase interfaces (e.g., at electrodes). These methods are among the most accurate and sensitive tools for analyzing chemicals and are widely used in chemistry, biochemistry, pharmaceuticals, ecology, and other fields.

Fundamentals of electrochemical methods: Electrochemical methods are based on measuring changes in electrical quantities, such as potential, current, voltage, during chemical reactions on the surface of electrodes. They allow studying the qualities and quantities of chemical compounds through their electrochemical properties.

The main types of electrochemical methods: Potentiometry; Coulometry; Voltammetry; Potentiostable methods (galvanostatics); Impedance spectroscopy.

Potentiometry is a method of measuring the electrical potential between two electrodes in a solution without applying an external current. This allows the concentration of ions in a solution to be determined. The magnitude of the potential varies with the concentration of ions, which can be used to determine the composition of the sample.

Main types of potentiometry: Ionometry: Special ion-selective electrodes are used to measure the concentration of individual ions in solutions. For example, electrodes for determining the concentration of potassium ions, sodium ions, hydrogen ions (pH), etc.; pH-metry: Potentiometry is widely used to determine the acid-base state (pH) of solutions. Water, depending on the concentration of hydrogen ions, has a certain electrical potential, which can be measured using a pH electrode.

Advantages of potentiometry: High measurement accuracy; Continuous monitoring of ion concentration; Safe method, as it does not require the addition of chemical reagents.

Coulometry is a method that is based on measuring the amount of electrical charge required to completely oxidize or reduce a certain amount of a substance in a sample. Coulometry is used to accurately determine the amount of a reacting component.

Voltammetry is a method in which the current flowing through a solution is measured as the potential at an electrode changes. This method allows the investigation of electrochemical reactions at electrodes and the study of the concentration of solutes.

Potentiostatic methods (Galvanostatics). This method involves the use of a direct current to carry out a reaction at an electrode in which the potential does not change or changes within controlled values. It is mainly used to determine the characteristics of ions in a sample, as well as to correct reduction or oxidation reactions.

Impedance spectroscopy is a technique that measures the change in electrical impedance (total resistance) of a system as the frequency of an external current changes. This technique is used to analyze the surface and internal properties of materials, such as conductivity, dielectric characteristics, or surface processes at electrodes.

Thermochemical methods are analytical methods based on the measurement of thermal effects that occur during chemical reactions or phase transitions. They allow us to study the energy changes associated with oxidation, reduction, formation, or decomposition reactions of compounds, as well as to determine heat capacity, enthalpy, entropy, and other thermodynamic parameters. These methods are important for studying the thermodynamics of chemical processes, as well as for determining the energetic characteristics of materials.

Fundamentals of Thermochemical Methods. Thermochemical methods of analysis study the change in temperature or the heat released or absorbed during chemical reactions. This makes it possible to determine the energetic characteristics of such processes, which allows for a deeper understanding of the mechanism of reactions and to assess their efficiency.

Main thermochemical methods: Calorimetry; Thermogravimetry; Differential scanning calorimetry (DSC); Thermochemical titration; Thermal reactions (thermal analysis).

Calorimetry is a method of measuring the amount of heat released or absorbed during chemical reactions. Calorimeters allow the measurement of the heat of reaction at constant pressure or volume, which allows the determination of the energetic characteristics of reactions.

Thermogravimetry is a method that measures the change in mass of a sample as a function of temperature. This method allows you to study the thermal degradation of materials, as well as assess their composition and stability under temperature changes.

Differential scanning calorimetry (DSC) is a widely used thermal analysis technique that measures the heat flow associated with physical and chemical changes in a material as its temperature is varied. This method provides valuable insights into phase transitions such as melting, crystallization, glass transition, and oxidation reactions. By precisely monitoring the heat absorbed or released by a sample, DSC enables researchers to determine specific thermal properties, including heat capacity, enthalpy changes, and thermal stability. The technique is particularly useful in materials science, pharmaceuticals, and polymer research, where understanding thermal behavior is crucial for material characterization and quality control.

Thermochemical titration is an advanced analytical method that combines classical titration with calorimetric measurements, allowing for the quantitative determination of reaction enthalpies. By monitoring the heat exchange that occurs during a titration process, this method provides information about reaction kinetics, thermodynamic parameters, and equilibrium constants. It is especially useful in the study of acid-base reactions, complexation processes, and redox reactions. The technique is commonly applied in biochemistry, electrochemistry, and industrial chemistry, where precise concentration measurements and reaction enthalpy data are essential for process optimization and product development.

Thermal analysis encompasses a range of techniques designed to measure temperature changes and thermal effects associated with chemical and physical processes. These techniques include differential thermal analysis (DTA), thermogravimetric analysis (TGA), and dynamic mechanical analysis (DMA), among others. Thermal analysis plays a crucial role in studying material properties such as decomposition temperatures, phase stability, oxidation resistance, and thermal conductivity. It is extensively used in the development of new materials, the assessment of polymer degradation, and the evaluation of catalysts in chemical industries.

Thermochemical methods for determining the concentration of gases in the atmosphere are based on the measurement of heat effects that occur when gases undergo chemical reactions with other substances. These methods enable precise quantification of gaseous components by analyzing the heat released or absorbed during their interaction with reagents. For example, in the detection of carbon dioxide (CO_2), carbon monoxide (CO), nitrogen dioxide (NO_2), or ammonia (NH_3), thermochemical approaches provide a sensitive and reliable means of monitoring environmental pollution. By integrating calorimetric techniques with gas-phase reactions, researchers can develop highly accurate sensors and analytical tools for atmospheric studies, industrial emissions control, and air quality monitoring.

Furthermore, thermochemical gas analysis methods are advantageous due to their rapid response times, high sensitivity, and ability to operate in real-time conditions. These techniques are often employed in environmental science, energy production, and chemical process safety assessments. Advanced calorimetric instruments, including microcalorimeters and reaction calorimeters, enhance the precision and applicability of thermochemical analyses in diverse scientific and industrial domains. As the demand for accurate gas sensing technologies grows, thermochemical methods continue to evolve, offering improved analytical capabilities for detecting and quantifying gaseous pollutants with high precision.

Chromatographic methods for determining the concentration of gases in the atmosphere are one of the most accurate and widely used methods for analyzing gas mixtures. These methods are based on the distribution of gas components between two phases — mobile and stationary — which allows them to be effectively separated and the amount of each component to be determined. Chromatographic methods are one of the most accurate and effective for determining the concentration of gases in the atmosphere. They allow obtaining highly detailed and reliable results that are important for environmental monitoring, climate change research, industrial emissions control, and human safety.

Biosensor methods for determining the concentration of gases in the atmosphere are a promising and rapidly developing technology based on the use of biological components (biosensors) to detect gases, especially toxic or harmful ones. These methods combine the high sensitivity of biological systems with technological advances in sensor devices, which allows obtaining accurate and rapid measurements of gas concentrations in real time.

The principle of operation of biosensor methods: Biosensors are devices that use biological material (enzymes, antibodies, cells, DNA molecules and other biological components) to detect specific gas molecules. In the event of gas interaction with the biosensor, physicochemical changes occur, which are recorded by the sensor and can be converted into an electrical signal for further analysis.

Biosensor methods are promising for rapid, accurate and safe determination of gas concentrations in the atmosphere. They combine the high sensitivity of biological components with advanced sensor technologies, which allows for effective control of environmental pollution and ensuring safety in industrial and residential areas.

A similar approach with weighting factors can be used to compare physical, chemical, electrochemical, thermochemical, chromatographic and biosensor methods for determining the concentration of gases in the atmosphere. Here are the evaluation criteria for these methods:

Evaluation criteria:

Sensitivity (from 1 to 5) is the ability of the method to detect low concentrations of gases.

Measurement speed (from 1 to 5) is the time required to obtain a result.

Accuracy (from 1 to 5) — the ability of the method to produce stable and accurate results.

The cost of equipment (from 1 to 5) is the economic component of the method.

Application in real-world conditions (from 1 to 5) — is the method convenient to use in field conditions or for mass monitoring.

Weighting factors:

- Sensitivity — 0.25;
- Measurement speed — 0.2;
- Accuracy - 0.2;
- Equipment cost — 0.15;
- Application in real conditions — 0.2 ;

Comparison of methods

1. Physical methods

- Sensitivity: 4;
- Measurement speed: 4;
- Accuracy: 4;
- Equipment cost: 3;
- Application in real conditions: 5;

Rating: 4.3.

2. Chemical methods
- Sensitivity: 4;
- Measurement speed: 3;
- Accuracy: 3;
- Equipment cost: 3;
- Application in real conditions: 4;

Rating: 3.7.

3. Electrochemical methods
- Sensitivity: 4;
- Measurement speed: 5;
- Accuracy: 4;
- Equipment cost: 2;
- Application in real conditions: 5;

Rating: 4.3.

4. Thermochemical methods
- Sensitivity: 3 ;
- Measurement speed: 3
- Accuracy: 3;
- Equipment cost: 4;
- Application in real conditions: 4;

Rating: 3.5.

5. Chromatographic methods
- Sensitivity: 5;
- Measurement speed: 3;
- Accuracy: 5;
- Equipment cost: 2;
- Application in real conditions: 3;

Rating: 4.05.

6. Biosensor methods
- Sensitivity: 3;
- Measurement speed: 4;
- Accuracy: 4;
- Equipment cost: 3;
- Application in real conditions: 4;

Rating: 3.85.

Evaluation results (table 1.2):

Table 1.2

The comparison of methods showed significant differences in efficiency

Method	Rating
Physical methods	4.3
Electrochemical methods	4.3
Chromatographic methods	4.05
Chemical methods	3.7
Biosensor methods	3.85
Thermochemical methods	3.5

According to the comparison results, physical methods and electrochemical methods receive the same highest score (4.3), which makes them optimal for determining the concentration of gases in the atmosphere among all the proposed methods.

Physical methods prevail due to their high sensitivity, measurement speed, accuracy, and ease of application in real-world conditions.

Electrochemical methods also have high speed and accuracy, but the cost of equipment can be slightly higher compared to physical methods.

Therefore, both of these methods are optimal, but the choice between them may depend on specific requirements and application conditions.

Absorption spectroscopy. Absorption spectroscopy is based on the ability of gases to absorb electromagnetic radiation of a certain wavelength. Each gas has a unique absorption spectrum, which allows you to determine its concentration in the air. This law allows you to quantitatively estimate the concentration of a gas in the air by analyzing the degree of attenuation of light intensity when passing through a gas mixture.

Raman spectroscopy. Raman spectroscopy is based on the inelastic scattering of light by gas molecules. When monochromatic light (usually laser radiation) passes through a gas mixture, most of the photons are scattered elastically (the Rayleigh effect), retaining their original energy. However, a small fraction of photons undergo inelastic scattering - their energy changes due to interactions with molecular vibrations, rotations, or electronic transitions.

Raman's Law. The change in energy of photons during scattering is determined by the difference between the energy levels of the molecule.

Optical-acoustic spectroscopy (OAS) is a materials research method that combines optical and acoustic techniques to obtain detailed information about the physical and chemical properties of materials. It is based on the study of the interaction of electromagnetic radiation (usually in the visible or infrared range) with a material and the subsequent generation of acoustic waves due to the absorption of this radiation.

Chromatographic methods for determining the concentration of gases in the atmosphere are among the most accurate and widely used methods for analyzing gas mixtures. These methods are based on the distribution of gas components between two phases — mobile and stationary — which allows them to be effectively separated and the amount of each component determined.

Chromatographic methods are among the most accurate and efficient for determining the concentration of gases in the atmosphere. They allow obtaining highly detailed and reliable results, which are important for environmental monitoring, climate change research, industrial emission control, and ensuring human safety.

To compare absorption spectroscopy, Raman spectroscopy, and optoacoustic spectroscopy, we will again apply an approach that evaluates various criteria by weighting factors. The criteria, as before, will include sensitivity, measurement speed, accuracy, equipment cost, and application in real conditions.

Evaluation criteria:

Sensitivity (from 1 to 5) is the ability of the method to detect low concentrations of gases.

Measurement speed (from 1 to 5) is the time required to obtain a result.

Accuracy (from 1 to 5) — the ability of the method to produce stable and accurate results.

The cost of equipment (from 1 to 5) is the economic component of the method.

Application in real-world conditions (from 1 to 5) — is the method convenient to use in field conditions or for mass monitoring.

Weighting factors:

- Sensitivity — 0.25 ;
- Measurement speed — 0.2 ;
- Accuracy — 0.2 ;
- Equipment cost — 0.1 5;
- Application in real conditions - 0.2 .

Comparison of methods

1. Absorption spectroscopy

- Sensitivity: 5;
- Measurement speed: 4;
- Accuracy: 5;
- Equipment cost: 3;
- Application in real conditions: 4;

Rating: 4.4.

2. Raman spectroscopy

- Sensitivity: 4;
- Measurement speed: 3;
- Accuracy: 5;
- Equipment cost: 2;
- Application in real conditions: 4;

Rating: 4.05.

3. Optical-acoustic spectroscopy

- Sensitivity: 4;
- Measurement speed: 5;

- Accuracy: 4;
- Equipment cost: 3;
- Application in real conditions: 4;

Rating: 4.3.

Evaluation results (table 1.3):

Table 1.3

Comparison of purely optical methods

Method	Rating
Absorption spectroscopy	4.4
Optical-acoustic spectroscopy	4.3
Raman spectroscopy	4.05

Absorption spectroscopy has the highest score (4.4) due to its high sensitivity, accuracy, and good applicability in real-world conditions, making it the optimal method for determining gas concentrations among the listed methods.

Optical-acoustic spectroscopy has also shown good results, in particular due to its high measurement speed, which makes it useful for rapid monitoring of gas concentrations.

Raman spectroscopy lags behind due to higher equipment cost and slightly slower measurement times, but remains an effective method for accurate and detailed measurements.

Considering that the optical absorption infrared method proved to be more suitable for measuring the concentration of gas components , there is a need to consider it in more detail for further work.

In the IR range of the spectrum there are specific features of the absorption of the gas being analyzed due to the presence of vibrational-rotational absorption bands. The magnitude of the radiation flux that has passed through the measuring cell with the gas being analyzed can be determined by the Bouguer-Lambert-Beer law [15]

$$F_{\lambda}(\lambda) = F_{\lambda 0}(\lambda) \cdot e^{-\chi(\lambda) \cdot \mathrm{C_i} \cdot l}, \qquad (1.1)$$

where $F_{\lambda}(\lambda), F_{\lambda 0}(\lambda)$ is the spectral density of the radiation flux at a given wavelength *;* $\lambda\chi(\lambda)$ - mass absorption coefficient of a substance for a given wavelength λ ; C_{and} - concentration of the substance that absorbs optical radiation; l is the thickness of the layer of medium that absorbs radiation.

The known value of χ of the gas being analyzed for the wavelength of the source is used, or, if the width of the source band is comparable to the width of the gas absorption band, the effective value of the absorption coefficient χe averaged over the source emission spectrum. In this case, the radiation flux integrated over the source spectrum, which is precisely recorded by the photodetectors, is taken into account. Then the Bouguer-Lambert-Beer law is expressed as [3]

$$F = F_0 \cdot e^{-\chi \cdot C_i \cdot l}, \qquad (1.9)$$

where χ and l are known, and the ratio of the gas flow passing through the layer l to the incoming flow F/F_0 or their difference at weak absorption is measured.

The IR range is characterized by narrow absorption bands of gases and relatively broad spectral bands of probing radiation sources. Let us consider how this affects the dependence of the intensity of radiation that has passed through the gas on the content of the gas being measured. The photodetector responds to the integrated radiation flux that has passed through the gas

$$F = \int_{\lambda 1}^{\lambda 2} F_\lambda(\lambda) d\lambda, \tag{1.10}$$

where λ_1 and λ_2 are the limits of the source radiation spectrum.

Then we consider layers of thickness l as the result of integration over the wavelength

$$F = \int_{\lambda 1}^{\lambda 2} F_{\lambda 0}(\lambda) \cdot e^{-\chi(\lambda) \cdot C_i \cdot l} d\lambda. \tag{1.11}$$

In this expression, it is not possible to isolate the parameter φ, that is, to represent the function in the form

$$F = F_0 \cdot F_1(C_i) \int_{\lambda 1}^{\lambda 2} F_2[\chi(\lambda)] d\lambda, \tag{1.12}$$

where $F_1(C_{and})$, $F_2[\chi(\lambda)]$ are functions with separated variables, and therefore the dependence

$$\ln \frac{F}{F_0} = -\chi(\lambda) \cdot C_i \cdot l, \tag{1.13}$$

is not fulfilled, especially in the case of strong absorption. Note that it is inappropriate to say here about the violation of the Bouguer-Lambert-Beer law, because its use is limited to the case of monochromatic radiation or to cases where non-monochromaticity can be neglected, as discussed above.

For weak absorption, the Bouguer-Lambert-Beer law can be represented as in the form of

$$\Delta F_\lambda(\lambda) = -F_{\lambda 0}(\lambda) \cdot \chi(\lambda) \cdot \mathrm{C_i} \cdot l \tag{1.14}$$

or

$$\Delta F_\lambda(\lambda) - F_{\lambda 0}(\lambda) = -F_{\lambda 0}(\lambda) \cdot \chi(\lambda) \cdot \mathrm{C_i} \cdot l. \tag{1.15}$$

Integrating (1.15) over the wavelength interval, we obtain

$$F - F_0 = -\int_{\lambda 1}^{\lambda 2} F_{\lambda 0}(\lambda) \cdot \chi(\lambda) \cdot \mathrm{C_i} \cdot l d\lambda \tag{1.16}$$

or

$$F - F_0 = -C_i \cdot l \int_{\lambda 1}^{\lambda 2} F_{\lambda 0}(\lambda) \cdot \chi(\lambda) d\lambda, \tag{1.17}$$

that is, there is a linear dependence of the difference in the radiation that has passed through the gas being analyzed and the fluxes that enter from the volume fraction of the substance, regardless of the shape of the emission bands of the source and the absorption band of the gas being determined. Here, the function $\chi(\lambda)$ can be replaced by its effective value χ_e, and then expression (1. 1 6) takes the form

$$F - F_0 = -\rho \cdot l \cdot \chi_e \int_{\lambda 1}^{\lambda 2} F_{\lambda 0}(\lambda) d\lambda = F_0 \cdot \chi_e \cdot \rho \cdot l, \qquad (1.\ 1\ 8)$$

or, if the ratio *F/F0 is measured*

$$\frac{F}{F_0} = 1 - \chi_e \cdot \rho \cdot l. \qquad (1.19)$$

In order to determine the value of the quantity χe , measure *F/F $_0$* for a gas with known concentration *C $_{and}$* , or *(F –F $_0$)* for a known *C $_{and}$* and a fixed value of *F $_0$* , or the output signals of the instrument corresponding to these values. In general, in the case when the absorption cannot be considered weak, i.e. the ratio (1.13) is not satisfied, calibration curves are constructed by measuring the electrical signal at the output of the instrument for a number of reference gas mixtures with a known content of the gas being determined.

The magnitude of the difference signal at weak absorption in accordance with the expression (1.18) turns out to be proportional to the volume fraction *Φ $_0$* of the gas being measured. Let us consider the dependence of this signal on the volume fraction at the magnitude of absorption sufficient for the relation (1.13) not to be fulfilled. Let us subtract from the right and left sides of the equation (1 . 8) $\Phi_{\lambda 0}$ and change the sign in both its parts

$$F_{\lambda 0}(\lambda) - F_{\lambda}(\lambda) = F_{\lambda 0} \cdot [1 - e^{-\chi(\lambda) \cdot Ci \cdot l}]. \qquad (1.20)$$

Integrating this expression over the wavelength interval, we obtain

$$F_0 - F = F_{\lambda 0}(\lambda) - F_{\lambda}(\lambda). \qquad (1.21)$$

The wavelength interval can be limited to the region where *χ(λ)* is noticeably different from zero. With a sufficiently narrow absorption line compared to the band of the probing optical radiation, $F_{\lambda 0}$ in this wavelength interval changes weakly and, according to the theorem, can be taken out $F_{\lambda 0}$ of the integration sign, replacing it with some average effective value $F_{\lambda 0e}$. Under the same conditions and not very strong absorption *χ(λ*) can also be replaced by *χe* , and the function $\exp(-\chi_e \cdot \rho \cdot l)$ taken out of the integral sign. Then

$$F_0 - F = F_e \cdot [1 - \exp(-\chi_e \cdot \rho \cdot l)], \qquad (1.22)$$

where $F_e = F_{\lambda 0e}(\lambda_2 - \lambda_1)$.

With very strong absorption, when the spectrum has passed through a cuvette with gas of IR radiation, in expression (1.22) the values of $F_{\lambda 0e}$ *and* can no longer be considered constant parameters, since they change their value.

The above represents the process of transition from the ideal condition of monochromaticity of optical radiation, for which the Bouguer-Lambert-Beer law is formulated, to a real situation, very far from ideal. However, the type of dependence and the conditions under which the assumptions made are valid are determined. A direct solution to the problem would require the exact value of the functions $F_{\lambda 0}(\lambda)$ and *χ(λ),* which would lead to cumbersome expressions that can be calculated only by numerical integration methods and are devoid of clarity. The final result would have less value, since it is suitable only for absolutely specific $F_{\lambda 0}(\lambda)$ and *χ(λ).*

Assuming that the transformation of radiation fluxes in the entire path from the photodetector to the indicator is linear, instead of expression (1.18) we can write

$$F_{вих} = \Delta F = F_e \cdot [1 - \exp(-k \cdot C_i)], \tag{1.23}$$

where k is the light absorption coefficient ·

From (1.22) and (1.23) it is seen that the values of ΔF and F_e depend on F_0, i.e. a highly stable source of optical radiation is required. In this case, equation (1.23) can be represented in the form

$$I_{ext} = I_0 \cdot [1 - \exp(-k \cdot C_i)], \tag{1.24}$$

where $I_{ext.}$ – intensity of incident light ; I_0 – intensity of transmitted light , k – light absorption coefficient ; C_i – the concentration of the component, which depends on the amount of substance in the sample.

The magnitude of the radiation flux that has passed through the measuring cell with the gas being analyzed can be determined by the Bouguer-Lambert-Beer law (1.24) . To check the compliance of the calibration curve, we differentiate the expression (1.24)

$$\frac{dI_{ext}}{d\varphi} = I_0 \cdot b \cdot \exp(-b \cdot C_i)], \tag{1.25}$$

and we take the resulting expression in logarithm

$$\ln(\frac{dI_{ext}}{d\varphi}) = \ln(I_0 \cdot b) - b \cdot C_i \tag{1.26}$$

or

$$y = c - b \cdot C_i, \tag{1.27}$$

where $y = \ln(\frac{dI_{ext}}{dC_i}), c = \ln(I_0 \cdot b)$.

We will take the theoretically obtained dependence 1.24 and use it to analyze the adequacy of the developed (in section 2) empirical mathematical model for determining the concentration of gases based on the optical absorption method.

To analyze the schemes of optical means of controlling the concentration of gas components , a review of patents and sources was carried out [3]. The review was conducted among the schemes whose action is based on the optical method of infrared absorption spectroscopy, since this method is the basis of the developed means of controlling the concentration of gas components .

Analikh showed that there are many developed and patented means of controlling the composition of gases . However, most of them use two cuvettes (working and with “zero” gas), and this type of optical means schemes technically outdated. This is explained by the complexity of its design control tools and their low accuracy. In addition, they all use a single radiation source and filters, but this approach significantly reduces the speed of the tool (due to the fact that the sample travels a longer path in the optical path).

All the analyzed control means do not provide for the use of other measuring channels for the assessment and compensation of influencing factors. Because of this, measurements using these means will not have the necessary accuracy. Therefore, it is advisable to provide in the developed The gas component concentration control device has additional measuring channels .

In fig. 1.5 presents the diagram of a two-beam photometer with two photodetectors.

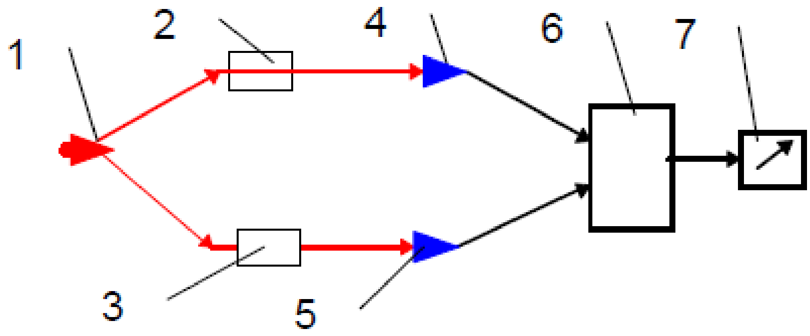

Fig. 1.5. Scheme of a two-beam photometer with two photodetectors : 1 - source, 2 - working cell, 3 - cell with "zero" gas, 4, 5 - optical radiation receivers, 6 - differential amplifier-converter, 7 - registrar.

In two-beam photometers, optical radiation from source 1 is split into two identical beams. One of them passes through cuvette 2 with the gas being measured , and the other through the same cuvette 3 filled with a "zero" gas that does not contain the measured component. Then each beam of optical radiation is directed to separate photodetectors 4 and 5, the signals from which are fed to the differential amplifier 6.

In the case of weak light absorption in the measuring cell, the difference in photocurrents of both photodetectors is proportional to the mass concentration of the substance, and for strong absorption, the logarithm of the ratio of the signals from the photodetectors will be proportional to the concentration. In order to have a direct value of the concentration of the gas being determined on the indicator 7 of the device, the signals from both channels must be processed accordingly.

In two-beam schemes, optical radiation can be modulated in intensity by a modulator 5 (Fig. 1.6) in antiphase to each other , and then both streams are directed to one optical radiation receiver 4, and then to an amplifier-converter 6.

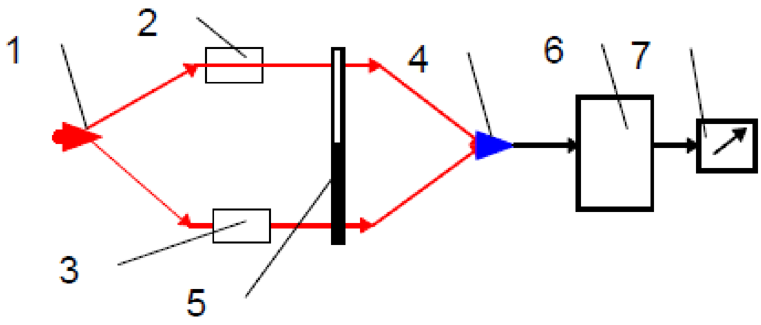

Rice. 1.6. Scheme of a two-beam photometer with a modulator:
1 - radiation source; 2 - working cell; 3 - cell with "zero" gas; 4 - optical radiation receiver; 5 - modulator; 6 - amplifier-converter; 7 - recorder.

In optical gas analysis, particularly in systems that use modulated light beams, the behavior of the signal received by the photodetector can vary depending on the degree of radiation absorption by the target gas. When the absorption is weak, the amplitude of the alternating (modulated) component of the photocurrent generated by the photodetector is directly proportional to the concentration of the absorbing gas. This linear relationship simplifies the analysis and calibration processes, making it easier to detect small variations in concentration.

However, in the case of strong absorption, the relationship becomes nonlinear. Here, the concentration is proportional to the logarithm of the ratio between the maximum and minimum levels of the signal received from the photodetector over the course of a modulation cycle. This behavior aligns with the Beer-Lambert law, which governs the attenuation of light as it passes through an absorbing medium. The stronger the absorption, the more significant the reduction in light intensity, and the more complex the mathematical relationship between the detected signal and the actual gas concentration.

In situations of weak absorption, nonlinearity in the photodetector’s response can usually be ignored. This is because the useful signal — that is, the component corresponding to the presence of the absorbing gas — constitutes only a small part of the overall signal, which is dominated by the background illumination. As a result, the photocurrent remains in a nearly linear regime with respect to the incoming radiation. It is important, however, to ensure that both the photodetector and the primary amplifier are operating within their linear range, i.e., not in saturation. Saturation can distort the signal and lead to inaccurate readings.

Regarding dual-channel detection systems that use two photodetectors, the requirement for these detectors to have identical characteristics is not very stringent. Minor discrepancies in their sensitivity or response can be effectively compensated through electronic or optical adjustments. For example, in the electronic domain, a voltage divider can be used to reduce the signal level from the more sensitive photodetector. Alternatively, an optical method such as partially blocking or diaphragming one of the optical paths can be used to equalize the intensity of light reaching each photodetector.

These strategies ensure that the overall system remains balanced and accurate, even when there are small variations in the components. This flexibility is particularly useful in practical implementations, where perfect symmetry between optical and electronic components is difficult to achieve.

It can be seen that the signal from the photodetector, which perceives the radiation flux that has passed through the cuvette with the "zero" gas, depends only on the radiation flux of the source and remains constant at a constant radiation flux. Then the entire comparison channel of the photometer can be replaced a source of constant voltage or current corresponding in magnitude to the signal from the photodetector when the measuring cell is full " zero " gas. This greatly simplifies the design of the device and reduces its cost. Such a photometer becomes single-beam. Fig. 1. 7 shows the scheme of the HL ZV.

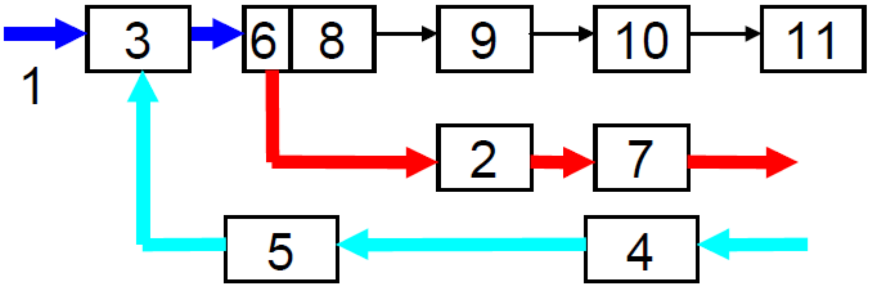

Fig. 1.7. Structural diagram of the HL ZV :
1 - intake pipe; 2 - rotameter; 3 - gas switch; 4 - filter-absorber; 5 - cal and brator; 6 - HL reactor; 7 - pump; 8 - optical radiation receiver; 9 - amplifier; 10 - processor; 11 - indicator.

The gas to be analyzed enters the intake pipe of the device and through The switch enters the CL reactor 6. Chemiluminescence radiation is converted into an electrical signal by means of an optical radiation receiver 8 , amplified in an amplifier 9, and converted into a digital code, is subjected to functional processing in the processor 10 and the result is displayed on the display of the indicator 11. To correct changes in the sensitivity of the CL sensor, a built-in generator of the standard mass concentration of the measured gas (calibrator) 5 is used. Block 10 when supplying gas from the calibrator sets such parameters of conversion of the electrical signal from the optical radiation receiver so that the indicator readings correspond to the concentration being determined. Then, when measuring an unknown concentration, the indicator will display the value directly in units of mass concentration. Fig. 1.8 shows the IR SWR diagram.

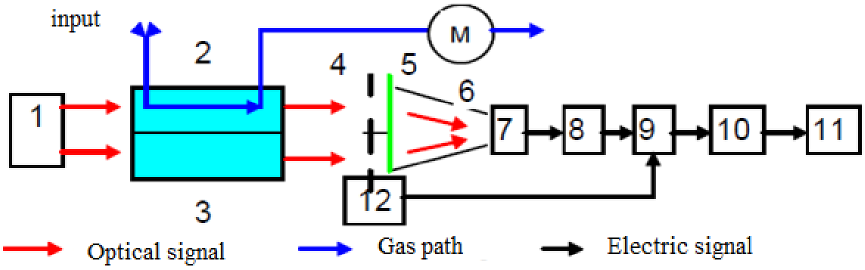

Fig. 1.8. Structural diagram of IR receiver

IR radiation from source 1 enters two cuvettes 2 and 3 located next to each other and parallel to each other 3. Next The optical radiation beams are modulated in antiphase to each other by means of the shutter 4, which is rotating disk with slots. Then the optical radiation passes through interference filter 5, which has maximum transmission (as an example τ = 80% on λ = 4.2 μm) . The absorption line of carbon dioxide falls into this band. carbon. Then both modulated beams are directed to the pyroelectric photodetector using the concentrator 6 . 7 the photodetector converts the flow radiation into a variable electric current proportional to its magnitude signal and its preliminary amplification takes place. Then the signal is amplified in the main amplifier 8 and divided into components corresponding to the radiation fluxes through the cuvettes 2 and 3 in the synchronous detector 9. Operation The detector is synchronized with the rotation of the shutter using a photosensor 12. Then the signals are sent to the processing unit 10, where they are subtracted and the result signal is displayed on indicator 11.

Measuring instruments designed to quantitatively determine the concentration of gas components are called gas analyzers and gas chromatographs [7] . These technical devices, depending on their purpose, are divided into portable and stationary. Portable gas analyzers and chromatographs are used to quantitatively determine the concentration of gas components when performing research work in laboratory conditions, as well as during special inspections, tests and adjustment of various industrial heat engineering installations. Stationary gas analyzers are designed for continuous automatic measurement of the volumetric percentage of a component in a gas mixture. Stationary gas analyzers are widely used to control the combustion process in combustion devices of steam generators, furnaces and other units for the analysis of technological gas mixtures, etc.

The most common method for determining the composition of gaseous fuels and products of incomplete combustion is gas chromatography [14]. Modern chromatographs allow for the determination of the composition of incomplete combustion products with high accuracy within a few minutes: H_2 , CO, CO_2 , CH_4. The general scheme of the chromatograph is presented in Fig. 1.9.

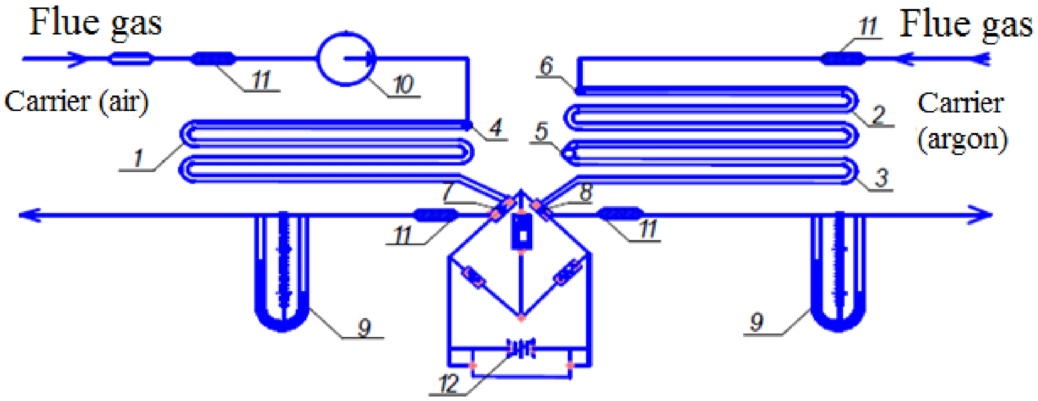

Fig. 1.9. General diagram of the chromatograph: 1-3 – separation columns, 4-6 – dosing devices, 7-8 – sensitive elements, 9 – rheometers, 10 – microcompressor, 11 – filter dryers, 12 – rectifier

The carrier gas (air) is supplied to the separation column 1 by means of a membrane-type microcompressor 10 and enters the working chamber of the detector 7 with a sensitive element located therein, in which a platinum filament is “embedded” in a layer of aluminogel made in the form of a ball. Another carrier gas (argon) washes the series-connected separation columns 2 and 3 and enters the working chamber of the detector 8, in which a sensitive element is also located. The flow rate of the carrier gases entering the device simultaneously is controlled by means of a rheometer 9. The sensitive elements are included in the circuit of a measuring bridge powered by a DC stabilizer 12.

The disadvantage of chromatography is the nonlinearity of adsorption isotherms, which leads to asymmetry of peaks. This nonlinearity is associated with the geometric and chemical heterogeneity of the surface of conventional active adsorbents. The heterogeneity and high adsorption, and sometimes catalytic activity of conventional adsorbents limits their use in gas chromatography. Therefore, such adsorbents are mainly used only for the analysis of gaseous substances that do not contain active functional groups, the adsorption isotherms of which at the concentrations and temperatures used in chromatography are close to linear.

Gas analyzers are essential tools used to determine the composition of gas mixtures in various industrial, scientific, and environmental applications. These devices are commonly calibrated in volume percentages because, under changing conditions of pressure and temperature, the relative proportions of the individual gas components in the total volume generally remain consistent. This approach provides a practical and reliable means of comparison, ensuring accuracy and uniformity across different operational settings.

Mechanical gas analyzers operate on the principle of detecting and quantifying specific physical or molecular-mechanical properties of a gas or gas mixture. These devices do not rely on electrical or optical measurements but instead focus on parameters such as pressure, volume, mass, or density to infer the concentration of a particular gas component. Mechanical gas analyzers are often appreciated for their robustness and simplicity, especially in environments where electronic equipment might not be feasible or reliable.

One of the most widespread types of mechanical gas analyzers is the chemical gas analyzer. These instruments function by measuring the reduction in the volume of a gas sample after a targeted component has been selectively removed. The principle behind this method is that by extracting a known component from the mixture, the resulting decrease in gas volume can be directly correlated to the concentration of that specific component in the original mixture.

The removal of the gas component is typically achieved through selective absorption or separate combustion. In selective absorption, the gas sample is exposed to a chemical reagent that reacts specifically with the target gas, absorbing it from the mixture. For example, carbon dioxide may be absorbed by a solution of potassium hydroxide, while oxygen can be absorbed using alkaline pyrogallol. In separate combustion, combustible gases such as hydrogen or hydrocarbons are burned in a controlled chamber, and the resulting reduction in volume is measured.

These chemical-mechanical methods offer a relatively straightforward and cost-effective way to analyze gas compositions, particularly when electronic analyzers are either unavailable or impractical. Although modern gas analysis has shifted largely toward electronic and sensor-based technologies, mechanical and chemical gas analyzers still play a crucial role in certain industrial and educational settings due to their reliability and ease of use.

Optical gas analyzers are based on the use of the dependence of the change in one or another optical property of the analyzed gas mixture on the change in the concentration of the measured component. Optical gas analyzers use such optical properties as spectral absorption, optical density, refractive index, spectral emission of the gas mixture, etc.

The group of electric gas analyzers includes gas analyzers, the principle of operation of which is based on measuring some electrical characteristic of the gas itself or the liquid with which the gas has reacted. In this case, an electrical parameter is selected that depends on the concentration determined by the component. Modern electrochemical gas analyzers, designed to optimize and control combustion modes in boiler plants, operate on various types of fuel, in addition to measuring volumetric particles (CO, O_2, NO and other components), also calculate the following parameters: efficiency by reverse balance, excess air coefficient, heat loss with gases, heat loss due to chemical incomplete combustion of fuel, heat loss with water vapor.

Thermal gas analyzers include devices based on measuring thermal properties, which determines the component of a gas mixture, which is a measure of its concentration. The measured values in gas analyzers of this type are the thermal conductivity of the gas mixture and the useful thermal effect of the catalytic oxidation reaction, which depend on the concentration of the mixture being determined. Thermal gas analyzers are divided into thermal conductometric (by the thermal conductivity of the gas mixture) and thermochemical (by the useful thermal effect of the catalytic oxidation reaction).

Magnetic gas analyzers are based on measuring the magnetic properties of oxygen and are designed to determine the mass fraction of oxygen in a mixture. The magnetic properties of gases are usually characterized by the values of the bulk magnetic susceptibility and the specific or mass magnetic susceptibility. All known gases are divided into diamagnetic and paramagnetic by the nature and absolute value of the magnetic properties. For diamagnetic gases, the bulk magnetic susceptibility κ has a negative value, for paramagnetic gases it is positive. The specific magnetic susceptibility χ is determined by the ratio of the bulk magnetic susceptibility κ to the gas density ρ.

Photocolorimetric gas analyzers are based on a color-selective reaction of chemical interaction between the components of a gas mixture, the concentration of which is being determined, and an indicator solution. Fig. 1.10 presents the systematization of gas analyzers.

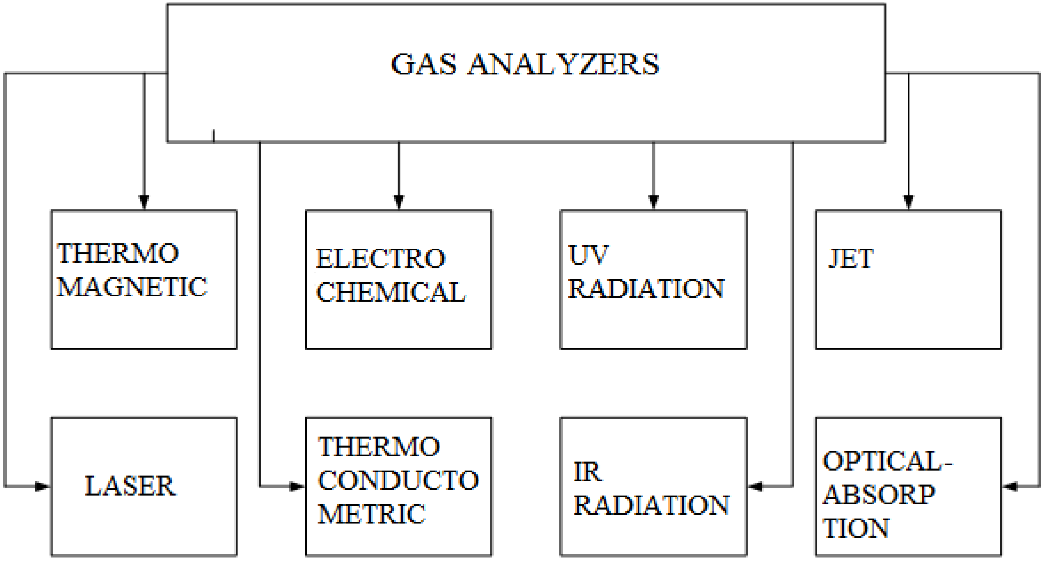

Fig. 1.10. Systematization of gas analyzers

An overview of modern means of measuring the quantitative value of the concentration of flue gas components is presented in Table 1.4.

Table 1.4

Means of measuring the concentration of gas components (via the CO_2 channel)

Instrument	Temperature range, °C	Working pressure, kPA	Measurement range, %	Insensitivity zone, with	Error, % / Control probability *	Drift, %
A-8M	up to 50	35	0.01 to 99.9	< 10	± 1 / 0.8	< ± 1
NDIR Gas sensor MH-410D	-20 - 60	5	20 to 100	30	5 / 0.85	< ± 1
Ezodo CTH - 37	up to 400	40	0- 50	10	5/ 0.94	< ± 1

The principle of operation of a number of well-known gas analyzers such as: "Jarrelach" (USA); "R iken Keiki" (Japan); "Multi - warn" , "Raid 1", "Microii", "Polytector" (Germany) ; "Detector mx 21" (France) is built on continuous or periodic calibration of equipment used for signal processing. But the algorithms of these devices are limited in terms of controlling components in the areas of qualitative and quantitative analysis, as well as in the area of changing influencing variables, which does not meet the requirements of adaptability.

Therefore, we can conclude that there is an imbalance in the parameters of information processing time - accuracy - sensitivity - price, and, therefore, the development of a device for controlling the concentration of gas components is relevant.

This section provides a comprehensive analysis of methods and technologies used to determine the concentration of gas mixtures. Various gas analysis techniques are reviewed, with a focus on their principles of operation, accuracy, sensitivity, and applicability for different tasks. The advantages and disadvantages of each method are considered, highlighting the challenges associated with gas detection and quantification in complex environments. Special attention is given to the influence of interfering components and external factors on measurement accuracy, as well as the need for improving selectivity and sensitivity in gas analysis techniques.

Among the numerous gas analysis methods available, the most widely used include electrochemical, chromatographic, mass spectrometric, and optical methods. Electrochemical sensors, while relatively inexpensive and easy to use, suffer from limited selectivity and potential cross-sensitivity to other gases. Chromatographic methods, such as gas chromatography (GC), offer high precision but require complex instrumentation and extended analysis times. Mass spectrometry, although highly accurate and capable of detecting trace gas concentrations, is expensive and requires extensive calibration.

A common drawback of most conventional gas analysis techniques—except for optical methods — is their low selectivity. This means that the presence of multiple gas components in a sample often interferes with accurate concentration determination. Another significant limitation is the sensitivity threshold, which determines the ability of an analytical method to detect low concentrations of gases. High sensitivity is primarily characteristic of electrochemical and optical methods, making them more suitable for applications where trace gas detection is required.

The review indicates that optical methods offer the most promising approach for gas concentration measurement due to their high selectivity, rapid response times, and non-invasive nature. Among these, optical absorption spectroscopy stands out as the most effective solution for addressing the identified challenges. Optical absorption techniques, particularly those based on infrared (IR) and ultraviolet (UV) spectroscopy, enable precise and real-time detection of gases by measuring the absorption of light at specific wavelengths corresponding to molecular transitions. These methods are widely used in environmental monitoring, industrial process control, and medical diagnostics.

Given the advantages of optical methods, an important objective of future research is to further enhance and optimize the most effective technique for gas component concentration control. The goal is to develop a unified and standardized approach tailored to the characteristics of the specific control object. Achieving this requires solving a series of theoretical and practical challenges, including improving sensor stability, minimizing measurement errors, and developing advanced algorithms for data processing and interpretation. Future work should also explore the integration of optical gas sensors with modern data acquisition and machine learning techniques to enhance the accuracy and reliability of gas concentration measurements across various applications.

CHAPTER 2

DEVELOPMENT OF A MATHEMATICAL MODEL FOR A CARBON DIOXIDE CONCENTRATION MEASUREMENT DEVICE IN FLUE GASES OF BOILER PLANTS

Analysis of absorption spectra of sensors of the control device. To determine the lengths of the photodetectors in the control device for the concentration of carbon dioxide in gases, we will analyze the absorption spectra of gases [16] , which are products of combustion. Appendix presents the absorption bands of the main combustion products (flue gases) .

Analysis of the absorption spectra of the main components of gases in the full infrared range of 0.75-15 μm (13330-667 cm $^{-1}$) is presented in Fig. 2.1-2.5.

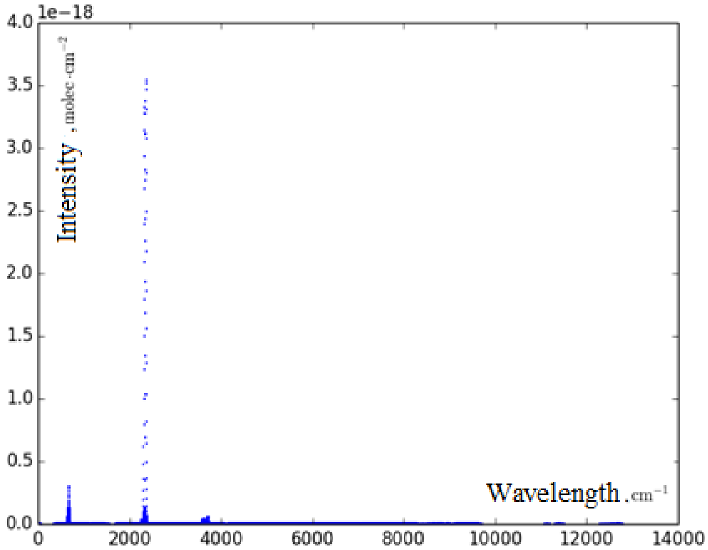

Fig. 2.1. CO_2 absorption spectrum in the range of 0.75-15 microns

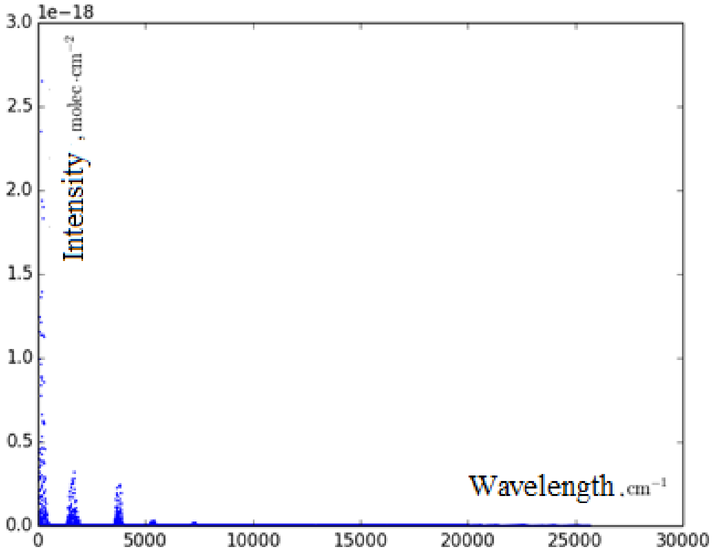

Fig. 2. 2. Absorption spectrum of H_2O in the range of 0.75-15 microns

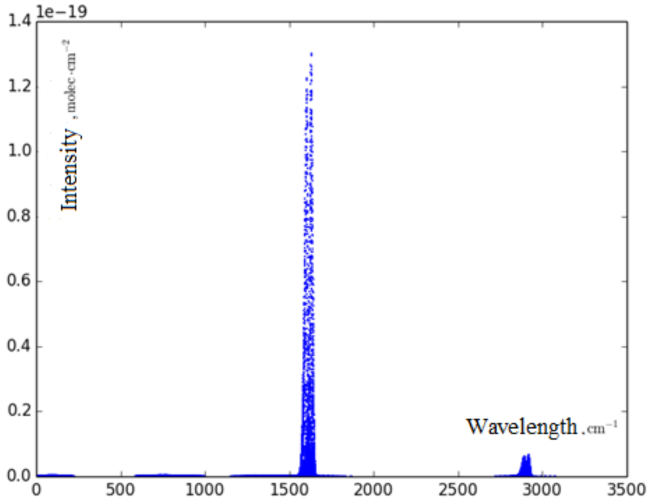

Fig. 2. 3. Absorption spectrum of N_2O in the range of 0.75-15 microns

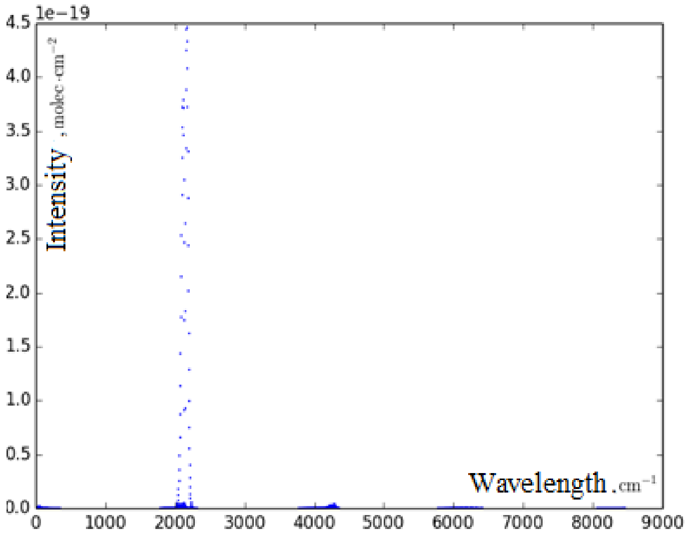

Fig. 2. 4. Absorption spectrum of CO in the range of 0.75-15 microns

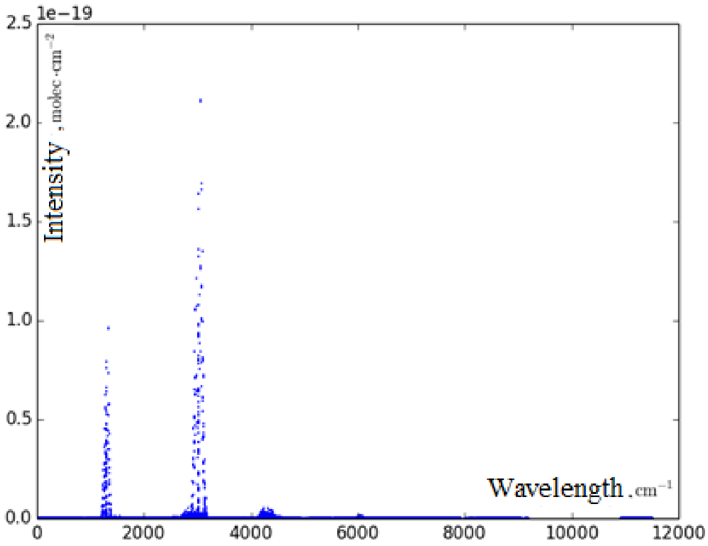

Fig. 2. 5. Absorption spectrum of CH_4 in the range of 0.75-15 microns

From the analysis of the spectra it was concluded that the most active region is within 2200-2500 cm $^{-1}$. Fig. 2.6 shows the absorption of the main components of gases in the range of 4 - 4.5 microns (2200 - 2500 cm $^{-1}$).

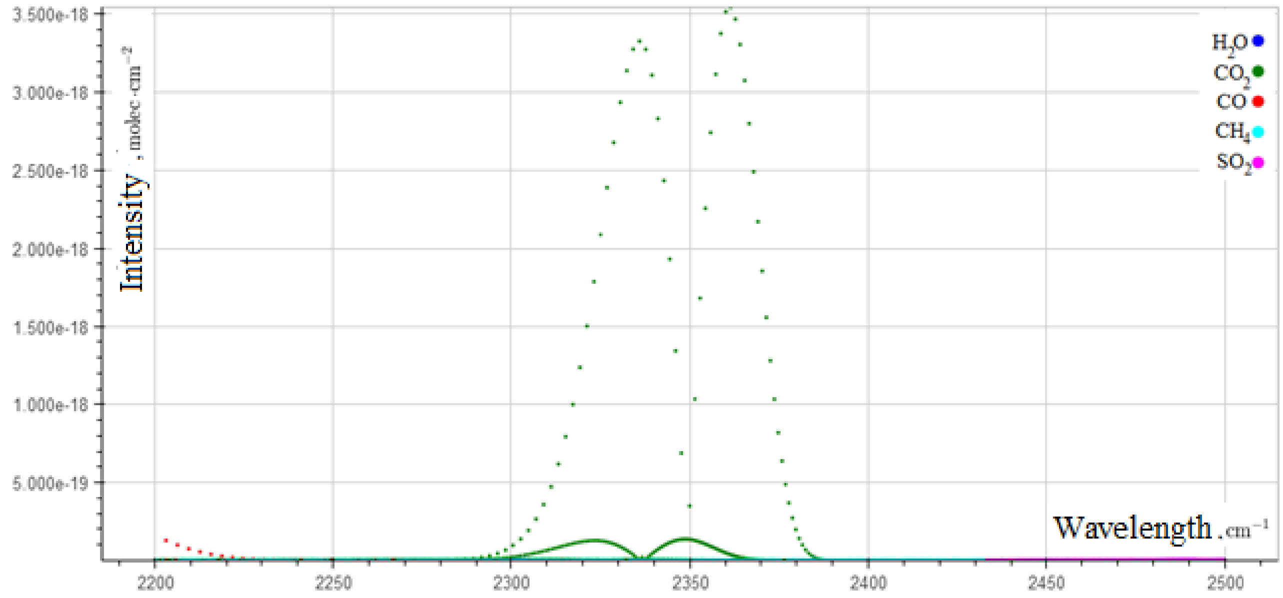

Fig. 2.6. Absorption spectrum of the main components of flue gases in the range of 4 – 4.5 microns

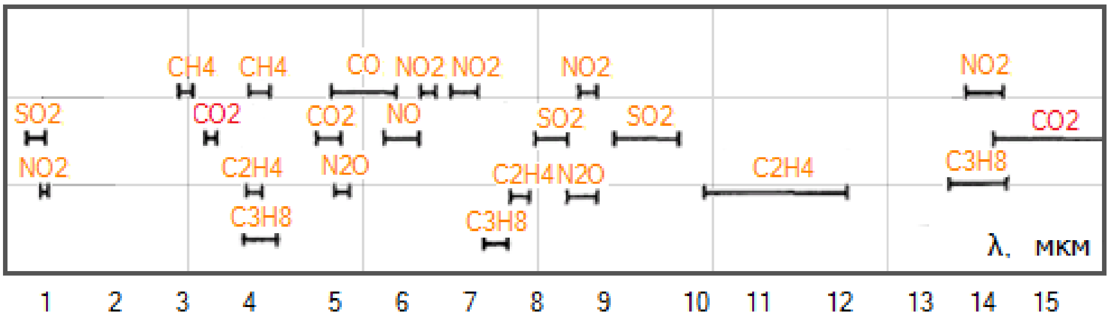

Fig. 2.7. Absorption bands of flue gases in the spectral range 0.25...15 microns

As can be seen from the analysis of the absorption spectra of the main flue gases, almost all absorption bands are located next to each other (in some cases overlap). In addition, water vapor present in gases occupies a wide range of absorption band lengths. Therefore, a necessary condition is not only the selection of gas absorption lengths in such a way that they do not overlap, but also the use of high-precision radiation sources and receivers (the width of the spectrum of which does not allow the ingress of "neighboring" gases). After analyzing the absorption lengths of flue gases, it is necessary to select infrared emitters and receivers based on the already known input data.

Thus, it is possible to determine the parameters of photodiodes and photodetectors, while taking into account the intersection of absorption lines. That is, the control points for each gas look in such a way that there are no absorption lines of other gases nearby that could affect the measurement results.

The model of radiation attenuation in the flue gas environment is presented in Fig. 2.8.

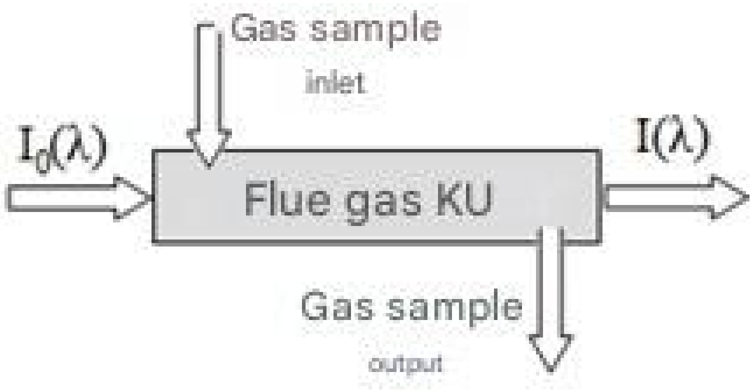

Fig. 2.8. Model of radiation attenuation in the flue gas environment

Let us present the Bouguer-Lambert-Beer law derived in the first section, which relates the intensity of radiation passing through the flue gas to the concentration of the gas under study, the length of the absorption path, and the absorption coefficient in the form

$$I_l = I_0 \cdot e^{-\varepsilon C l}, \tag{2.1}$$

where C is the concentration of the gas under investigation, l is the absorption path length, ε – attenuation indicator .

The attenuation indicator is the sum of two components

$$\varepsilon = k_n + k_p, \tag{2.2}$$

where k_p and k_p are the absorption and scattering indices, respectively.

Thanks to the condenser lens, the scattering index in formula (2.2) disappears. Therefore, (2.2) can be rewritten as

$$I_l = I_0 \cdot e^{-k_n C l}. \tag{2.3}$$

If the concentration is expressed in mol/l, then the absorption coefficient k_p is replaced by the molar specific absorption coefficient χ (units of measurement - [l/(mol·cm)])

$$I_l = I_0 \cdot e^{-\chi C l}. \tag{2.4}$$

Since in formula (2.4) the concentration of gas C *is* expressed in mol/l, and the unit of measurement of concentration in the work is % vol. , it is necessary this dependency add the correction factor m . To begin with, let's present the concentration in *mg /m* ^{3} .

$$C_{\text{mg/ m3}} = C \cdot M \cdot 10^6, \tag{2.5}$$

where $C_{\text{mg/ m3}}$ –gas concentration (*mg/* m^3) , M is the molar mass of the gas under study (*g/ mol*) .

The gas concentration in *mg/* m3 is related to the volume concentration in *%vol* by the following relationship (assuming 1% vol = 10000 ppm) :

$$C_{\%o.} = \frac{C_{\textit{мг}\backslash \textit{м}^3} \cdot \dfrac{R \cdot T}{P}}{M \cdot 10^4}. \tag{2.6}$$

Substituting (2.5) into (2.6) we obtain

$$C_{\%} = C \cdot 10^2 \cdot \frac{R \cdot T}{P}. \tag{2.7}$$

Temperature and pressure have a significant impact on the value of the absorption index χ and, accordingly, on the correctness of the results of concentration determination [14] . In order to assess this effect, we will write down the analytical dependence of χ on T and P . We will solve this problem in two stages. In the first stage, we will move from molar to spectral absorption. In the second stage, we will isolate T and P through the known Clapeyron- Mendeleev –law .

Therefore, the molar and spectral absorption indices are related by the following relationship:

$$\chi = k_n(\lambda) \cdot \frac{V}{\mu}, \tag{2.8}$$

where V is the volume of gas (l), μ is the number of moles of gas (mol).

In turn, μ depends on the molar volume under normal conditions V_m (22.4 l/mol) and the volume occupied by the gas being analyzed under normal conditions V_0 (l).

$$\mu = \frac{V_0}{V_m}. \tag{2.10}$$

Let us assume that the process of controlling the concentration of carbon dioxide in flue gases is a thermodynamic process that occurs with a constant mass at a constant value of the volume of the gas being analyzed. That is, we actually assume that the process is isochoric [16]

$$\frac{P}{T} = const \tag{2.11}$$

Mendeleev law [17] in the form of the system

$$\begin{cases} PV = \mu RT; \\ P_0 V_0 = \mu R T_0, \end{cases} \tag{2.12}$$

where R is the universal gas constant.

By defining the parameter μR and solve the system with respect to V_0 we will get

$$V_0 = \frac{PVT_0}{TP_0}. \tag{2 .1 3}$$

Substituting (2 .1 3) into (2.10) we obtain

$$\mu = \frac{PVT_0}{TP_0 V_m} \tag{2.14}$$

Let us reduce expression (2.14). To do this, substitute the values of P_0 and T_0 under normal conditions determined according to IUPAC . Then

$$\mu = 1{,}2 \cdot 10^{-4} \frac{PV}{T}. \tag{2.15}$$

We substitute the resulting expression into (2.9):

$$\chi = k_n(\lambda)\cdot\frac{8333,(3)\cdot T}{P}\,. \qquad (2.16)$$

From the researched publications it is not known about the existence of an adequate analytical model of the pressure value brought to the control object. It is known that through the inlet and outlet openings of the chimney air is combined with the atmosphere, which leads to pressure equalization (but not complete). In The flue gas is under the chimney. absolute pressure, which consists of atmospheric and excess pressure (vacuum pressure 40-80 Pa). Absolute pressure is equal to the sum of atmospheric pressure and vacuum (taken with a minus sign). Then

$$P_{a.} = P_{at} - P_{p.} \qquad (2.23)$$

However, it should be noted that the atmospheric pressure according to the requirements of the international code FM 12 SYNOP is reduced to sea level. To calculate the pressure at altitude h (the altitude at which the gas concentration control device operates) from the sea level pressure P_0 (this pressure is substituted into the well-known formula 2.23) and air temperature T, we use the formula

$$P_{at.} = P_0 \cdot e^{-\frac{M_{\text{м}}\cdot g\cdot h}{R\cdot T}}\,, \qquad (2.24)$$

where M is the molar mass of dry air (0.029 $\frac{kg}{mol}$), g is the acceleration of gravity, h is the height, which is the sum of the height of the chimney and the surface of its base above sea level (for example, KU PTVM-30 (Vinnytsia city) is located at an altitude of 294 meters above sea level with a height of 90 meters).

Then the absolute pressure at the control object is expressed as

$$P_{a.} = P_0 \cdot e^{-\frac{M_{\text{м}}\cdot g\cdot h}{R\cdot T}} - P_p\,. \qquad (2.25)$$

There are tabulated values of the spectral absorption index $k_n(\lambda)$ for the main gases, but they are given for normal or standard conditions, which is unacceptable for the control object, because [19] the spectral absorption index depends on pressure and temperature, and, as a result, the half-width of the spectral line depends on them.

As mentioned in the first section, the absorption ability of gas molecules in the IR region is due to the vibrational-rotational mechanism of molecular oscillations. From the analysis of the absorption spectra, CO_2 has the most intense absorption band with a central length of 4.264 μm. The contour of this band is described by the Lorentz function [18] (we will write this function in terms of the length λ)

$$k_i(\lambda) = \frac{S(\lambda_i)}{\pi}\cdot\frac{\sigma}{\sigma^2 + (\frac{1}{\lambda} - \frac{1}{\lambda_i})^2}, \qquad (2.26)$$

where *S* is the intensity of the absorption band, λ and λ_0 are the length and center of the absorption band, σ is the width of the absorption band.

In turn

$$S(\lambda_s) = \int_0^{\infty} k_s(\lambda)d\lambda. \qquad (2.27)$$

λ *and* λ of the same intensity and width .

The necessary information about the gas (intensity and spectral half-width of the lines) can be found in the HITRAN database [19]. The gas data is stored in a text file and is a table where the columns present the name of the gas, wave number, gas line intensity, and spectral half-width of the lines.

Table 2.1

Physical properties of flue gas absorption bands

Serial number of the gas mixture	Wave number (υ)	Gas line intensity (S)	Spectral half-width of lines (σ)
23	2373.455087	2.058E-30	.06800
63	2373.470292	1.330E-28	.06440
23	2373.473365	1.213E-25	.06010
21	2373.477165	7.860E-28	.07730
21	2373.484763	5.652E-27	.05860
24	2373.507231	2.038E-30	.05680
21	2373.524463	2.052E-29	.05610
23	2373.529430	1.972E-29	.07280
24	2373.556092	1.370E-30	.05660
11	2373.572984	9.372E-28	.01980
21	2373.576440	5.582E-28	.07940
61	2373.587840	1.521E-29	.04700
24	2373.629919	1.621E-23	.06580
61	2373.630875	6.218E-29	.04500
24	2373.636738	1.411E-30	.05660
21	2373.661105	3.602E-28	.08150
21	2373.665624	1.034E-18	.06810
61	2373.671538	3.617E-29	.04500
63	2373.681517	2.192E-28	.02240

HITRAN (HIgh-resolution TRANsmission molecular absorption) Database is one of the most comprehensive and widely used resources for molecular spectroscopic data. It contains information on the absorption and emission characteristics of gases, with a primary focus on the infrared and microwave regions of the electromagnetic spectrum. This database plays a pivotal role in atmospheric science, remote sensing, environmental monitoring, climate modeling, and other fields that involve the study of molecular interactions and absorption in the atmosphere.

The HITRAN database is a collection of spectroscopic parameters that describe the interactions of molecular species with electromagnetic radiation. These parameters are used to model and understand how gases absorb, emit, and scatter radiation, which is crucial for various applications, including atmospheric science, remote sensing, environmental monitoring, climate modeling, and industrial applications such as gas monitoring in combustion or chemical manufacturing processes.

Molecular Species: HITRAN includes data for a wide range of molecular species, including greenhouse gases such as CO_2, methane (CH_4), water vapor (H_2O), nitrous oxide (N_2O), and ozone (O_3), as well as many other atmospheric and industrial gases.

Spectroscopic Parameters: The core of HITRAN consists of detailed spectroscopic parameters, including transition frequencies (the frequencies at which molecules absorb or emit radiation), line intensities (the strength of absorption or emission lines), line shapes (describing how absorption lines broaden or shift), pressure-induced line shifts (the change in frequency of absorption lines due to pressure), and temperature dependence (how line intensities and shapes change with temperature).

Isotopologues: The database includes data for isotopologues, which are molecules that differ in their isotopic composition. These can affect the absorption spectra in measurable ways and are essential for accurate atmospheric modeling and remote sensing applications.

Line Mixing and Broadening: HITRAN provides data on line mixing and broadening effects, which are particularly important for understanding the behavior of gases in dense media or under extreme conditions. These effects influence the shape and width of spectral lines.

Collision-Induced Absorption (CIA): For certain gases, especially in dense atmospheres, HITRAN includes data on collision-induced absorption, where molecular collisions contribute to the absorption process. This is especially relevant for atmospheric gases at high pressures.

The HITRAN database is organized in a standard format that allows users to access and manipulate the data easily. The data is typically stored in ASCII files that can be read by various software programs. The format includes fields such as molecule name, spectral region, transition data (frequency, intensity, quantum numbers, etc.), isotopic information, and temperature and pressure dependencies. The data is categorized by different spectral regions, including infrared, microwave, and millimeter-wave spectra, with the majority of the database focusing on the infrared region (from 2.5 μm to 25 μm).

Atmospheric Modeling: HITRAN data is extensively used in atmospheric radiative transfer models to simulate how gases interact with radiation at various altitudes and latitudes. It helps researchers predict climate change, analyze air quality, and study the transport of gases in the atmosphere.

Remote Sensing: The HITRAN database is crucial for interpreting measurements from instruments like spectrometers and spectroradiometers on satellites or ground-based observatories. By matching observed spectra with the HITRAN database, scientists can deduce the concentrations of specific gases in the atmosphere.

Climate Studies: HITRAN's detailed molecular absorption data is key to understanding how gases like CO_2 and CH_4 absorb infrared radiation and contribute to the greenhouse effect. It is instrumental in climate models that predict global warming and the effects of greenhouse gases.

Astronomy: In astronomy, HITRAN helps interpret molecular absorption spectra observed from distant stars, planets, and interstellar clouds. It is vital for understanding the chemical composition of extraterrestrial environments.

Industrial and Environmental Monitoring: HITRAN is also applied in industrial settings to monitor the concentrations of gases such as carbon monoxide, sulfur dioxide, and volatile organic compounds. By using HITRAN’s spectroscopic data, engineers and scientists can develop sensors and systems for detecting trace gases in the environment.

Chemical and Combustion Processes: In chemical engineering, HITRAN data is used to model and optimize combustion processes. By understanding the absorption spectra of various chemicals, engineers can improve the efficiency and safety of combustion systems.

The HITRAN database is periodically updated to include new spectral data, correct errors, and improve the precision of existing parameters. These updates often reflect advancements in spectroscopic techniques and the discovery of new molecular species. The most recent versions are often made available to the public through institutions like the Harvard-Smithsonian Center for Astrophysics (CfA), which maintains the database.

HITRAN is usually released in different formats to accommodate a wide range of users, from researchers working with atmospheric models to engineers designing monitoring systems. Additionally, it is made available through online portals and interfaces that allow easy access to the data.

The HITRAN database is a fundamental tool in scientific research, engineering, and environmental monitoring. Its detailed molecular absorption data is indispensable for modeling and understanding the interaction of gases with electromagnetic radiation. By providing accurate and comprehensive spectroscopic data, HITRAN enables researchers and industry professionals to better analyze and interpret the behavior of gases in diverse fields, from atmospheric science to industrial processes.

Graphical modeling of a fragment of the HITRAN database is presented in Fig. 2.9.

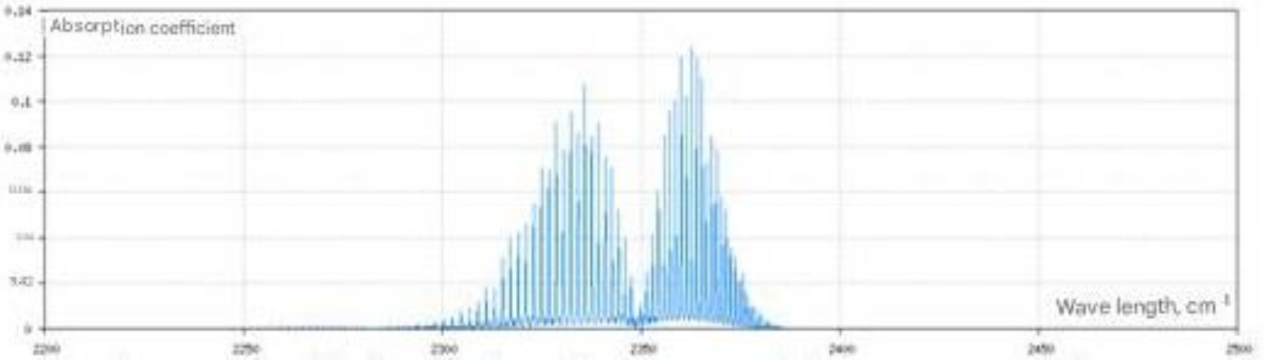

Fig. 2.9. Graphical modeling of a fragment of the HITRAN database

As can be seen from Fig. 2.8-2.9, the absorption spectrum The flue gas spectrum in a given range has a complex structure due to the superposition of the spectra of the gases contained in it, therefore the absorption coefficient *k (λ)* of the band is expressed as the sum of the absorption coefficients of individual lines.

$$k(\lambda)=\sum_i \frac{S(\lambda_i)}{\pi}\cdot\frac{\sigma}{\sigma^2+(\frac{1}{\lambda}-\frac{1}{\lambda_i})^2}. \quad (2.28)$$

At the same time, each of the spectral lines has the following important characteristics [17]:

1. λ_0 – the center of the absorption band (resonant frequency) does not depend on *T* and *P*.
2. Intensity *S* does not depend on *P* , but depends on *T.*
3. *line* width σ_L has a certain temperature dependence

Model 2.28 takes into account different $\lambda_{0\,and}$ and $S(\lambda_{and})$ for each individual absorption line, but the value of σ_L must be equal (thus, a certain assumption is introduced for the calculation of the series 2.28). The spectra of the absorption coefficients of all gases are given in the spectral band (2.6 µm ±). Thus, the model 2.28 will take into account the influence of the influencing gases.

to determine the absorption *of* CO_2 in gases [17] .

To calculate the absorption value in the spectral interval 4.1–4.3 µm (2300–2400 cm $^{-1}$), an analytical model of the spectral distribution of gas absorption coefficients was used, calculated on the basis of tables of the intensity of lines S (λ_0) of gas radiation in the specified spectral range [17], which corresponds to the following approximations:

1. The spectrum of the gas absorption coefficient is described by the sum of Lorentz distributions with different λ_0 and $S(\lambda_0)$, but the same values of σ_L .
2. The absorption coefficient spectra of all gases are given in the spectral band 2300-2400 cm $^{-1}$ (radiation wavelengths 4.1 - 4.3 microns) with a step of 0.01 cm $^{-1}$. Fulfilling this condition is necessary for the convenience of analyzing gas mixtures and taking into account the influence of influencing gases.
3. The model takes into account only lines with an intensity S ≥0.1 [cm·atm] under normal measurement conditions.

Therefore, by substituting formulas 2.7 into 2.4, 2.25 into 2.15, 2.28 into 2.16, the general form of the model will be as follows:

$$I_l = I_0\cdot e^{\frac{\int_0^\infty k_s(\lambda)d\lambda}{\pi}\cdot\frac{\sigma}{\sigma^2+(\frac{1}{\lambda}-\frac{1}{\lambda_i})^2}\frac{-0{,}0083\cdot T}{P_0\cdot e^{-\frac{M_M\cdot g\cdot h}{R\cdot T}}-P_{p.}}\cdot\frac{C}{M}\cdot l}. \quad (2.29)$$

The simulation results are presented in Fig. 2.10 -2.11 .

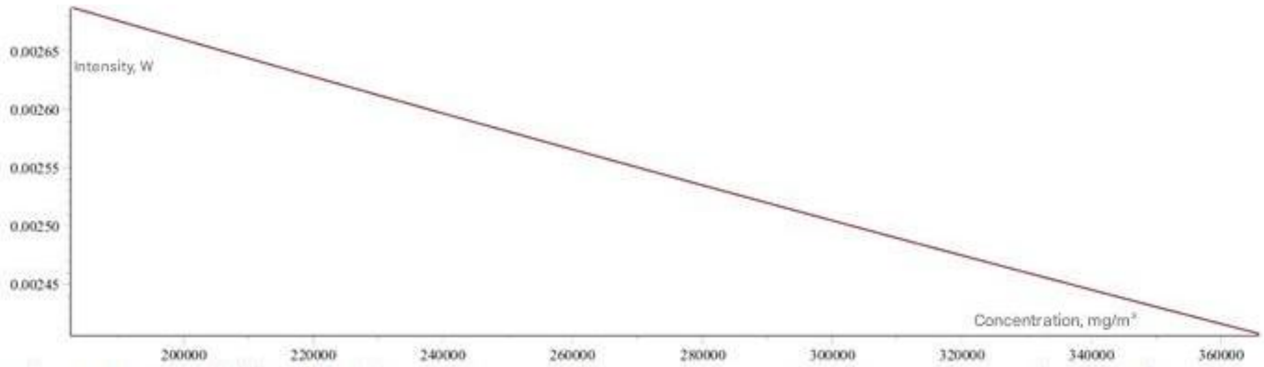

Fig. 2.10. Modeling the dependence of flue gas concentration on intensity (in the operating range)

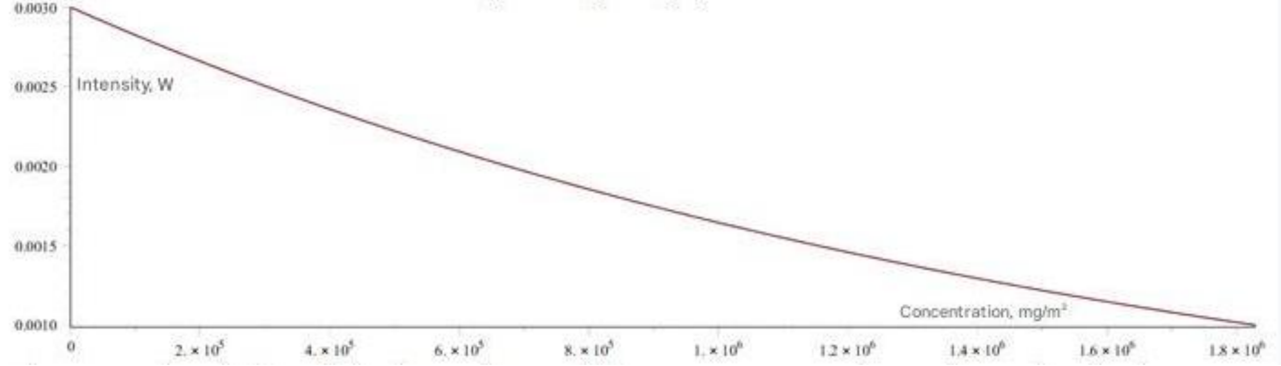

Fig. 2.11. Simulation of the dependence of flue gas concentration on intensity (in the full range)

Thus, the mathematical model (2.29) and its simulation Fig. 2.10-2.11 describe the process of radiation attenuation in an optical measuring transducer and take into account the main factors related to the features of the control object that affect its correctness.

IR emitter. An IR emitter (infrared emitter) is a device that generates and emits infrared (IR) radiation, i.e. electromagnetic waves with a wavelength ranging from approximately 0.75 microns to 1 mm, i.e. outside the visible spectrum, on the longer wavelength side.

IR emitters operate on the principle of electrical or thermal excitation of materials capable of emitting in the infrared range. Typically, IR emitters are used to transmit energy or signals in the infrared spectrum, as well as to heat various objects.

Main types of IR emitters:

Thermal IR emitters are devices that generate infrared radiation using heat. They can be made in the form of lamps or elements that heat up to a high temperature, emitting IR rays. Such devices are often used in infrared heaters or to provide thermal effects in technological processes.

Semiconductor IR emitters are devices that generate infrared radiation due to electrical transitions in semiconductor materials. Such emitters are used, for example, in IR diodes or lasers (IR lasers), which are capable of generating coherent IR radiation. They are used in telecommunications, sensor systems, and in various measuring instruments.

Gas-discharge IR emitters - These devices produce infrared radiation by means of gas discharges excited by electrical pulses. They are often used in spectroscopy when it is necessary to emit IR waves of a specific wavelength for the analysis of materials.

IR emitters are widely used in various fields, such as:

IR heating: Used in industrial heaters, drying units, heaters, etc.

Telecommunications: IR lasers and diodes are used in fiber optic systems for data transmission.

Security and monitoring: They are used in night vision systems, motion sensors, and other security technologies because infrared radiation allows the detection of thermal signatures of living objects.

Medical applications: IR radiation is used in physiotherapy, where IR rays are used to treat joint and muscle diseases.

The main characteristics of IR emitters are the spectral region of emission (which determines the wavelength of infrared light), the radiation power, and the efficiency of converting electrical energy into infrared waves.

A light-emitting diode (LED) was used as a source of IR radiation. The line width of infrared radiation generation of LED is 40–1000 nm. This meets the requirements of the task, because the radiation generation lines are chosen in such a way that at a distance of the width of the radiation generation line there are no intense absorption lines of other gases.

The main disadvantage of LED is the dependence of the radiation power on the temperature of the medium. As the temperature increases, the power emitted by the diode decreases [13].

Photodetector. A photodetector is an electronic device designed to detect and record light signals. Its main task is to convert light energy into an electrical signal, which can then be processed or used in various systems, such as measurement, automation, communication, and others.

A photodetector works on the principle of the photoelectric effect, which is that certain materials can change their electrical properties (for example, conduct electricity) when exposed to light. The main element of a photodetector is a sensor that detects light and converts it into an electrical signal. There are different types of photodetectors, depending on how they react to light:

1. Photodiodes are semiconductor devices that change their electrical resistance or generate an electric current when exposed to light. They are highly sensitive to light signals and are used in a wide range of applications, from simple lighting systems to high-precision measuring instruments.
2. Phototron is a type of vacuum tube in which light striking the cathode causes electrons to be ejected, which then create an electric current. These devices were widely used in the past, but are now being gradually replaced by more modern technologies.
3. Photosensors (optical sensors) are devices that can detect the presence or changes in the intensity of light signals. They can be used in various applications, such as automatically turning on lights, measuring distance, or detecting motion.
4. Pixelation and Photographic Plates - In some cases, photodetectors are more complex systems consisting of a large number of small photosensors or pixels.

This is often found in cameras or other optical systems where precise image representation is required.

Photodetectors are used in various fields such as telecommunications, science, medicine, photography, and automatic control systems. For example, in telecommunications, photodetectors are used to receive signals in fiber optic systems, and in medical devices, to collect information about the intensity of light passing through tissues (e.g., in pulse oximeters).

Key characteristics of photodetectors are light sensitivity (how effectively the device responds to different levels of light), spectral sensitivity (what part of the light spectrum is perceived), and response speed, which determines how quickly the photodetector can respond to changes in light intensity.

Due to their ability to convert light into an electrical signal, photodetectors are the basis of many modern technologies and are widely used in a variety of scientific, technical, and consumer devices.

In the article [14] the results of theoretical studies of the photoelectric measuring area-voltage conversion are presented, the main mathematical relations describing it are obtained. In such converters the area of the photosensitive layer of the photodetector, which is illuminated, changes under the action of the measured physical quantity. As a result, the output voltage of such a converter is a function of the measured physical quantity.

Fig. 2. 12 shows the principles and equivalent circuits of a photodetector based on a photodiode - operational amplifier pair.

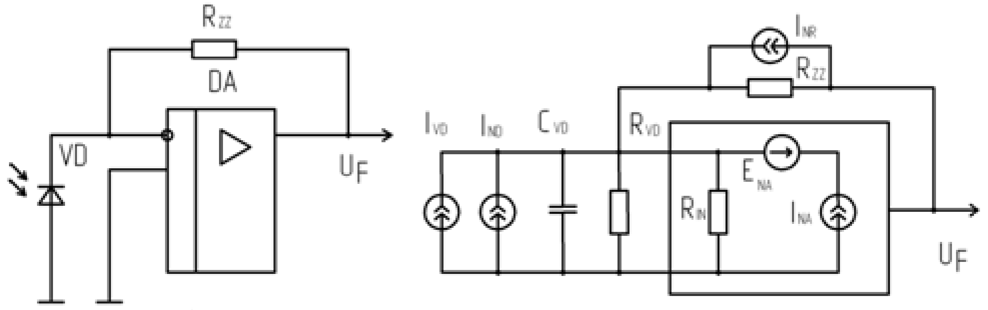

Fig . 2.12 . Photodetector based on a pair photodiode-operational amplifier

In the above circuit, the photodiode VD acts as a current generator, and the operational amplifier DA , covered by feedback , converts this current into voltage. The dependence of the current flowing through the photodiode on the irradiation flux is described by the expression [15]

$$I_{VD} = \frac{\Phi \cdot S_{I0}}{\sqrt{1+(\Omega \tau_{VD})}} - I_s \cdot (\exp(e_e \cdot U_{VD} / kT) - 1), \qquad (2.29)$$

where I_{VD} is the photodiode current; Φ – irradiation flux, S_{I0} – integral current sensitivity of the photodiode under unmodulated irradiation; I_S – dark current of the photodiode; U_{VD} – voltage drop across the photodiode; T – absolute temperature; k – Boltzmann constant; e_e – electron charge; Ω – cyclic frequency of irradiation flux modulation; τ_{VD} – time constant of the photodiode, which depends on the values of the internal resistance of the photodiode R_{VD} and the parasitic capacitance of the photodiode C_{VD}.

The output voltage of a photodetector based on a photodiode-operational amplifier pair, taking into account the zero offset, the difference in input currents, and the noise voltage, is described by the expression [16]

$$U_F = \frac{I_{VD} \cdot R_{ZZ}}{1 + \frac{R_{ZZ}}{K_0 \cdot R_{IN}} + \frac{1}{K_0}} + \Delta I \cdot R_{ZZ} + U_{SM} + U_N, \qquad (2.30)$$

where K_0 - the transfer coefficient of the operational amplifier; R_{IN} - the input resistance of the operational amplifier; - the U_{SM} zero $\Delta \mathrm{I}$ offset voltage of the operational amplifier; - the difference of the input currents of the R_{ZZ} operational amplifier; - the resistance in the feedback loop of the operational amplifier; U_N - the noise voltage at the output of the photodetector, which depends on the noise current I_{NR} of the resistor in the feedback loop, the noise current of the photodiode I_{ND}, the noise current of the operational amplifier I_{NA} and the noise voltage of the operational amplifier E_{NA}.

Substituting (2.29) into (2.30) and performing the transformation, we obtain

$$U_F = \frac{\Phi \cdot S_{I0} \cdot R_{ZZ}}{\left(1 + \frac{R_{ZZ}}{K_0 \cdot R_{IN}} + \frac{1}{K_0}\right) \cdot \sqrt{1 + (\Omega \tau_{VD})}} - \frac{I_S \cdot R_{ZZ} \cdot (\exp(^{e_e \cdot U_{VD}}/_{kT}) - 1)}{1 + \frac{R_{ZZ}}{K_0 \cdot R_{IN}} + \frac{1}{K_0}} + \qquad (2.31)$$
$$+ \Delta I \cdot R_{ZZ} + U_{SM} + U_N$$

When using a light source with a condenser lens, it is possible to obtain a plane-parallel radiation flux, the same on the entire plane. In this case, the intensity of the radiant flux and the area of the photosensitive layer of the photodiode being irradiated are related by the relation [17]

$$\Phi = I \cdot S, \qquad (2.32)$$

where I - intensity; S - area of the photosensitive layer of the photodetector that is illuminated.

Substitute formula (2.32) into formula (2.31) and we obtain

$$U_F = \frac{I \cdot S \cdot S_{I0} \cdot R_{ZZ}}{\left(1 + \frac{R_{ZZ}}{K_0 \cdot R_{IN}} + \frac{1}{K_0}\right) \cdot \sqrt{1 + (\Omega \tau_{VD})}} - \frac{I_S \cdot R_{ZZ} \cdot (\exp(^{e_e \cdot U_{VD}}/_{kT}) - 1)}{1 + \frac{R_{ZZ}}{K_0 \cdot R_{IN}} + \frac{1}{K_0}} + \qquad (2.33)$$
$$+ \Delta I \cdot R_{ZZ} + U_{SM} + U_N$$

As follows from expression (2.33), the output voltage of a photodetector based on a photodiode-operational amplifier pair linearly depends on the intensity of the radiation.

Substituting (2.28) into (2.33) we obtain

$$U_F = \frac{I_0 \cdot \exp^{-K \cdot C_{\text{‰}} \cdot l} \cdot S_{I0} \cdot S \cdot R_{ZZ}}{(1 + \frac{R_{ZZ}}{K_0 \cdot R_{IN}} + \frac{1}{K_0}) \cdot \sqrt{1 + (\Omega \tau_{VD})}} - \frac{I_S \cdot R_{ZZ} \cdot (\exp(^{e_e \cdot U_{VD}} / _{kT}) - 1)}{1 + \frac{R_{ZZ}}{K_0 \cdot R_{IN}} + \frac{1}{K_0}} + \qquad (2.34)$$

$$+ \Delta I \cdot R_{ZZ} + U_{SM} + U_N$$

The relation (2.34) describes the photoelectric measurement conversion of concentration-voltage.

Thus, a mathematical model of the functional relationship between the output voltage of the photodetector, based on the photodiode-operational amplifier pair, with the concentration of gas components, the dark current of the photodiode, the noise component, the bias voltage and the difference of the input currents of the operational amplifier, the values of the transfer coefficient and the input resistance of the operational amplifier was obtained.

Simulation. Noise current density of the feedback resistor [18]

$$I_{NR} = \sqrt{\frac{4 \cdot k \cdot \text{O} \cdot \Delta f}{R_{zz}}}, \qquad (2.35)$$

where Δf is the effective bandwidth of the electronic path.

Noise current density of a photodiode operating in photovoltaic mode [13]

$$I_{ND} = \sqrt{\frac{4 \cdot k \cdot \text{O} \cdot \Delta f}{R_{VD}}}. \qquad (2.36)$$

The modulus of the output noise voltage is determined by the expression [14]

$$U_N = \sqrt{E_{NA}^2 + (I_{NA}^2 + I_{ND}^2 + I_{NR}^2) R_{ZZ}}, \qquad (2.37)$$

Expression (2.33) can be simplified. If the light flux is unmodulated or the cyclic modulation frequency of the irradiation flux Ω is much less than the cutoff frequency of the photodiode and the operational amplifier, then the influence of their frequency properties can be neglected. The difference in input currents ΔI for modern operational amplifiers is units of nA, and the bias voltage U_{SM} is units of mV. Under the conditions $U_F \rangle\rangle U_{SM}$ and $\text{I}_{\text{VD}} \rangle\rangle \Delta \text{I}$, the values of U_{SM} and ΔI can be neglected. When using an element base with a low noise level, the noise component U_N expression (2.33) can be neglected. Due to the small value of the dark current, which is in the order of nanoamperes, it can be assumed that $I_S \approx 0$. The input resistance of modern operational amplifiers is tens or hundreds of MΩ, which significantly exceeds the resistance R_{ZZ} in the feedback loop and the internal resistance of the photodiode. The transfer coefficient of modern operational amplifiers is also very high and can reach tens of thousands. Based on this, the valid expression

$$\lim_{\substack{K_0 \to \infty \\ R_{IN} \to \infty}} \left(1 + \frac{R_{ZZ}}{K_0 R_{IN}} + \frac{1}{K_0} \right) = 1. \qquad (2.38)$$

Taking into account all these conditions, expression (2.33) takes the form

$$U_F = I_0 \cdot e^{\frac{\int_0^\infty k_s(\lambda) d\lambda}{\pi} \cdot \frac{\sigma}{\sigma^2 + (\frac{1}{\lambda} - \frac{1}{\lambda_i})^2} \frac{-0{,}0083 \cdot T}{P_0 \cdot e^{-\frac{M_M \cdot g \cdot h}{R \cdot T}} - P_{p.}} \cdot \frac{C}{M} \cdot l} \cdot S_{I0} \cdot S \cdot R_{ZZ}. \qquad (2.39)$$

From expression (2.39) it follows that the output voltage of a photodetector based on a photodiode-operational amplifier pair is directly proportional to the area of the photosensitive layer of the photodiode that is illuminated, if we neglect the influence of the dark current, the noise component, the bias voltage and the difference of the input currents of the operational amplifier, the final values of the transfer coefficient and the input resistance of the operational amplifier, etc.

Modeling the dependence of CO2 concentration on voltage in the operating and full range is presented in Fig. 2. 13 -2. 14 .

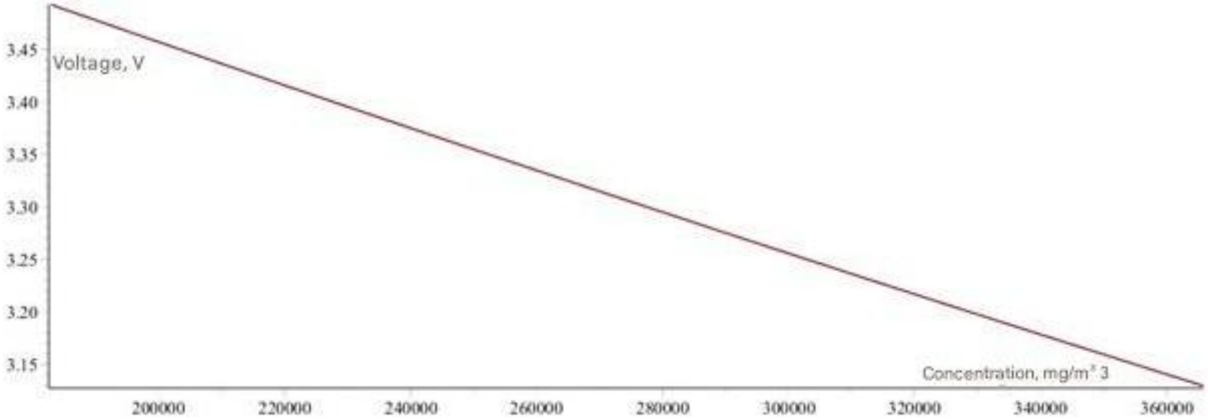

Fig. 2.13 . Voltage-concentration dependence (working range)

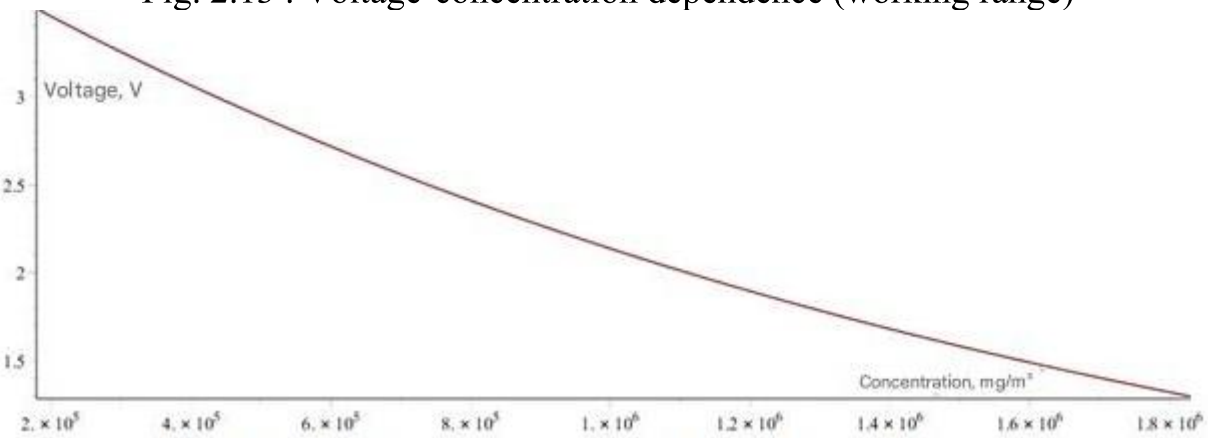

Fig. 2.14. Voltage-concentration dependence (full range)

The simulation was performed at an input intensity of 3 mW, a feedback resistance of 9.88 MΩ (series E 192), an integrated current sensitivity of the photodiode of 5.06 $\frac{A}{м^2}$, and an area of the photosensitive layer of the photodetector of 26 mm^2.

Fig. 2.15. presents the factors that lead to a change in the voltage at the output of the optical sensor and, as a result, affect the value of the carbon dioxide concentration.

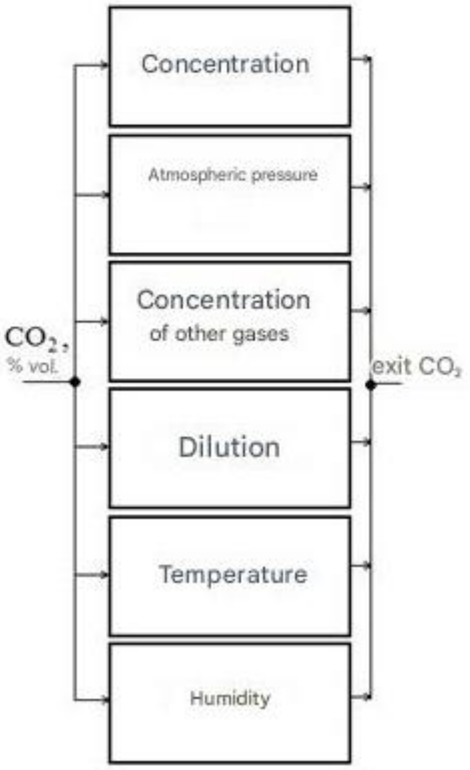

Fig. 2.15. Factors that lead to a change in the voltage at the output of an optical sensor

Considering that the controlled parameter is not only the CO $_{2 \text{ concentration itself}}$, but also other factors, which are also arguments in the mathematical model of radiation transfer into the gas environment, they should be considered separately.

A generalized structural diagram of the temperature and rarefaction measuring channel is presented in Fig. 2.16.

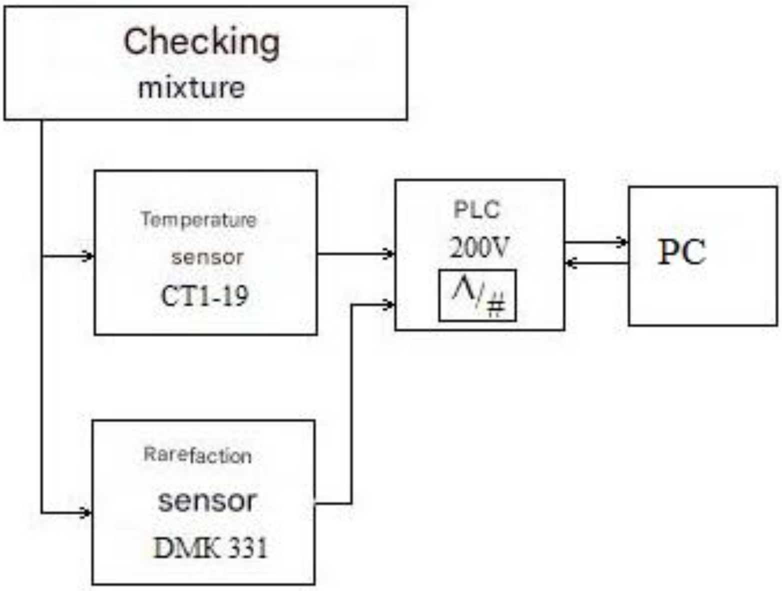

Fig. 2. 16. Generalized structural diagram of the temperature and rarefaction measuring channel

Temperature sensor. Accurate temperature measurement is critically important when monitoring gas concentrations because the physical properties of gases are closely tied to temperature conditions. As temperature changes, so do the volume, pressure, and density of gases, which directly affect the readings recorded by sensors or analyzers.

Most gas analyzers operate based on physical or chemical processes that depend on temperature. For instance, the rate of molecular diffusion, reactivity, or even the optical properties of gases can change significantly with temperature. If these changes are not taken into account, the measurements will be inaccurate, potentially leading to false assessments of concentration levels.

In industrial environments, precision in measuring gas concentrations is vital for worker safety, equipment protection, and compliance with environmental regulations. Exceeding permissible levels, even slightly, can pose risks of explosions, poisoning, or serious environmental damage.

In scientific research, temperature control ensures the repeatability of experiments. If temperature conditions are unstable or improperly accounted for, comparing results becomes impossible, which undermines the reliability of the entire study.

Thus, accurate temperature measurement is not just a technical requirement, but a foundation for reliability, safety, and scientific validity when working with gases.

After analyzing modern means of measuring temperature under given conditions [42], an additional temperature measurement channel was introduced into the device based on the thermoresistive industrial sensor (TRD) ST1-19 - a semiconductor resistor with a nonlinear current-voltage characteristic, a distinctive feature of which is a sharply pronounced temperature dependence of electrical resistance. The sensor has high sensitivity, stability and accuracy (± 0. 1 ^{0} C), display variation (±0. 0 1 ^{0} C), a wide measurement range (-60–300 ^{0} C). The resistance of the sensor decreases with increasing temperature, that is, it is a thermistor with a negative temperature coefficient of resistance. Depending on the temperature of the gas mixture, the thermistor has an electrical resistance that is related to the temperature by a nonlinear function, which is described by the Steinhardt Hart formula (parametric identification method) [33, 34, 35, 36].

$$T = \frac{1}{C_0 + C_1 \cdot \ln R + C_2 \cdot (\ln R)^3}, \tag{2.40}$$

where T is the temperature acting on the turbofan; R is the resistance of the turbofan; $C_{1,2,3}$ are coefficients that are selected under the condition of the best approximation to the obtained experimental dependence.

In our case, the ST1-19 type turbofan has a nonlinear “resistance-temperature” dependence, which was obtained experimentally by using reference measuring transducers with accuracy class 0.2.

The graph of the experimental dependence “resistance-temperature” of the ST1-19 type turbojet engine is presented in Fig. 2.17.

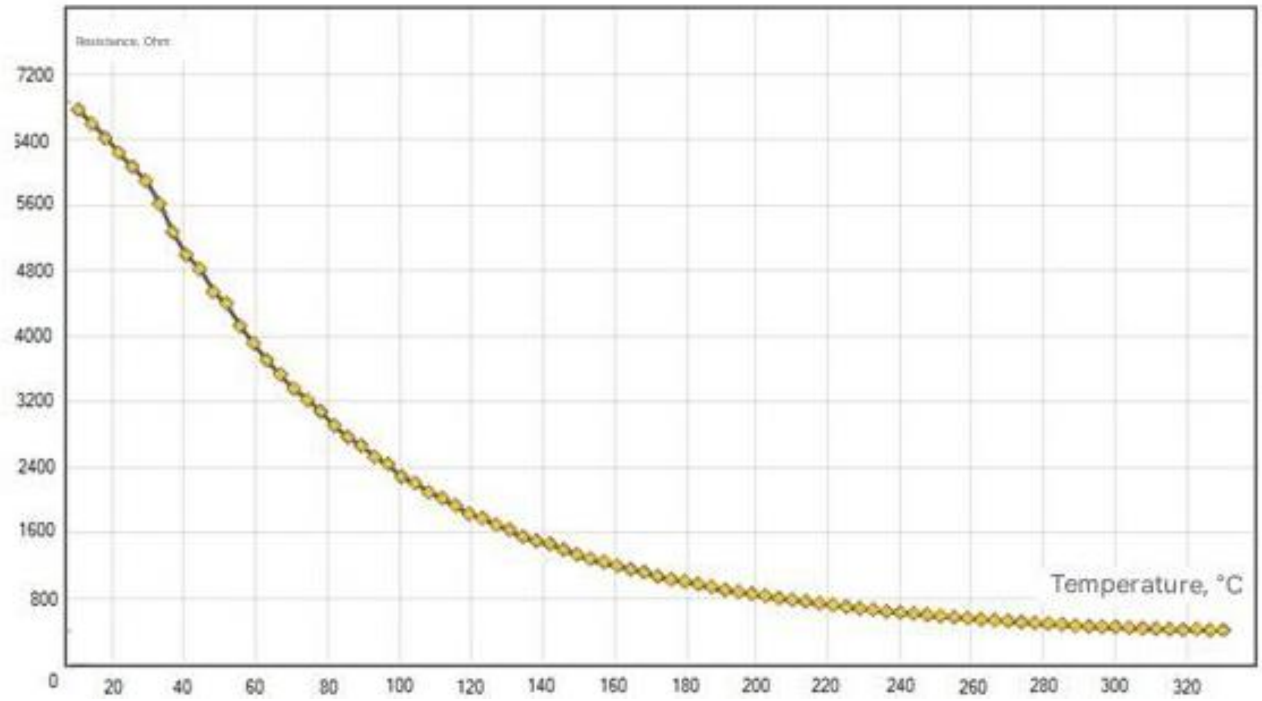

Fig. 2.17. Dependence of the resistance of the ST1-19 turbojet engine on temperature

The analytical dependence has the form

$$T = \frac{1}{0.18 - 0.056 \cdot \ln R + 0.0006 \cdot (\ln R)^3}\,. \qquad (2.41)$$

The dependence of the change in the temperature of the gas mixture on time is presented in Fig. 2.18 [5] (measurements were carried out within $2{,}4 \cdot 10^6$ seconds during operation of the DE-25-14 GM boiler).

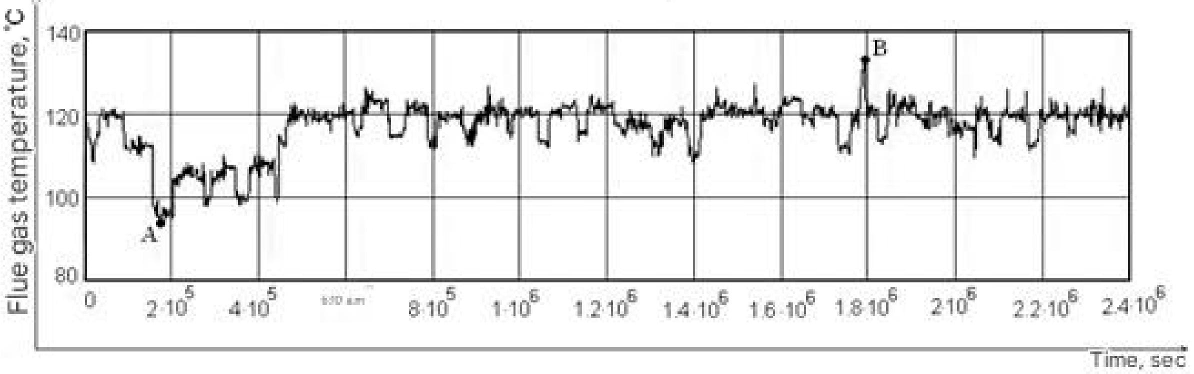

Fig. 2.18. Change in temperature of the gas mixture, that came out of the furnace, in time

The extreme points A and B were determined on the obtained dependence. Using an experimental setup [6] , which includes a cooler and a heater, with the help of which the gas entering the optical sensor is heated, cooled, and maintained at a given temperature.

The voltage at the output of the temperature sensor has the following analytical dependence

$$U_T = 12.5 \cdot 10^{-3} \cdot T + 0.5 . \tag{2.42}$$

The dependence of the voltage at the sensor output on temperature is presented in Fig. 2.19

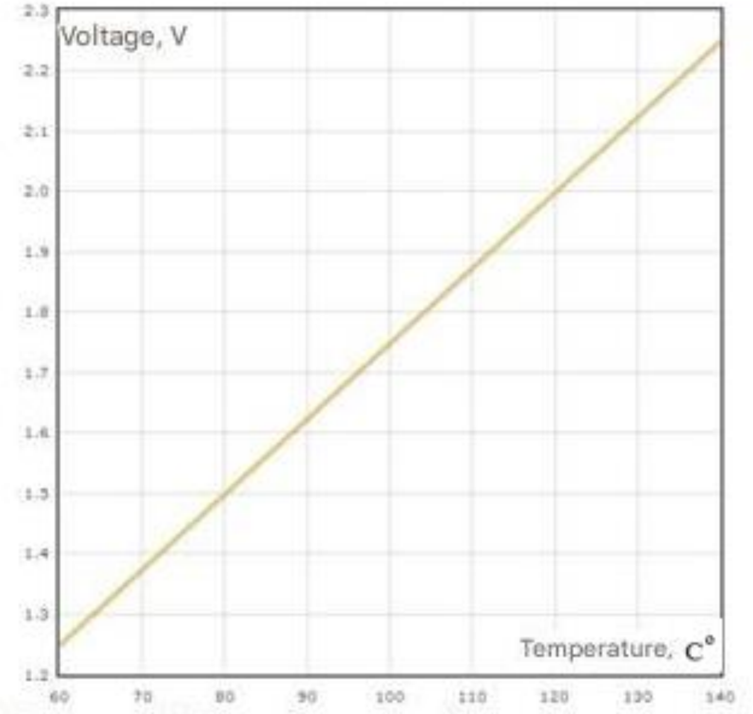

Fig. 2.19. Dependence of the voltage at the sensor output on temperature

The voltage at the sensor output will be a function of temperature and the ADC code has the form

$$N_T = \frac{U_T}{U_0} \cdot 2^n , \tag{2.43}$$

where N_T is the ADC output code and the temperature sensor , U_T is the voltage value at the temperature sensor output , U_0 is the voltage of the reference power supply, n is the ADC bit depth.

Then the ADC code at the output of the temperature sensor (with a PLC bit depth of 12 and a reference voltage of 5.5 V)

$$N_T = \frac{\dfrac{12.5 \cdot 10^{-3}}{C_0 + C_1 \cdot \ln R + C_2 \cdot (\ln R)^3} + 0.5}{5.5} \cdot 2^{12}. \tag{2.44}$$

The dependence of the ADC code at the sensor output on temperature is presented in Fig. 2.20

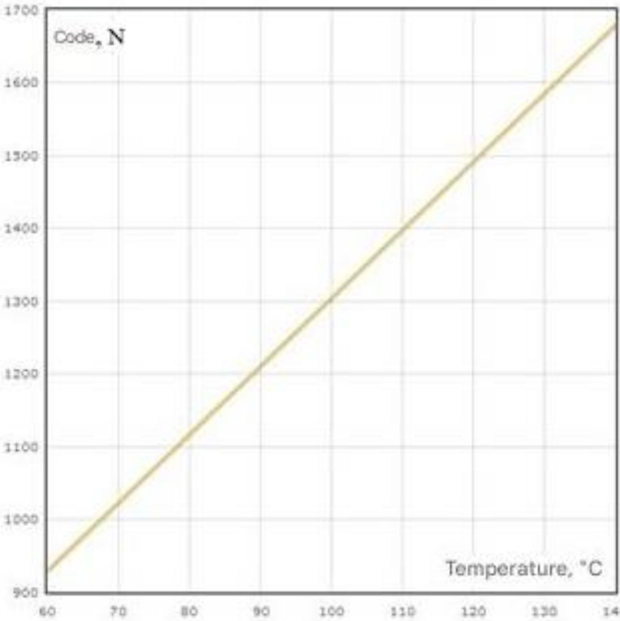

Fig. 2.20. Dependence of the ADC code at the sensor output on temperature

When measuring the temperature of a gas flow over time, the receiver may not have time to monitor the change in this temperature due to a certain value of the thermal inertia index, which depends on the geometric shape and dimensions of the sensing element, the heat capacity and density of the material from which the sensing element is made, as well as the heat transfer coefficient between the flow and the receiver [41]. If the transient operating mode of the VP is too inertial and significantly affects the value of the total error of the measuring channel (device), you can use the work [42] , where methods for measuring rapidly changing temperatures of gas flows by introducing corrections into the readings of inertial temperature receivers are considered and the methodology for conducting such measurements is described.

Vacuum sensor. Knowing the pressure value is fundamentally important when measuring gas concentrations because pressure directly influences the behavior and characteristics of gases. According to the ideal gas law (PV=nRT), the amount of gas in a given volume is proportional to its pressure. Therefore, any change in pressure will cause a change in gas concentration if temperature and volume remain constant.

In practical applications, gas concentration is often expressed in terms of either volume (e.g., parts per million, ppm) or mass per unit volume. Since gases are compressible, their volume can vary significantly with pressure. If pressure increases, gas molecules are packed more densely, effectively increasing the concentration. Conversely, a drop in pressure results in fewer gas molecules in a given volume, reducing the measured concentration.

Many types of gas sensors and analyzers are sensitive to pressure changes. Without proper pressure compensation, sensor readings may become inaccurate. For example, infrared sensors, electrochemical cells, and photoionization detectors all rely on the density of gas molecules to produce an output. If the pressure deviates from the expected value, the sensor may under- or overestimate the actual concentration.

In safety-critical environments, such as chemical plants, oil refineries, or confined spaces, inaccurate readings due to pressure fluctuations can lead to serious consequences. Undetected gas leaks, incorrect alarm thresholds, or failure to meet regulatory standards can pose risks to human health and the environment.

Moreover, in scientific research and industrial quality control, consistent and reliable gas measurement is essential for reproducibility and process optimization. Pressure readings allow for proper calibration of instruments and ensure that comparisons between datasets are meaningful and accurate.

Finally, many international standards and regulatory frameworks require gas measurements to be normalized to standard temperature and pressure (STP) conditions. This normalization is only possible if the actual pressure at the time of measurement is known.

In conclusion, accurate knowledge of pressure is a crucial parameter in gas concentration measurement. It ensures the reliability of results, the safety of operations, and the compliance with scientific and regulatory standards.

A BD sensor was used to measure vacuum pressure. sensors DM K 331 [9] is an industrial sensor, the feature of which is the ability to work in an aggressive environment. Measurement range 5-120kPa. Relative error no more than 0.25%. The sensor has a linear dependence of the input and output signals. The conversion equation has the form:

$$U_P = 3.33 \cdot 10^{-5} \cdot P_{vacum} + 0.99 \, , \tag{2.45}$$

where U_P – voltage at the sensor output.

The dependence of the voltage at the sensor output on the pressure is presented in Fig. 2.21

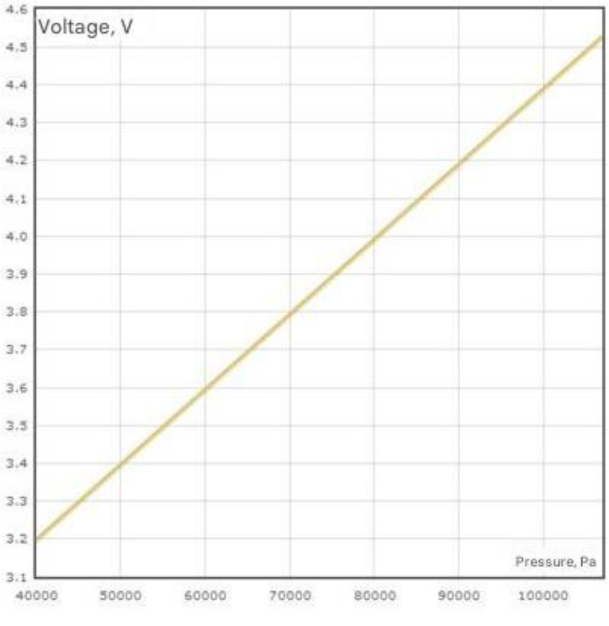

Fig. 2.21. Dependence of the voltage at the sensor output on the pressure

Taking into account the signal conversion in the ADC, the general equation will be:

$$N_P = \frac{U_P}{U_0} \cdot 2^n = \frac{3.33 \cdot 10^{-5} \cdot P_p + 0.99}{5.5} \cdot 2^{12} \tag{2.46}$$

The dependence of the ADC code at the sensor output on pressure is presented in Fig. 2.22.

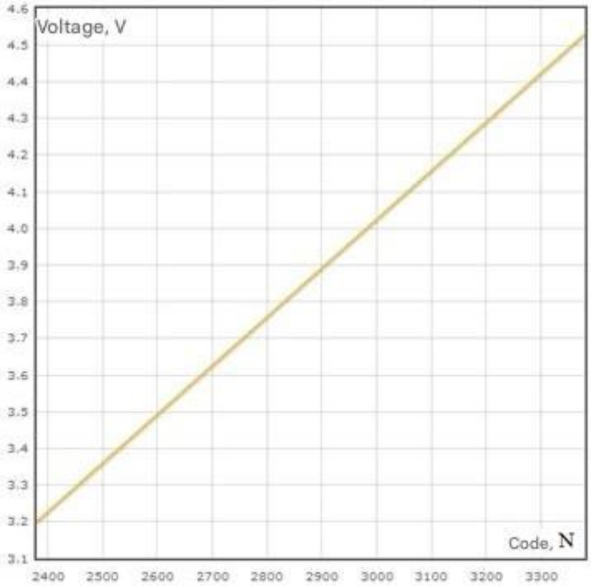

Fig. 2.22. Dependence of the ADC code at the sensor output on pressure

Humidity. Humidity, or the amount of water vapor present in the air, plays a critical role in the accurate measurement of gas concentrations. Water vapor can influence both the physical and chemical behavior of gases, and its presence must be accounted for to ensure precision and reliability in gas analysis.

One of the key reasons humidity is important is that it affects the density and composition of the gas mixture. When water vapor is present, it displaces other gas molecules in a given volume, thereby reducing the partial pressures of those gases. This is particularly significant in environments where measurements are reported on a dry basis (excluding water vapor) or on a wet basis (including water vapor). Without knowing the humidity level, it's impossible to correctly convert between these two common reporting methods.

Humidity also directly impacts the performance of many gas sensors. For example, electrochemical and metal oxide sensors can absorb water molecules, which may alter their sensitivity and response time. In some cases, high humidity can cause condensation, which interferes with sensor function or even damages sensitive components. On the other hand, low humidity may cause sensor drift or a reduction in accuracy over time.

In certain industrial and environmental monitoring applications, humidity can react with target gases or with the materials in the system, leading to chemical interference or false readings. For instance, high humidity levels can cause the formation of corrosive substances when mixed with gases like sulfur dioxide or nitrogen oxides.

Moreover, scientific and regulatory measurements often require corrections for humidity. Without accounting for the water vapor content, results can be misleading or non-compliant with established standards, such as those set by environmental protection agencies or occupational safety bodies.

Finally, consistent humidity control ensures comparability of measurements over time and between different locations. Whether in research, process control, or air quality monitoring, understanding and adjusting for humidity is essential for trustworthy data.

In summary, monitoring humidity is essential for accurate gas concentration measurement, sensor performance, data comparability, and regulatory compliance.

In works [44, 45], humidity analyzers of gas mixtures were developed. Based on experimental studies, it was determined that the analyzer meets the following requirements: fast response, no influence of aggressive impurities. In the classical case, the problem of taking into account the humidity factor of gases is solved by introducing an additional measuring channel into the control device. The signal at the output of the humidity channel determines the correction to the CO_2 concentration readings. However, given that the work involves the task of developing methods for compensating for the influence of influencing gases, including water vapor, the problem of humidity compensation is solved by introducing a reference optical channel (discussed in detail in section 2.7).

Dustiness. Dustiness, or the presence of airborne particulate matter, is a crucial factor to consider when measuring gas concentrations. While gas analyzers are designed to detect specific gaseous compounds, the presence of dust can interfere with these measurements in various ways, potentially compromising accuracy, safety, and reliability.

First, dust particles can physically obstruct or scatter light in optical-based sensors, such as infrared or laser-based analyzers. These sensors often rely on the unobstructed passage of light through a gas sample to detect specific absorption wavelengths. When dust is present, it can cause scattering or attenuation of the light beam, leading to distorted readings or signal loss.

Second, dust can settle on or within the sensor components over time, especially in environments with poor air filtration. This buildup may degrade the sensor’s performance, slow down response time, or cause calibration drift. In long-term use, such contamination might require frequent maintenance or replacement of sensitive parts, increasing operational costs.

Third, some gas measurement techniques involve chemical reactions at the sensor surface. Dust particles can coat these reactive surfaces, reducing their sensitivity or altering the reaction pathways. In some cases, dust can also carry moisture or other reactive contaminants, introducing unexpected chemical interferences that skew results.

In industrial environments, high dust levels often coexist with hazardous gases. Failing to account for dustiness can lead to underestimation of gas concentrations, potentially putting workers at risk due to a false sense of safety. In environmental monitoring, ignoring dust levels can affect air quality indices and compliance with legal regulations, particularly when particulate matter is itself a pollutant of concern (e.g., PM2.5 or PM10).

Moreover, for accurate comparisons over time or between different locations, measurement conditions — including dust levels — must be consistent or properly corrected. Dustiness can vary greatly between urban, rural, and industrial settings, and without compensation, gas concentration data may be misleading or incomparable.

In conclusion, dustiness is more than just a nuisance — it’s a key environmental factor that can significantly impact gas concentration measurements. Accounting for it ensures accurate data, reduces equipment wear, and supports safe and compliant operations.

After studying the effect of dustiness on the performance of optical sensors in [13], an engineering decision was made to build a means of controlling the concentration of gas components with an open optical channel (discussed in detail in section 3).

Based on 2.33, we write the Bouguer-Lambert-Beer law in the form

$$U(C,\lambda,I_0)=U_0(I_0,\lambda)\cdot\exp[-\alpha(\lambda)\cdot L\cdot C] \tag{2.47}$$

A device that converts the input value C into the measured value $U\,(\,I\,C\,,\,\lambda\,)$, is a measuring transducer. In a gas composition control device, the function of the measuring transducer is performed by an optical sensor.

In recent years, optical sensors have been built on the basis of light-emitting diodes and photodiodes [20], which allow significant improvements to be made to the sensor design: to abandon mechanical modulators, interference filters, reduce power consumption and dimensions. Further prospects for improving IR gas analyzers are associated with the creation of a new, more efficient element base for gas sensors, primarily sources and receivers of IR radiation. The block diagram of the developed optical sensor is presented in Fig. 2.23.

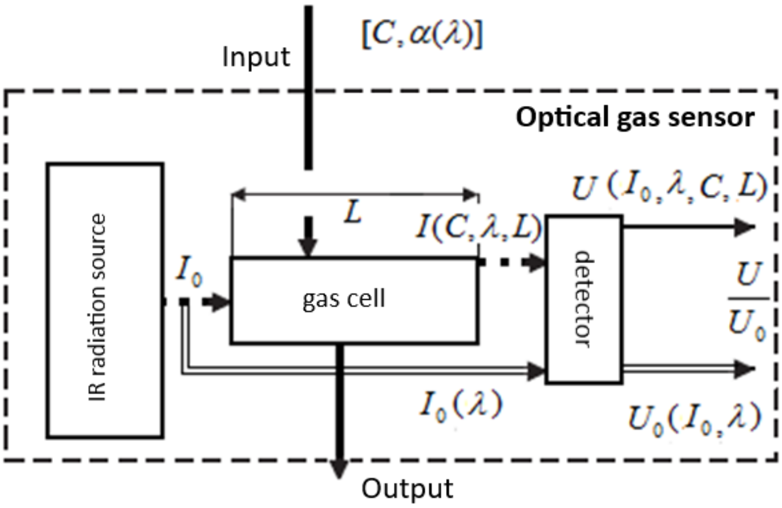

Fig. 2.23. Block diagram of the developed optical gas sensor

As the output signal of the optical sensor, we will present the radiation transmittance in the cell with gas

$$k_{np}(C,L,\alpha(\lambda)) = \frac{U(I_0,\lambda,C,L)}{U_0(I_0,\lambda)}. \tag{2.48}$$

When using LED and PD with spectral characteristics that overlap a certain frequency band $\lambda = \lambda_2 - \lambda_1$. The shift of the spectral characteristics of the radiation source and receiver due to changes in temperature and pressure is inherent in all LED and PD. To assess the influence of temperature and pressure acting on the optical sensor and, as a result, on the gas concentration value, we introduce the parameters T and P into the functions of the spectral characteristics of the source and receiver of IR radiation. The photodetector measures the integral signal and the transfer function of the optical sensor is described by the integral expression

$$k_{np}(C,L,P,T) = \frac{\int_{\lambda_1}^{\lambda_2} S_{PhD}(\lambda,T,P)\cdot I_{LED}(\lambda,T,P)\cdot \exp[-\alpha(\lambda)\cdot L\cdot C]d\lambda}{\int_{\lambda_1}^{\lambda_2} S_{PhD}(\lambda,T,P)\cdot I_{LED}(\lambda,T,P)d\lambda}, \tag{2.49}$$

where $S_{PhD}(\lambda, T)$ is the spectral sensitivity of the photodetector, $I_{LED}(\lambda, T)$ is the spectral power of the source, $\alpha(\lambda)$ is the spectrum of the gas absorption coefficient, L is the length of the optical path (the length of the interaction of radiation with the gas).

Previous studies have shown that to increase sensitivity, it is necessary to narrow the width of the emission spectrum [19]. To increase the sensitivity of an optical gas sensor, we will solve the following problems:

- to improve the optical part of the gas control device by introducing a filter into its composition;
- to analyze the effect of the width of the source's radiation spectrum on the sensitivity and accuracy of an optical gas sensor.

To analyze ways to increase sensitivity, a study was conducted of the width of the spectral response of the power of the IR radiation source on the sensitivity of the optical gas sensor.

The characteristic of the LED is presented in Fig . 2.23. For an analytical description of the characteristic, we use the equation [10]:

$$S_C = S_0 \cdot \exp(-b^2{}_u \cdot (\lambda - \lambda_0)) = \frac{F_0}{\sqrt{\pi}} \cdot \frac{\ln 2}{\Delta\lambda_0} \cdot (\lambda - \lambda_0), \tag{2.50}$$

where S_0 is the spectral sensitivity of the radiation power, Φ_0 is the optical radiation power, λ_0 is the central wavelength of the optical characteristic, b_u is a coefficient that depends on the half-width of the spectral characteristic $\Delta\lambda_0$.

The optical signal at the output of the gas cell is presented in the form [18]:

$$S_{out}(\lambda, C_{\%}, l) = S_C(\lambda) \cdot k_k(\lambda, C_{\%}, l) \tag{2.51}$$

where k is the transmittance of the cell with the gas being analyzed.

The output signal of the radiation receiver can be written in the form [18]:

$$F_{outFD}(\lambda, C_{\%}, l) = \int_{\lambda_1}^{\lambda_2} S_{вux}(\lambda, C_{\%}, l) d\lambda, \tag{2.52}$$

The information parameter of an optical gas sensor is the change in intensity after infrared radiation passes through a gas sample.

$$D = \frac{F_{FD}}{F_C} = \frac{\int_{\lambda_1}^{\lambda_2} S_{out}(\lambda, C_{\%}, l)d\lambda}{\int_{\lambda_1}^{\lambda_2} S_{out}(\lambda, l)d\lambda}, \tag{2.53}$$

Using the developed mathematical model of the CO_2 . The dependence of D on % $_{vol}$ was obtained . The dependence of the information parameter of the optical gas sensor on the concentration of carbon dioxide is presented in Fig. 2.24.

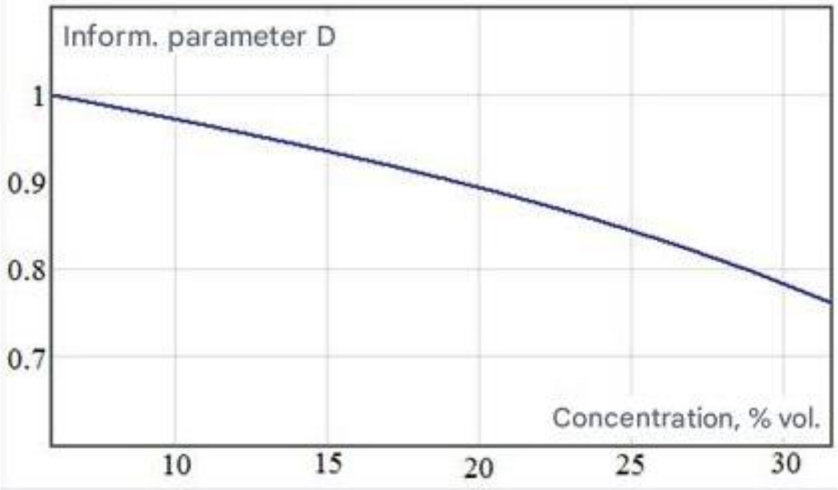

Fig. 2.24. Dependence of the information parameter of an optical gas sensor on the concentration of carbon dioxide

The sensitivity of a sensor is a characteristic that determines how the sensor's output changes in response to a change in the measured quantity. In simple terms, it is the sensor's ability to respond to small changes in the object being measured. The higher the sensitivity of a sensor, the more it responds to a small change in the parameter it is measuring.

Determining sensitivity helps you understand how accurately a sensor can measure changes in environmental parameters. If sensitivity is high, the sensor can detect even small changes, which is important for tasks where high accuracy is required, such as in medical devices or scientific experiments.

Knowing the sensitivity helps you choose the right sensor for a particular task. If you need to measure a very small change in a parameter, for example, detecting small fluctuations in temperature or pressure, you will need a sensor with high sensitivity. For tasks where stability at large values of the measured parameter is important, a sensor with lower sensitivity may be sufficient.

If a sensor has high sensitivity, it can produce a signal even when the variable changes by very small amounts. However, excessive sensitivity can also be a disadvantage, as the sensor can react to noise or background signals, which reduces the accuracy of the measurement. Determining sensitivity helps to understand whether the sensor is able to provide the desired balance between sensitivity and stability.

Knowing the sensitivity of a sensor allows you to better tune your instrument or system for the best results. For example, when processing signals, it is important to consider the sensitivity of the sensor to avoid skewing the results due to readings that are too high or too low.

Sensitivity determines the minimum amount of change in a parameter that a sensor can detect. This is important for systems such as detectors or security systems, where it is important to detect the smallest changes to prevent potentially dangerous situations.

Thus, sensor sensitivity is an important parameter that helps assess how effectively a sensor can perform its functions in real-world conditions.

The sensitivity of the optical gas sensor was calculated using the formula

$$k_{led} = \frac{\Delta y C_{\%o.}}{\Delta C_{\%o.}} = -0.01 \frac{1}{\%_{o.}}. \qquad (2.54)$$

Based on the data obtained, we can conclude that the sensitivity of the optical gas sensor is quite high due to the selection of LEDs with a narrow emission spectrum.

It can also be concluded that the dependence of the information parameter on % has a certain nonlinearity. To obtain the most linear dependence, an optical filter was used, which emits radiation in the wavelength range of 40-60 nm. The dependence of D on % with and without the use of an optical filter is presented in Figure 2.25.

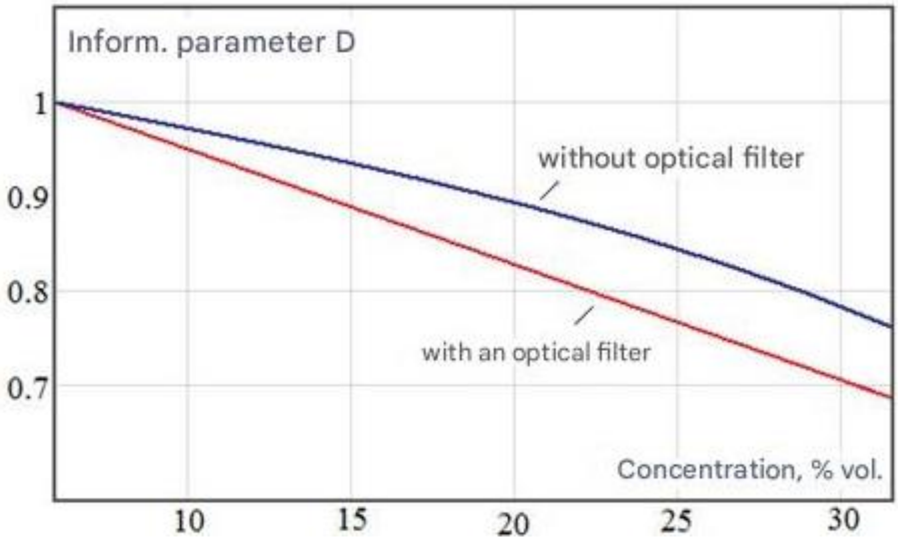

Fig. 2.25. Dependence of the information parameter of an optical gas sensor on the concentration of carbon dioxide with an optical filter, without an optical filter

Sensitivity of optical gas sensor with filter

$$k_{led} = \frac{\Delta y C_{\%o.}}{\Delta C_{\%o.}} = -0.011 \frac{1}{\%_{o.}}. \qquad (2.55)$$

Thus, the sensitivity of the optical gas sensor increases by approximately 10% and the dependence of D on id % is linear in nature throughout the operating range.

The dependence of the relative measurement error with and without an optical filter is presented in Fig. 2.26.

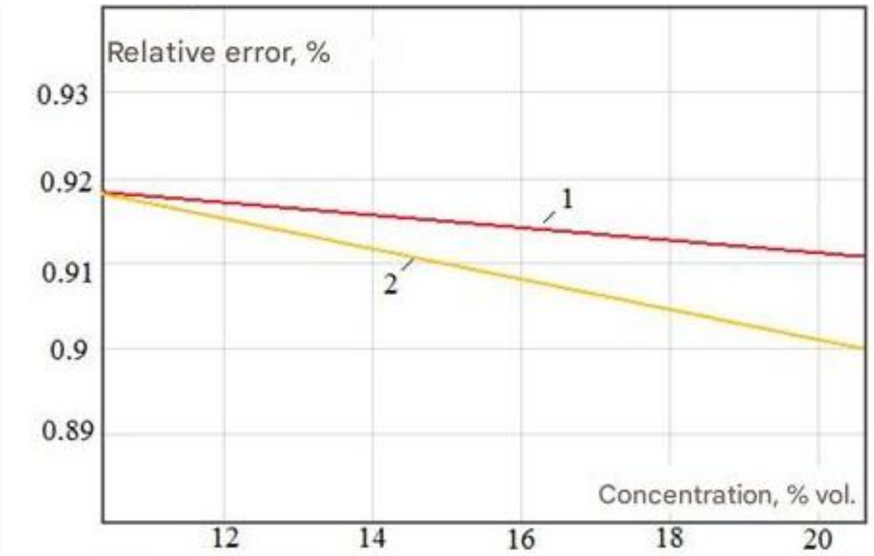

Fig. 2.26. Dependence of relative measurement error with optical filter, without optical filter

Thus, the relative error of the optical gas sensor is reduced to approximately 0.05% depending on the range.

From the analysis of the spectra, we can conclude that the absorption of carbon dioxide in the range of 1900 cm $^{-1}$ is almost zero. Then, as a source of IR radiation for the reference optical channel, we will use a laser with a working length *of* $\lambda=1900\ cm^{-1}$. It should be noted that in this range, the absorption of CO , NO_2 , SO_2 , CH_4 is from 10 $^{-21}$ to 10 $^{-23}$ cm/mol, which is several orders of magnitude higher than the absorption *of* CO_2 in this range.

The working and reference wavelengths and the absorption sensitivity are presented in Fig. 2.27.

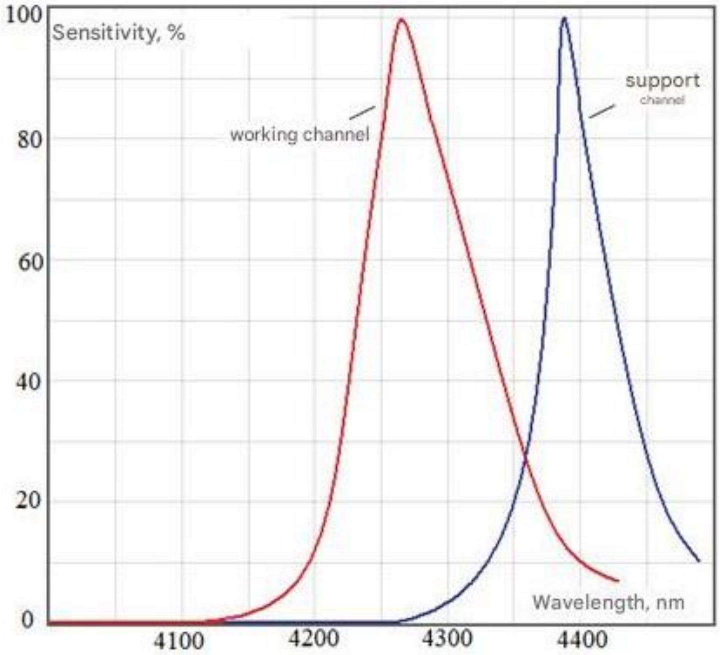

Fig. 2.27. Sensitivity dependence absorption by wavelength

Model of the influence of factors that lead to a change in the voltage at the output of an optical sensor. Fig. 2.28 presents the factors that lead to a change in the voltage at the output of an optical sensor.

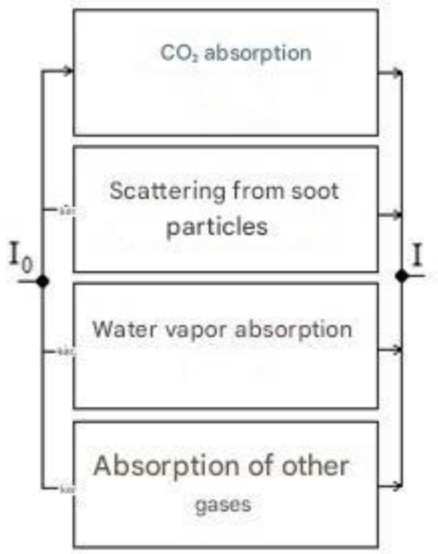

Fig. 2.28. Factors that lead to a change in the voltage at the output of an optical sensor

A non-specific factor affecting the output intensity of the radiation at the output of the optical path is scattering from soot particles, in contrast to absorption, which is described by the Bouguer-Lambert-Beer law. The flux is attenuated due to scattering of light when it hits soot particles. The problem is that soot particles are not uniform and of different sizes, and their number can change over time.

The total intensity of light scattered when hitting soot particles depends on the parameter ε

$$\varepsilon = 2 \cdot \pi \cdot r_{ч.с.}, \tag{2.56}$$

where r is the size of the soot particle.

If $\varepsilon < 1$ (soot size up to 0.1 μm), then the scattering intensity is proportional to $r^6_{ч.с.}$, when $\varepsilon = 1$ (soot size up to 1 μm) – the scattering intensity is proportional to $r^4_{ч.с.}$, when $\varepsilon > 1$ (soot size more than 1 μm) – the scattering intensity is proportional to $r^2_{ч.с.}$.

In the general case, the scattering intensity *I is* described by the Mie equation [17]

$$I_p = \frac{\lambda^2}{2 \cdot \pi^2 \cdot l^2} \cdot (i_1 + i_2), \tag{2.57}$$

where λ is the wavelength, l is the distance from the radiation source to the soot particle, *and* $_1$ *and* $_2$ are the intensity of the scattered light (polarized perpendicularly and parallel to the scattering area).

There are methods for experimentally estimating the average size of soot particles, but such methods are inaccurate because they depend on many factors of combustion processes and fuel composition.

Development of the method of additive-multiplicative compensation of influencing factors. Additive-multiplicative compensation of influencing factors is a method used to correct or eliminate the influence of various factors that can distort the results of measurements or estimates in various systems. This approach combines two main methods of correction - additive and multiplicative, which are used depending on how exactly the factors affect the measured value.

In additive compensation, influencing factors are added to or subtracted from the measured value. This is suitable for cases where the influence of the factor is constant or linear and can be represented as a constant correction. For example, if a sensor gives a constantly overestimated value due to temperature fluctuations, a fixed amount corresponding to this effect can be subtracted from the obtained results.

Multiplicative compensation is used when the influence of a factor is proportional to the measured value. In this case, the influence of factors is corrected by multiplying or dividing by a certain coefficient. This is typical for situations where changing factors change the value not by a constant amount, but proportionally to the result. For example, if the sensitivity of the sensor changes depending on environmental conditions (temperature, humidity), then to compensate for the influence of such changes, a coefficient can be used that is multiplied by the measured value to obtain a correct result.

Adaptive-multiplicative compensation is a powerful method for correcting measurement errors, especially in conditions where the influence of factors varies depending on the circumstances. It allows you to increase the accuracy of measurements and provide more reliable results when determining physical quantities.

In [19] , two variants of the algorithm for compensating destabilizing factors for the parameters of the optical converter – linear and nonlinear – were considered. Based on the research data, algorithms for additive and multiplicative compensation of influencing factors were developed, which are adapted to the control object.

Intensity at the output of the working optical channel according to the model

$$I_{out.p.к} = I_{LEDp.к} \cdot e^{k1} \cdot e^{k2} \cdot e^{k3} \tag{2.58}$$

where $k_{1} = k_{sol.}$, $k_{2} = k_{CO2\ absorption}$, $k_{3} = k_{ch.\ H2O + CO + SO2 + CH4 + NO2}$.

Output voltage of the working optical channel according to the model

$$U_{outp.к} = I_{LEDp.к} \cdot e^{k1} \cdot e^{k2} \cdot e^{k3} \cdot S_{I0p.к.} \cdot S_{p.к} \cdot R_{zzp.к.} \tag{2.59}$$

Intensity at the output of the reference optical channel according to the model

$$I_{out.o.к} = I_{LEDo.к} \cdot e^{k1} \cdot e^{k3} \tag{2.60}$$

Voltage at the output of the reference optical channel according to the model

$$U_{outo.к} = I_{LEDo.к.} \cdot e^{k1} \cdot e^{k3} \cdot S_{I0o.к.} \cdot S_{o.к} \cdot R_{zzo.к.} \tag{2.61}$$

Let's assume that

$$\begin{cases} S_{I0p.к.} \approx S_{I0o.к.} \\ S_{p.к} = S_{o.к} \\ R_{zzp.к.} = R_{zzo.к.} \end{cases} . \tag{2.62}$$

The additive compensation of influencing factors expressed in terms of intensity has the form

$$\begin{aligned} Add &= I_{out.o.к} - I_{out.p.к} = I_{LEDo.к} - \Delta I_{роз.LED.o.к} - \Delta I_{k3o.к} \\ &- I_{0LEDp.к} - \Delta I_{co_2p.к} - \Delta I_{k3p.к} - \Delta I_{роз.LED.p.к} = \Delta I_{co_2p.к} \end{aligned} \tag{2.63}$$

The additive compensation of influencing factors expressed in terms of voltage has the form

$$\begin{aligned} Add &= U_{out.o.к} - U_{out.p.к} = I_{LEDo.к.} \cdot e^{k_{роз.}} \cdot e^{k3} \cdot S_{10o.к.} \cdot S_{o.к} \cdot R_{zzo.к.} - \\ &- I_{LEDp.к} \cdot e^{k_{роз.}} \cdot e^{k_{погл.CO_2}} \cdot e^{k3} \cdot S_{10p.к.} \cdot S_{p.к} \cdot R_{zzp.к.} = \Delta U_{co_2 p.к} \end{aligned} \tag{2.64}$$

Multiplicative compensation of influencing factors expressed through intensity has the form

$$Mul = \frac{I_{out.p.к}}{I_{out.o.к}} = \frac{I_{LEDp.к} \cdot e^{k1} \cdot e^{k2} \cdot e^{k3}}{I_{LEDo.к} \cdot e^{k1} \cdot e^{k3}} = e^{k_{погл.CO_2}} \tag{2.65}$$

Multiplicative compensation of influencing factors expressed through voltage has the form

$$\begin{aligned} Mul &= \frac{U_{outp.к}}{U_{out.o.к}} = \\ &= \frac{I_{LEDp.к} \cdot e^{k1} \cdot e^{k2} \cdot e^{k3} \cdot S_{10p.к.} \cdot S_{p.к} \cdot R_{zzp.к.}}{I_{LEDo.к.} \cdot e^{k1} \cdot e^{k3} \cdot S_{10o.к.} \cdot S_{o.к} \cdot R_{zzo.к.}} = e^{k2} \end{aligned} \tag{2.66}$$

Based on equation 2.66

$$k_{nCO2} = \ln Mul \tag{2.67}$$

The graphical dependence of the Add and Mul parameters on the CO_2 concentration in the range from 0 to 10% $_{vol.}$ is presented in Fig. 2.29.

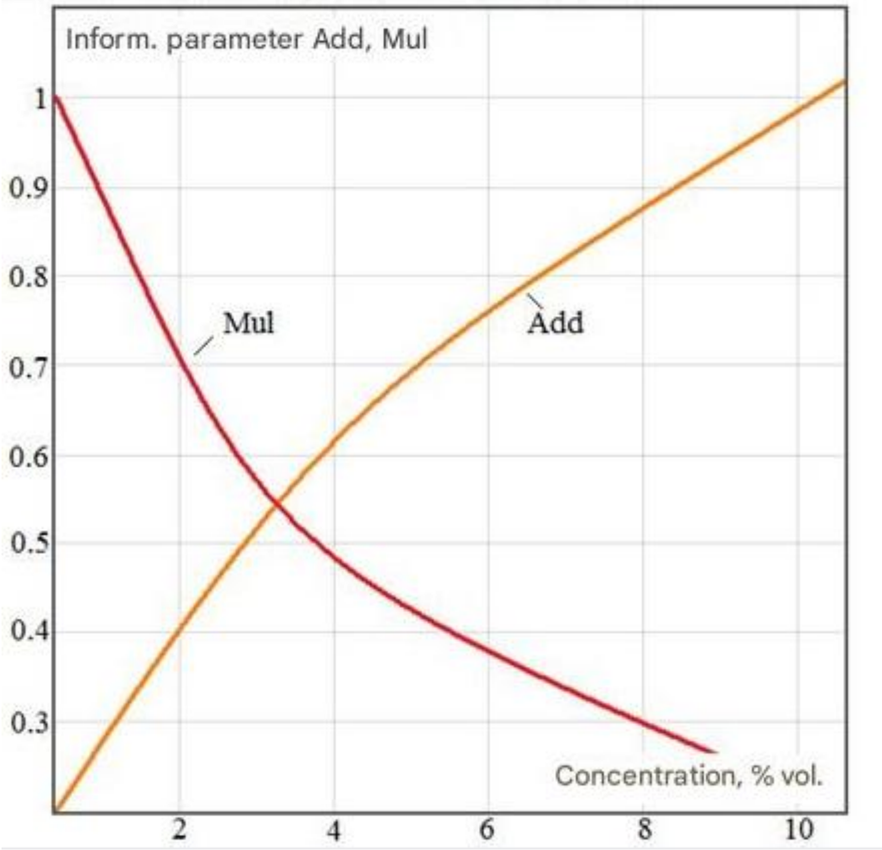

Fig. 2.29. Dependence of Add and Mul parameters on CO $_2$ concentration

Modeling of the parameters *Add* and *Mul* from the CO_2 concentration was performed based on experimental data with a step of 2.5% $_{vol}$. Theoretically, models

2.60 and 2.61 take into account the intensities at the output of the working and reference channels, but practically in these dependencies the voltage was used, i.e. $Add = U_{out.o.к} - U_{out.p.к} \Rightarrow Mul = \frac{U_{out.p.к}}{U_{out.o.к}}\ Mul = \frac{U_{out.p.к}}{U_{out.o.к}}$.

After analyzing the characteristic in Fig. 2.39, it was concluded that at a concentration of CO_2 up to 3% $_{\text{vol.}}$ it is more optimal to use an additive compensation algorithm, and for more than 3% $_{\text{vol.}}$ – a multiplicative one.

This section analyzes the physical and mathematical properties of the absorption of gases by infrared radiation.

An improved mathematical model of radiation transfer into the flue gas environment, which, unlike existing ones, takes into account the features of the control object, namely the pressure value in the general case is represented as atmospheric pressure and rarefaction, and the atmospheric pressure takes into account the height of the control device above sea level, which allowed to increase the reliability of control.

The method of measuring the concentration of carbon dioxide in gases in the main infrared region was further developed and a structural scheme with open measuring and compensation channels was developed for its implementation, which made it possible to reduce the number of controlled parameters (humidity, dustiness), which, unlike the known ones, differs in that the value of the carbon dioxide concentration is obtained based on the ratio of the intensities of the light fluxes that passed through the open measuring and compensation channels, and the ratio of the intensities of the light fluxes takes into account both additive and multiplicative correction factors depending on the measurement range.

The mathematical model of the photoelectric measuring converter of the intensity of the luminous flux has been improved, which takes into account the parasitic parameters of the constituent elements of the photodetector, and a transformation equation has been obtained that uniquely connects the output value - the value of the output voltage of the photodetector and the input value - the value of the intensity of the luminous flux, which has allowed to increase the reliability of control and the influence of the spectral width of the IR radiation receiver on the sensitivity of the optical channel of the gas sensor was investigated.

The results of the research presented in this section are published in the following works of the author [10].

CHAPTER 3

DEVELOPMENT OF A DEVICE FOR MONITORING CARBON DIOXIDE CONCENTRATION IN GASES AND EVALUATION OF ITS METROLOGICAL CHARACTERISTICS

The block diagram of a gas concentration control device describes the organization of the elements and subsystems that make up the measuring system. It provides an idea of the physical structure and components that interact with each other to make a measurement. The block diagram usually shows the sensors that determine the gas concentration in the environment. These can be different types of sensors, depending on the principle of their operation, for example, chemical, electrochemical or infrared sensors. After the sensors measure the physical quantities, the signal is transmitted to amplifiers to increase its amplitude so that it can be further processed. Computing units, such as microprocessors, analyze the signal, converting it into digital or analog form, which can be used to display the results. In addition, the block diagram includes input and output interfaces for convenient data transfer to the display, indicators or for connection to other systems. Also important are the elements that provide power and control of all subsystems.

The functional diagram focuses on the processes and functions that are performed in a gas concentration control device. It describes how the system processes information and makes measurements. First, sensors record physical changes that correlate with the gas concentration. After that, the signal coming from the sensors is processed by amplifiers and filters in preparation for further processing. The computing unit analyzes the received data, comparing them with reference values to determine the exact level of gas concentration. When the analysis is complete, the results are displayed through interfaces such as displays or indicators. Depending on the level of gas concentration, the system can activate alarms, transmit data to other devices, or make automatic corrections if the indicators exceed permissible limits.

The difference between a structural diagram and a functional diagram is that a structural diagram depicts the physical components of a system and their relationships, while a functional diagram focuses on describing the processes and interactions between the functions of different elements of the system during the execution of measurements and data processing. A structural diagram is important for understanding the hardware part of the system, while a functional diagram provides a clear picture of how the system works at the signal processing and function execution level. Both types of diagrams are important for developing effective and accurate means of monitoring gas concentrations.

A structural and functional diagram of a means of controlling the concentration of carbon dioxide in gases and an optical sensor in particular has been developed. Recommendations for the design of a means of measuring control of carbon dioxide in gases have been presented . The main metrological characteristics of the developed control means have been assessed.

The developed means of controlling the concentration of carbon dioxide in gases includes the following main structural components (Fig. 3.1):

- test gas mixture;
- radiation source;
- optical measuring transducer;
- radiation receiver;
- industrial logic controller
- ADC (built into PLC);
- MX (built into PLC);
- personal computer;
- pressure sensor ;
- temperature sensor .

Using a programmable logic controller (the integrated nodes of which are ADC and MX), multi-channel analog-to-digital conversion of measurement signals is carried out. Measurement signals are unified and come from industrial temperature and pressure sensors and an optical measuring converter. Using the RS -232 interface, data exchange between the PLC and a personal computer with the necessary software is ensured.

Fig. 3.1 presents a generalized structural diagram of a means of controlling the concentration of carbon dioxide in gases.

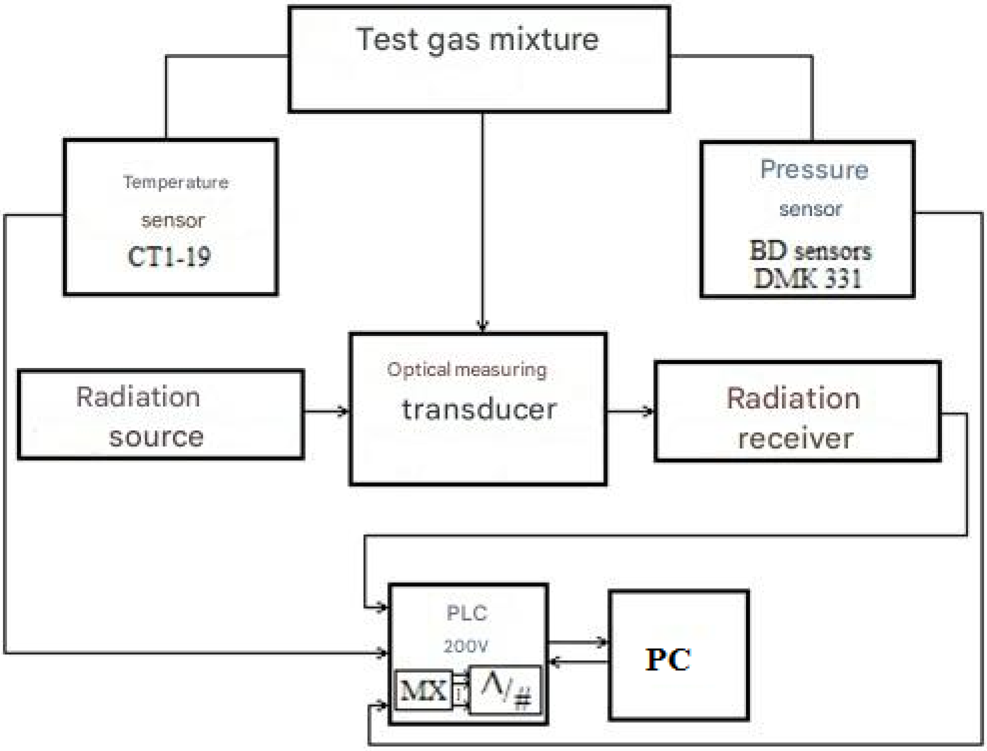

Fig. 3.1. Structural diagram of a means of controlling the concentration of carbon dioxide in gases

The functional units of the developed means of controlling the concentration of carbon dioxide in gases include (Fig. 3.2) :

1 – housing of the device for controlling the composition of carbon dioxide concentration in gases ;
2 – optical sensor housing ;
3 – gas sampling probe hose for pumping / pumping the sample into / from the control medium ;
4 – filter (from mechanical impurities) ;
5 – fans ;
6 – pressure sensor ;
7 – temperature sensor ;
8 – LED of the working channel ;
9 – FD of the working channel ;
10 – FD of the reference channel ;
11 – SVD of the reference channel ;
12 – board ;
13 – socket for connectors ;
14 – PLC with built-in ADC ;
15 – PC ;
16 – test gas mixture ;
17 – heater ;
18 – cooler ;
19 – alarm .

Fig. 3.2 shows a functional diagram of a means of controlling the concentration of carbon dioxide in gases.

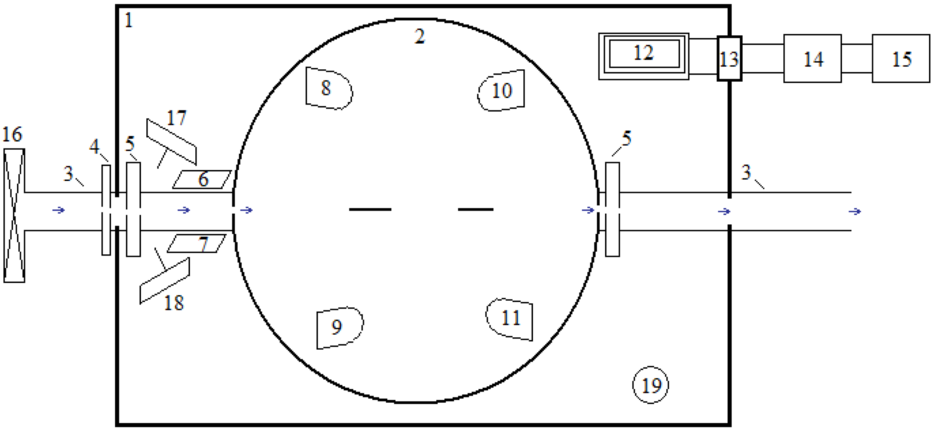

Fig. 3.2. Functional diagram of a means of controlling the concentration of carbon dioxide in gases

The means of controlling the concentration of carbon dioxide in gases works as follows: a sample with gas enters through a gas collection probe into the working and reference cuvettes located in parallel to each other. In parallel with the quantitative control of the concentration of carbon dioxide in gases, its temperature and vacuum pressure are measured by sensors. The signals from the sensors are fed to the PLC, which, in turn, processes them and the concentration value in % vol. is displayed to the operator on the PC. If the concentration of carbon dioxide in gases is outside the settings, an audible signal is triggered. Due to the fact that this sample of the control means is introduced into the laboratory practice, it is additionally equipped with a cooler-heater pair for forced change of the temperature parameters of the sample.

As was determined in the first section, in terms of their capabilities, optical methods of gas analysis surpass the electrochemical and catalytic methods used in this class of devices, providing high speed, selectivity, resistance to aggressive environments, and long service life.

In turn, there are different types of construction of the structural and functional organization of the optical gas sensors themselves.

Traditionally, IR analyzers use sensors based on heat sources and broadband radiation receivers together with narrowband (interference) filters. An example of such a structure is gas analytical systems (GAs), built on the principle of direct action [7] . The principle of operation is as follows - IR radiation from the source enters two cuvettes located next to each other and parallel to each other - working and comparative . The gas being analyzed is pumped through the working cuvette, and the comparative cuvette contains air free from this gas and forms a comparison channel (with a closed inlet and outlet). However, the disadvantage is the need to select a comparative cuvette for different types of boiler units, which does not allow adaptation of the gas composition control means. Therefore, the implementation of the working and reference channels is carried out on the principle that both cuvettes have an open inlet and outlet. The structural diagram of the reference and working optical channels is presented in Fig. 3.4.

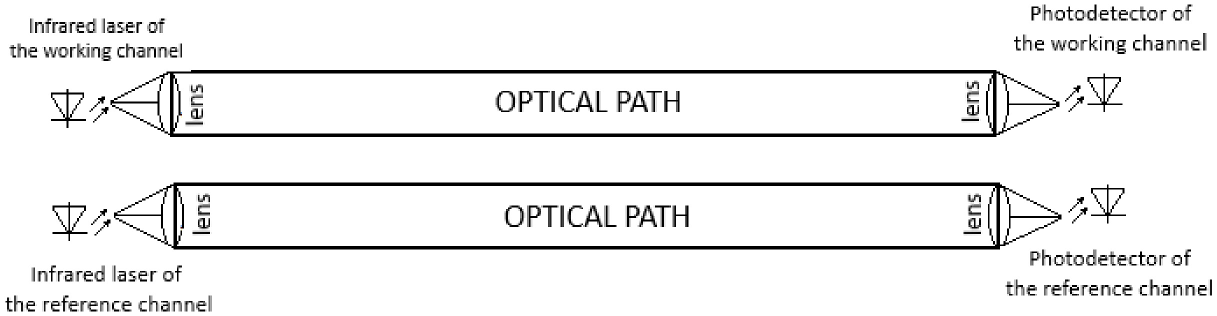

Fig. 3.4. Structural diagram of the reference and working optical channels

The cells are structurally identical, the only difference is in the operating wavelengths of the laser-photodiode pair.

To maintain the resource-saving operation mode of the boiler, it is necessary to ensure with high accuracy the optimal fuel-air ratio in the boiler, with the minimum possible excess air coefficient. To do this, on the one hand, depending on the amount of fuel supplied, it is necessary to supply the required amount of air to the boiler furnace, and on the other hand, to remove combustion products from it with a given intensity. This can be achieved using the following boiler control scheme : information from the gas analyzer (information about the composition of combustion products in the boiler furnace) is supplied to the PLC, which in turn controls the flow and outflow of air into the furnace (from the furnace) of the boiler within the normalized optimal limits. The control process is based on the presented models of material and heat balance of liquids and gas fractions of the boiler.

Input parameter stabilization unit (IPSU). The sample taken for gas mixture analysis directly from the flue pipe has a large “dispersion” of parameters, namely:

temperature, humidity, pressure, dustiness. If gas with unstabilized parameters is supplied directly to the measuring transducer, this will result in obtaining information about the composition of the flue gas with a large error at the output. Therefore, it is proposed to include an IPSU in the structure of the GS. The IPSU must meet the following requirements: high speed, effective and reliable cleaning from mechanical impurities, reduction to the required value of the mixture humidity, stabilization of temperature and pressure.

That is, thanks to the introduction of BSVP into the composition of the GS, the above-listed influencing factors are compensated. But there is an ambiguity: when the static component of the error decreases, the dynamic component increases (when the sample passes through BSVP (1)), and vice versa, when the dynamic component decreases, the static component increases (with an open optical channel (2)) [43].

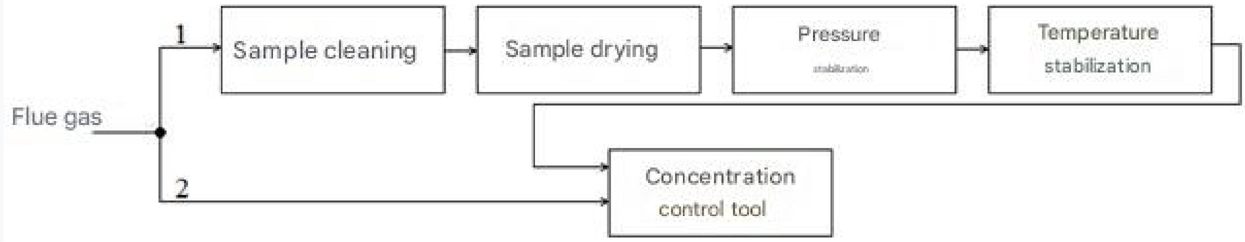

Fig. 3.5. Flue gas supply routes to the gas storage tank for its analysis

Indeed, the steady-state error is a static error. The presence of a transient process causes a dynamic error. The duration of the transient process for a given dynamic error is determined by the equation [31]

$$\Delta_D = k \cdot e^{-(\frac{t_{pp}}{\tau})}, \tag{3.1}$$

where t_{PP} – duration of the transition process; τ is the time constant; Δ_{DN} is the dynamic error of the measuring instrument; k is the transmission coefficient.

From the last equation, the duration of the transient process for a given dynamic error is determined by the formula

$$t_{ПП} = \tau \cdot \ln(\frac{k}{\Delta_D}). \tag{3.2}$$

Thus, in measuring instruments with an aperiodic transient process, which is described by a first-order transient, the dynamic error decreases with a decrease in the duration of the transient process.

The course of the transition process in the VP after changing the concentration of the gas The mixture is presented in Fig. 3.6. Transition characteristic $h(t)$ is constructed in the Scilab environment . The results of modeling the transient process with an open optical channel are presented in [14] , with a closed optical channel in [3] (optical gas analyzer GIAM-15M).

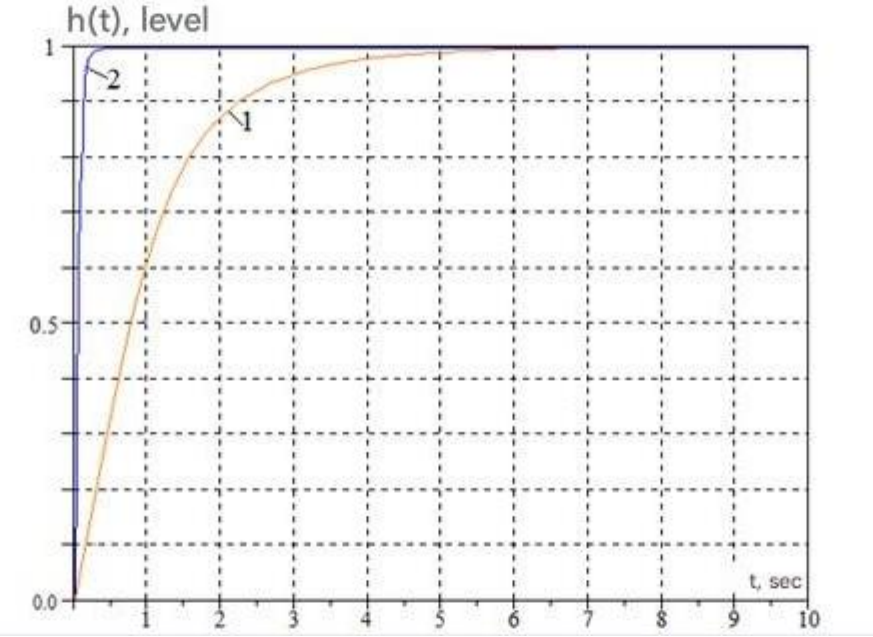

Fig. 3.6. Transient process in the VP with closed – 1 (open – 2) optical channel

At t ≈ from 0.0 to 3.0 – is the time spent on transporting the sample and is due to the inertia of the GS elements. At t ≈ from 0.0 to 0.1 s – is the time due to the inertia of the GS elements.

Therefore, there is a problem $\Delta_{DN1} > \Delta_{DN2}$, with $\Delta_{ST1} < \Delta_{ST2}$, and vice versa $\Delta_{DN1} < \Delta_{DN2}$, at $\Delta_{ST1} > \Delta_{ST2}$. The solution to this problem was started in section 2 by introducing additional measuring channels into the means of controlling the concentration of carbon dioxide in gases and will be continued in section 3.4 (through engineering solutions in the development of the structure of the optical sensor).

Measurement channel transformation equation . The measurement channel transformation equation describes the mathematical relationship between the input quantity (the physical parameter we want to measure) and the output signal of the measuring device. This equation reflects how the measurement channel (a collection of instruments, sensors, and electronic components) transforms the physical quantity we are measuring into a measured result.

Typically, a measurement channel has an input (e.g., temperature, pressure, velocity, voltage) and an output, which is a signal to be processed (e.g., the voltage at the output of a sensor or the reading of a digital device). The conversion equation describes this process of converting a physical parameter into an electrical or other type of signal that can be measured.

Mathematically, the measurement channel transformation equation usually has the form of a function that can be linear or nonlinear depending on the characteristics of the channel itself. Dependence of the output code N_x on voltage U_x

$$N_x = \frac{U_x}{U_0} \cdot 2^{n-1}, \tag{3.3}$$

where U_x - the voltage value at the sensor output at a given C; N_x - code value after analog-to-digital conversion; U_0 - reference voltage; n - ADC bit resolution.

Substituting equation (2.22) into equation (3.3) and the absolute value of the reference voltage, we obtain the equation of the measuring channel in terms of voltage

$$N_x = \frac{I_0 \cdot e^{\frac{\int_0^\infty k_s(\lambda)d\lambda}{\pi} \cdot \frac{\sigma}{\sigma^2+(\frac{1}{\lambda}-\frac{1}{\lambda_i})^2} \cdot \frac{-0{,}0083 \cdot T}{P_0 \cdot e^{-\frac{M_M \cdot g \cdot h}{R \cdot T}} - P_{p.}} \cdot \frac{C}{M} \cdot l} \cdot S_{I0} \cdot S \cdot R}{5.5} \cdot 2^{12}. \tag{3.4}$$

Graphical dependence of the source code N_x on the concentration C is presented in fig. 3.7 - 3.8.

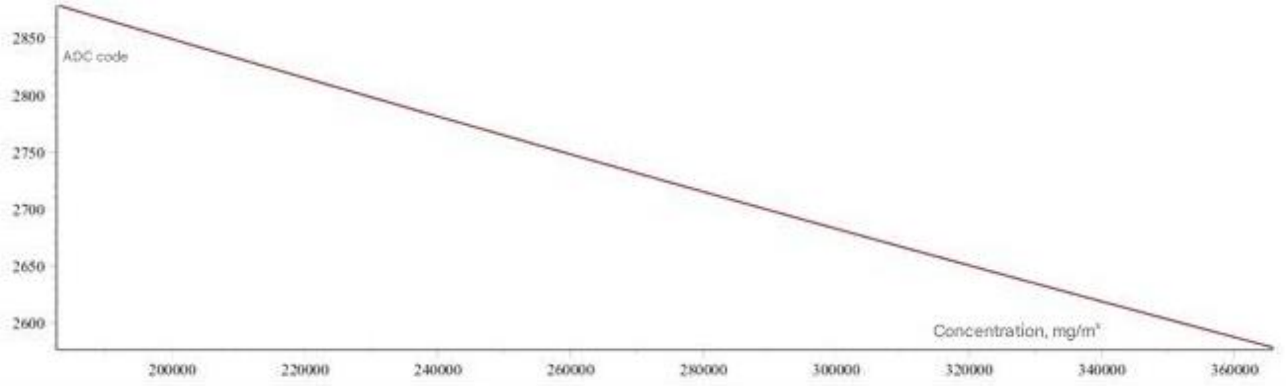

Fig. 3.7. Graphical representation of the equation of the measuring channel for the concentration of carbon dioxide in gases (in the operating range)

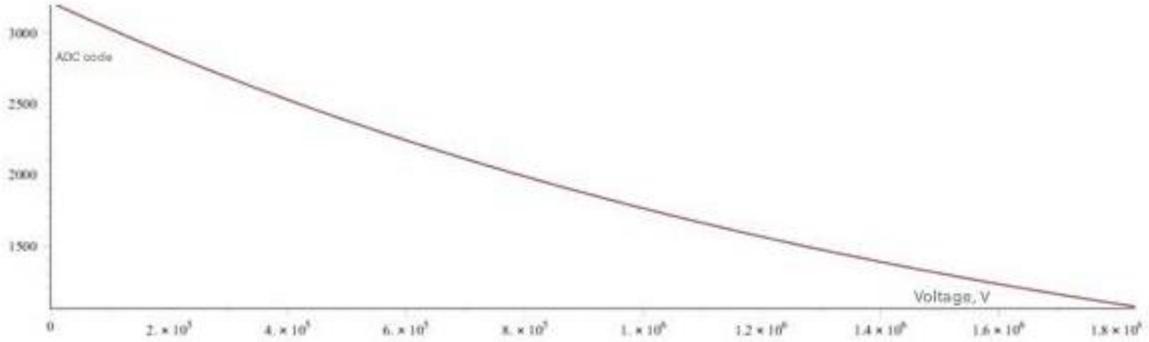

Fig. 3.8. Graphical representation of the equation of the measuring channel of carbon dioxide concentration in gases (in full range)

In turn, the radiation intensity at the output of the optical channel I_x is related to U_x the following relationship

$$I_0 = \frac{U_F}{e^{\frac{\int_0^\infty k_s(\lambda)d\lambda}{\pi} \cdot \frac{\sigma}{\sigma^2+(\frac{1}{\lambda}-\frac{1}{\lambda_i})^2} \cdot \frac{-0{,}0083 \cdot T}{P_0 \cdot e^{-\frac{M_M \cdot g \cdot h}{R \cdot T}} - P_{розр.}} \cdot \frac{C}{M} \cdot l} \cdot S_{I0} \cdot S \cdot R_{ZZ}}. \tag{3.5}$$

The dependence of the radiation intensity on the voltage (in the operating range of 10-20%) is presented in Fig. 3.9

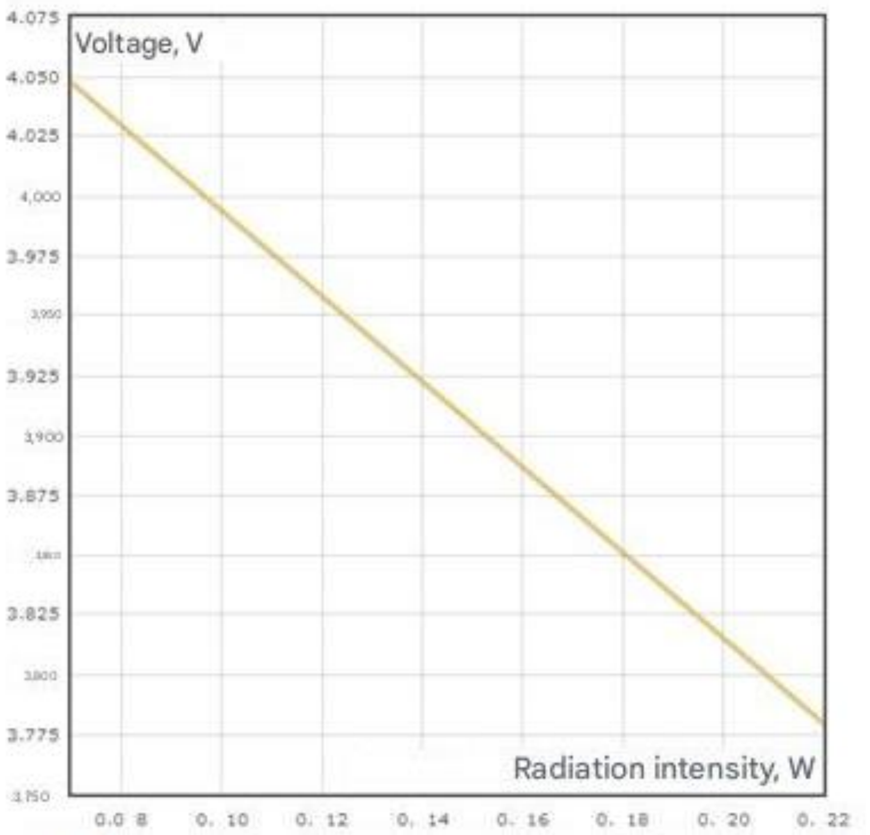

Fig. 3.9. Dependence of radiation intensity on voltage

The dependence of the radiation intensity on pressure and temperature is presented (at constant concentration) in Fig. 3.10.

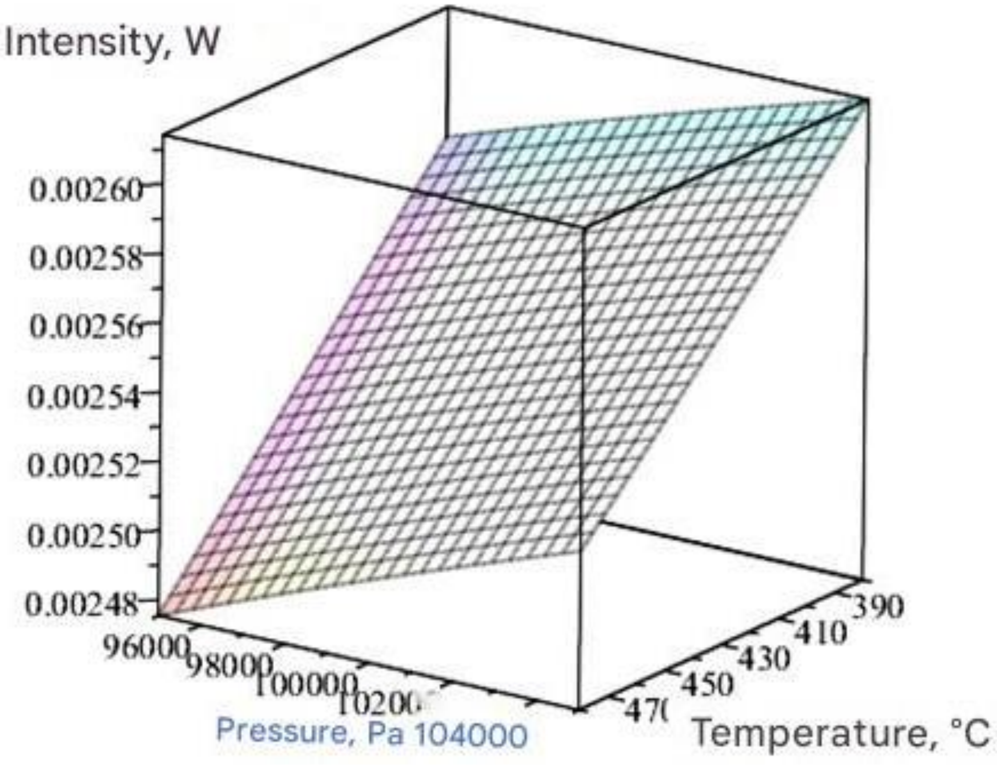

Fig. 3.10. The dependence of the radiation intensity on pressure and temperature is presented (at constant concentration)

The dependence of the voltage at the output of the optical sensor on pressure and temperature is presented (at constant concentration) in Fig. 3.11.

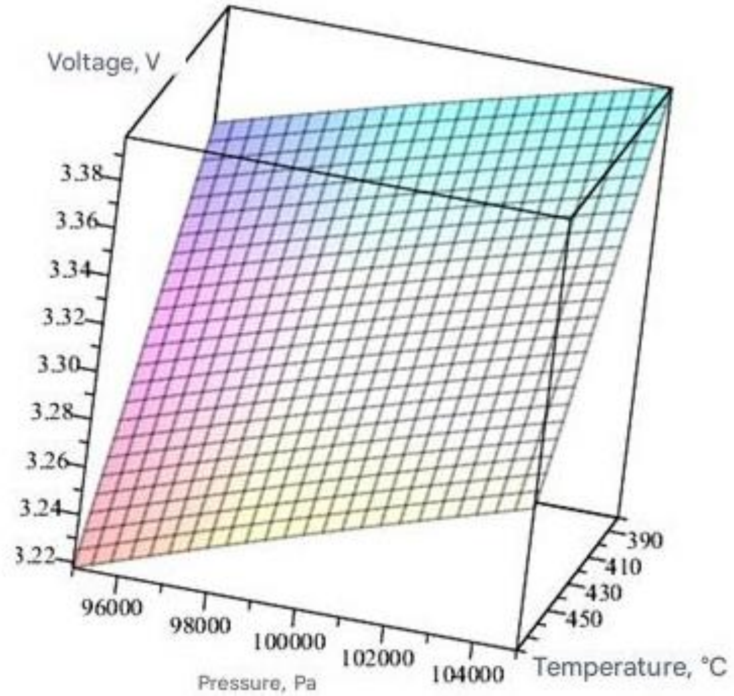

Fig. 3.11. The dependence of the voltage at the output of the optical sensor on pressure and temperature is presented (at constant concentration)

Decomposition of functional dependence into a Taylor series and study of the main static characteristics. The Taylor series expansion of a function and the study of basic static characteristics are important tools in mathematical analysis that allow us to study functions, their behavior, and properties. Let's consider them in more detail without using formulas.

The Taylor series expansion of a function is a way of representing a complex function as a sum of infinitesimal polynomial terms. It allows us to approximate the value of the function around a certain point, which is very useful in calculations where exact values of functions are difficult or impossible to calculate.

Let's imagine that we have a function that is difficult to calculate directly. Then we can use its approximation through a polynomial, in which each term depends on the derivative of the function at a certain point. The more terms of this polynomial we use, the more accurate the approximation will be. This approach allows us to obtain very good results, even if we do not have an exact expression for the function.

Taylor series expansion is often used to investigate complex functions or to approximate the values of functions for small changes in the argument. It allows you to replace complex functions with simpler polynomials that are easier to analyze and calculate.

Static characteristics of a function are properties that describe its behavior without regard to time (if the function varies over time) or without changes in its external parameters. These characteristics allow us to understand how the function behaves over certain sections or at certain points, and are used for stability analysis, optimization, and other aspects.

When we study a function, we are often interested in where it reaches its greatest or smallest values. The points at which a function reaches its maximum or minimum value are called extrema. To find such points, we need to understand where the function stops increasing and starts decreasing (or vice versa). This happens when the first derivative of the function is zero. If the second derivative of the function is positive at these points, then this is a point of minimum, and if it is negative, then this is a point of maximum.

Monotonicity of a function means that it either increases or decreases on certain sections. This helps to understand how the function changes on different intervals. If a function increases on a certain interval, this means that its values become larger as the argument increases. Conversely, if the function decreases, its values decrease. To determine the intervals of monotonicity, you need to consider the first derivative of the function: if it is positive, the function increases, if it is negative, it decreases.

An inflection point is a point on the graph of a function where it changes its curvature. This means that the function first curves in one direction and then begins to curve in the other. Such a point is important for understanding the behavior of the function because it indicates a change in the nature of its increase or decrease. To find inflection points, you need to analyze the second derivative of the function. If the second derivative is zero at a certain point, and the sign of the derivative changes around this point, then this is an inflection point.

An asymptote is a line that the graph of a function approaches but never reaches. There are different types of asymptotes: horizontal, vertical, and inclined. For example, a function may have a horizontal asymptote as its values approach a certain number as the argument goes to infinity. Asymptotes are often used to study the behavior of a function at large or small values of the argument, and to describe functions that do not have clear boundaries or discontinuities.

Continuity of a function means that its graph has no breaks or jumps. Discontinuities are points where the function changes abruptly. This is important because continuity usually indicates stable behavior of the function, while discontinuities may indicate physical or mathematical features that require further analysis. Examining the limit of a function at specific points helps to identify the locations of the breaks and establish the types of continuity.

The expansion of functions into Taylor series and the study of static characteristics have wide applications in science and technology. Taylor series allows to approximate complex functions to polynomials, which simplifies calculations in numerical methods and in models of physical processes, such as mechanics, electrodynamics or thermodynamics. The study of static characteristics allows to optimize systems and to understand their stable and unstable states, which is important for technical calculations, economic modeling and many other fields.

These mathematical methods make it possible not only to study functions in a theoretical context, but also to apply them to real problems and tasks that arise in various fields of science and technology.

The mathematical apparatus for studying static metrological characteristics is the use of the Taylor series expansion of the transformation function [31, 32] .

To estimate the errors of the measurement conversion , the method described in [14] was used. The concentration of carbon dioxide is expressed from the mathematical model of the measuring converter of the concentration of carbon dioxide in gases :

$$C = \frac{M \cdot \ln \dfrac{I_0}{U_F \cdot S_{I0} \cdot S \cdot R_{ZZ}}}{\dfrac{\int_0^{\infty} k_s(\lambda) d\lambda}{\pi} \cdot \dfrac{\sigma}{\sigma^2 + (\frac{1}{\lambda} - \frac{1}{\lambda_i})^2} \dfrac{0{,}0083 \cdot T}{P_0 \cdot e^{-\frac{M_M \cdot g \cdot h}{R \cdot T}} - P_{p.}} \cdot l}. \tag{3.6}$$

The measured and influential quantities of indirect measurement are presented in Figure 3. 12

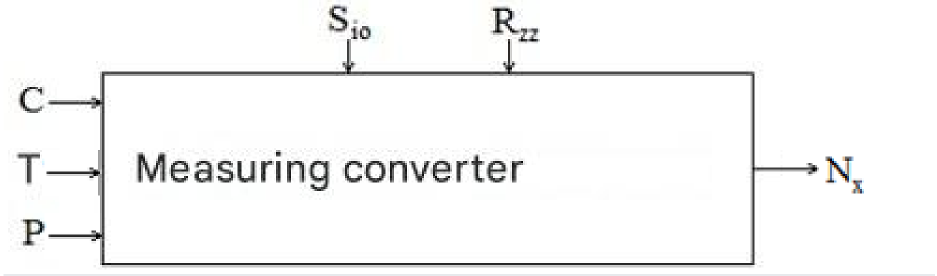

Fig. 3. 12. Representation of the measurement transformation

According to the representation of the measurement transformation, the transformation function has the form :

$$y = N_x = fun(\bar{x}, \bar{f}) = fun(C, T, P, S_{io}, R_{zz}), \tag{3. 7 }$$

where $\bar{x} = (C, T, P)$, $\bar{f} = (S_{io}, R_{zz})$.

Expanding 3. 7 in a Taylor series we get 3.9 and 3.9

$$y = fun(x_{1n}, x_{2n}, x_{3n}, f_{1n}, f_{2n}) + \sum_{i=1}^{3} \frac{\partial y}{\partial x_{i_\Phi}}(x_i - x_{in}) + \sum_{i=1}^{2} \frac{\partial y}{\partial f_{in_\Phi}}(f_i - f_{in}) +$$

$$+ \frac{1}{2} \sum_{i=1}^{3} \sum_{j=1}^{3} \frac{\partial^2 y}{\partial x_i \partial x_j}(x_i - x_{in}) \cdot (x_j - x_{jn}) + \frac{1}{2} \sum_{i=1}^{2} \sum_{j=1}^{2} \frac{\partial^2 y}{\partial f_i \partial f_j}(f_i - f_{in}) \cdot (f_j - f_{jn}) +$$

$$+ \sum_{i=1}^{3} \sum_{j=1}^{2} \frac{\partial^2 y}{\partial x_i \partial f_j}(x_i - x_{in}) \cdot (f_j - f_{jn}). \tag{3.8}$$

$$
\begin{aligned}
N_x = {} & fun(C_n, T_n, P_n, S_{ion}, R_{zzn}) + \frac{\partial N}{\partial C}(C - C_n) + \frac{\partial N_x}{\partial T}(T - T_n) + \frac{\partial N_x}{\partial P}(P - P_n) + \\
& + \frac{\partial N_x}{\partial S_{io}}(S_{io} - S_{ion}) + \frac{\partial N_x}{\partial R_{zz}}(R_{zz} - R_{zz\,n}) + \\
& + \frac{1}{2} \cdot \left[\begin{array}{l} \dfrac{\partial^2 N_x}{\partial C^2} \cdot (C - C_n)^2 + 2\dfrac{\partial^2 N_x}{\partial C \partial T}(C - C_n)(T - T_n) + 2\dfrac{\partial^2 N_x}{\partial C \partial T}(C - C_n)(P - P_n) + \\ 2\dfrac{\partial^2 N_x}{\partial T^2}(T - T_n)^2 + \dfrac{\partial^2 N_x}{\partial T \partial P}(T - T_n)(P - P_n) + \dfrac{\partial^2 N_x}{\partial P^2}(P - P_n)^2 \end{array} \right] + \\
& + \frac{1}{2}\left[\frac{\partial^2 N_x}{\partial S^2_{io}}(S_{io} - S_{ion})^2 + \frac{\partial^2 N_x}{\partial R^2_{zz}}(R_{zz} - R_{zz\,n}) + 2\frac{\partial^2 N_x}{\partial S_{io} \partial R_{zz}}(S_{io} - S_{ion})(R_{zz} - R_{zz\,n}) \right] + \\
& + \frac{\partial^2 N_x}{\partial C \partial S_{io}}(C - C_n)(S_{io} - S_{ion}) + \frac{\partial^2 N_x}{\partial C \partial R_{zz}}(C - C_n)(R_{zz} - R_{zzn}) + \\
& + \frac{\partial^2 N_x}{\partial C \partial S_{io}}(T - T_n)(S_{io} - S_{ion}) + \frac{\partial^2 N_x}{\partial T \partial R_{zz}}(T - T_n)(R_{zz} - R_{zzn})
\end{aligned}
\tag{3.9}
$$

d e 1. $\frac{\partial N}{\partial C}(C - C_n) + \frac{\partial N_x}{\partial T}(T - T_n) + \frac{\partial N_x}{\partial P}(P - P_n)$ – the sum of nominal conversion coefficients or the sensitivity of the VP;

2. $\frac{1}{2} \cdot \left[\begin{array}{l} \dfrac{\partial^2 N_x}{\partial C^2} \cdot (C - C_n)^2 + 2\dfrac{\partial^2 N_x}{\partial C \partial T}(C - C_n)(T - T_n) + 2\dfrac{\partial^2 N_x}{\partial C \partial T}(C - C_n)(P - P_n) + \\ 2\dfrac{\partial^2 N_x}{\partial T^2}(T - T_n)^2 + \dfrac{\partial^2 N_x}{\partial T \partial P}(T - T_n)(P - P_n) + \dfrac{\partial^2 N_x}{\partial P^2}(P - P_n)^2 \end{array} \right]$ – the sum of changes in sensitivity in the range of transformations;

3. $\frac{1}{2}\left[\frac{\partial^2 N_x}{\partial S^2_{io}}(S_{io} - S_{ion})^2 + \frac{\partial^2 N_x}{\partial R^2_{zz}}(R_{zz} - R_{zz\,n}) + 2\frac{\partial^2 N_x}{\partial S_{io} \partial R_{zz}}(S_{io} - S_{ion})(R_{zz} - R_{zz\,n}) \right]$ – influence of influencing variables on the output parameter N_x.

The modeling of the nominal transformation function, absolute nonlinearity error, relative nonlinearity error, absolute multiplicative error, and absolute additive error is presented in Fig. 3.13-3.17.

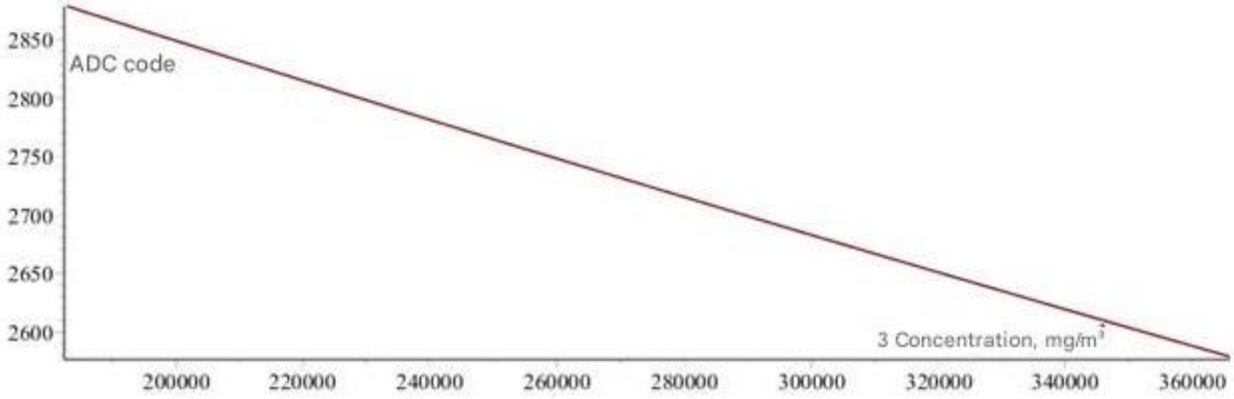

Fig. 3.13. Representation of the nominal transformation function

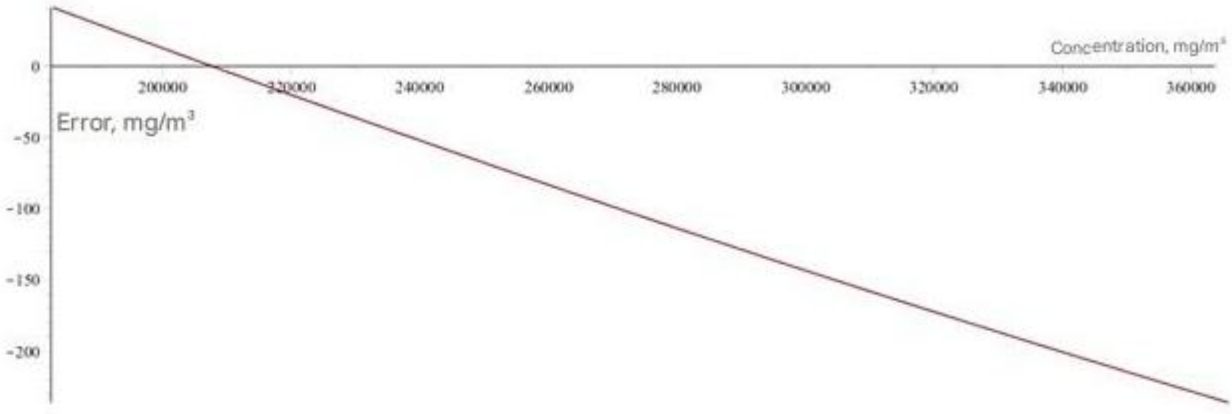

Fig. 3.14. Representation of the absolute error of nonlinearity

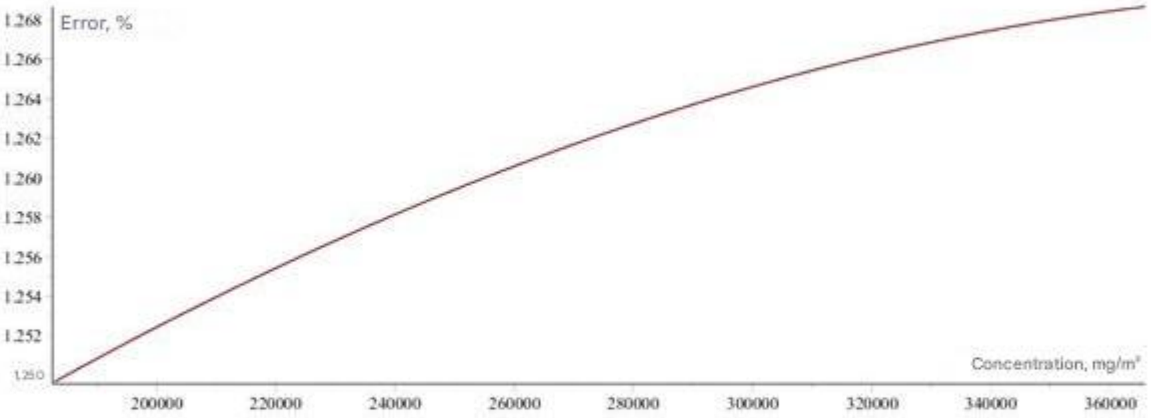

Fig. 3.15. Representation of the relative error of the nonlinearity of the nominal transformation function

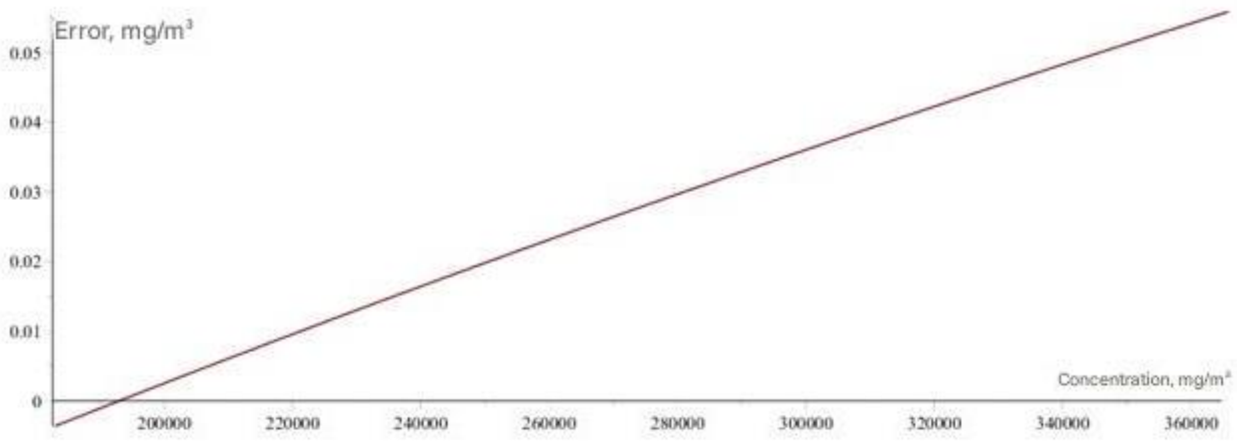

Fig. 3.16. Representation of absolute multiplicative error

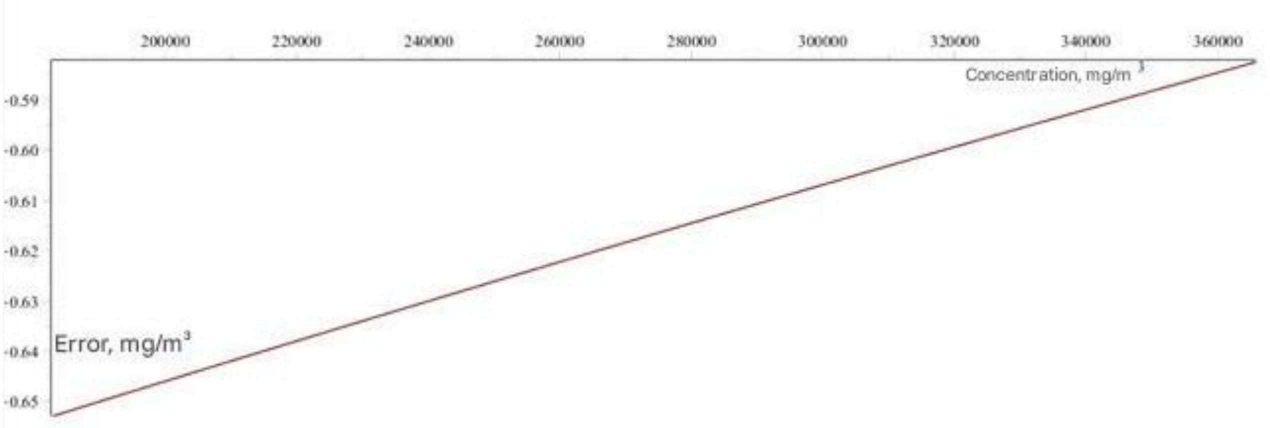

Fig. 3.17. Representation of absolute additive error

Maximum quantization error (in real conditions, the quantization error will be much smaller, since the maximum adequate ADC code is no more than 3200).

$$\sigma = \frac{1}{N_x} \cdot 100\% = 0.12\%. \tag{3.10}$$

Quantization error is the difference between the actual value of a signal (analog) and its quantized value (digital) after the analog signal has been converted to digital. Finding and estimating quantization error is important for several reasons:

When an analog signal is converted to digital using an analog-to-digital converter (ADC), the signal is "quantized," meaning its values are rounded to the nearest possible value that can be represented in digital form. The quantization error provides an idea of how accurately the digital signal represents the analog signal. If the error is large, the result of the digital conversion will be less accurate and may lead to signal distortion.

Quantization error directly affects the quality of signal processing. The smaller the error, the more accurate the digital signal recovery or processing will be. Taking into account the error helps to adjust quantization parameters, such as the number of bits, to minimize distortion and ensure the required signal quality. This is important, for example, in audio, video or radio engineering processing.

In modern measurement systems that utilize Analog-to-Digital Converters (ADCs), quantization error plays a critical role in determining the overall accuracy and performance of the system. Quantization error arises during the process of converting a continuous analog signal into a discrete digital signal. Since the ADC can only represent the input signal with a finite number of levels, this process introduces a small deviation from the actual signal value—known as quantization error. Although this error may seem negligible in some applications, it can become a significant component of total system error, especially in high-precision measurements.

When measuring physical quantities such as temperature, pressure, voltage, or current, understanding and minimizing quantization error is essential to ensure the reliability, accuracy, and validity of the measured results. In sensitive systems, even minor inaccuracies introduced by quantization can lead to incorrect interpretations or flawed decisions. Therefore, evaluating quantization error helps define the practical limits of measurement accuracy and guides engineers in system calibration and error budgeting.

One of the key areas where quantization error has a profound impact is in handling signals with a large dynamic range—that is, signals with substantial variations in amplitude. In such systems, preserving accuracy across the full range of signal values is challenging. By carefully analyzing the quantization error, system designers can determine whether the current bit resolution of the ADC is sufficient or if a higher-resolution ADC (with more bits) is required to reduce the error to an acceptable level. This analysis supports informed decisions that balance performance requirements with cost and hardware limitations.

Quantization error is also a vital consideration in the development of data compression algorithms, such as those used in audio, image, and video compression (e.g., MP3, JPEG, MPEG formats). In these applications, quantization is deliberately applied to reduce data size, but it must be controlled so that the resulting distortion remains imperceptible or acceptable to the end user. By understanding the characteristics of quantization error, developers can optimize compression levels, reducing storage or bandwidth usage without significantly sacrificing quality—a key concern in multimedia applications and communication systems.

In the realm of digital signal processing (DSP), modeling quantization error is crucial for predicting its impact on system behavior. Whether designing filters, control systems, or communications protocols, quantization introduces non-linearities that can degrade performance. Accurate modeling allows engineers to implement compensation strategies, such as dithering or error correction algorithms, to maintain signal integrity. This is especially important in mission-critical systems, such as medical devices, scientific instruments, and aerospace systems, where precision and reliability are paramount.

Furthermore, knowledge of quantization error supports resource optimization during system design. ADC resolution directly affects hardware requirements, including memory capacity, processing speed, and power consumption. By estimating the level of quantization error that can be tolerated in a given application, engineers can determine the minimum number of bits necessary to meet the required accuracy. This enables the design of cost-effective systems that deliver high performance without over-engineering.

In conclusion, quantization error is a foundational concept in both the theoretical and practical aspects of digital measurement and signal processing systems. Its proper understanding and management are essential to achieving a balanced design—one that meets performance expectations while remaining efficient in terms of hardware, software, and energy usage.

Quantization error is needed to understand how accurate a digital signal will be compared to its analog equivalent, and how this affects the overall quality of processing and measurements. Quantization error estimation allows you to optimize the system, reduce distortion, and improve the efficiency of hardware resources.

The dependence of the quantization error on the concentration is presented in Fig. 3.1 8 . – 3.1 9 .

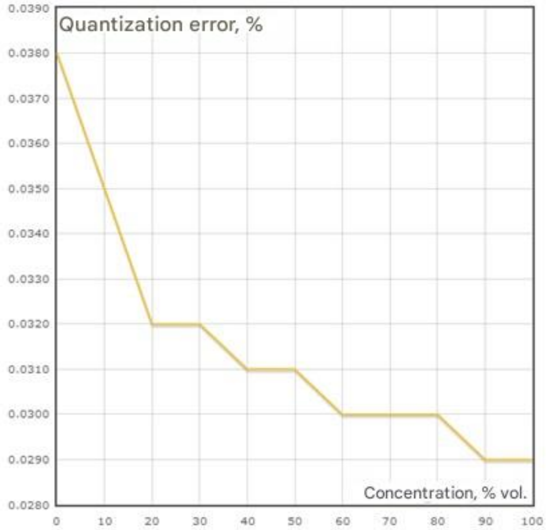

Fig. 3.18. Dependence of quantization error on CO_2

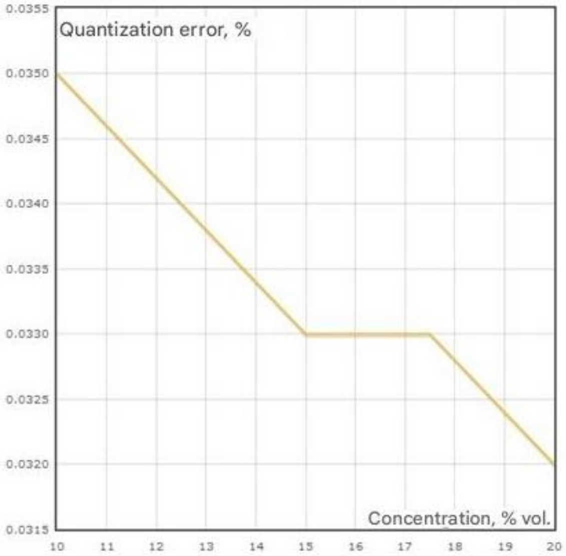

Fig. 3.19. Dependence of quantization error on CO_2 (in the operating range)

Study of the transient process. A transient process is a temporary change in the state of a system that occurs under the influence of an external influence or change in conditions until the system reaches a new steady state or equilibrium. It is characteristic of physical, chemical, biological and technical systems, when after a certain change in conditions (for example, a change in input parameters, a change in external load or environmental conditions), the system begins a transient process that continues until stability is achieved.

A transient process has a certain time duration, because the system changes its state gradually, not instantaneously. During this time, the system is between the initial and final states, which means that it is not in a stable state and can exhibit various variations of quantities, such as oscillations, acceleration or deceleration.

During a transient process, the parameters of a system typically change. For example, temperature, pressure, velocity, concentration of substances, etc. may change until the system reaches a new steady state. Changes in conditions, such as a change in external load or the introduction of energy into the system, are the main cause of transients. In response to these changes, the system reacts by changing its characteristics.

The transition process can be different depending on the nature of the change and the type of system. It can be a linear or nonlinear process, an oscillatory process (where the system begins to oscillate around a new steady state), or a process that changes abruptly or adapts smoothly to new conditions.

Dynamic error is represented through dynamic characteristics and is defined as the instantaneous difference between the value of the input signal calculated from the input signal and the value of the nominal static characteristic, and the instantaneous value of the signal at a given time [31, 32]. The most characteristic for measuring instruments are dynamic characteristics, which are described by first-order differential equations. The generalized equation that characterizes the aperiodic link has the form

$$\tau \cdot \frac{dy}{dt} + y = k \cdot x, \tag{3.11}$$

where k is the transmission coefficient; τ is the time constant determined by the parameters of the measuring instrument; $x\,(\,t\,)$ is the input value of the measuring instrument; $y\,(\,t\,)$ is the output value of the measuring instrument.

Inertial properties of a measuring instrument are characteristics that describe the ability of a measuring instrument or system to respond to changes in the measured quantity, as well as its ability to withstand or absorb these changes over time. These properties are important for understanding how quickly and accurately a measuring device responds to sudden changes in the measured quantity (for example, changes in temperature, pressure, or voltage level).

The inertia of a sensor or measuring element describes its ability to respond to changes in its environment or to changes in the quantity it is measuring. The greater the inertia, the slower the sensor responds to changes. This can be important in cases where rapid fluctuations or sudden changes need to be measured, such as in dynamic systems.

Measuring instruments have a certain time delay, which determines how quickly the instrument can respond to a change in the input signal. The time delay occurs due to the limitations of the sensor itself and the electronic system, which are not able to adapt to changes instantly. This delay can be critical when you need to monitor processes where changes occur very quickly, for example, in rapidly changing flows or in automated control systems.

The inertial properties of a measuring instrument affect its dynamic characteristics—the speed at which the measuring instrument is able to reach a new state after a change in the measured quantity. For measuring instruments with high inertia, the response to a change will be slower, and they may not reflect rapid fluctuations in the quantity.

When measuring signal levels in a dynamic process (e.g., in real time in electrical systems or when measuring temperature in furnaces), it is important to choose instruments with appropriate dynamic characteristics so that they can accurately reflect changes.

Inertial properties can also be related to damping, i.e. the ability of a measuring instrument to smooth out sudden fluctuations or noise that may occur in a system. Damping reduces the level of rapid fluctuations and allows for more accurate recording of stable values, which can be useful, for example, in industrial measurements where the influence of short-term but significant changes must be avoided.

The inertial properties of the device also determine its sensitivity to the rate of change of the measured quantity. If measurements are made under conditions of rapid change of the quantity (for example, when controlling the temperature in cooling or heating systems), inertia can affect the accuracy of the measurements. The lower the inertia, the more accurately the rapid change of the quantity will be displayed.

Inertial properties can affect measurement accuracy, as instruments with high inertia may not reflect rapidly changing quantities, resulting in a delay in measurement or smoothing of real fluctuations. In such cases, measurement results may be less accurate, especially with high dynamics of quantity change.

The inertial properties of a measuring instrument describe how a measuring device responds to changes in input quantities. They determine the ability of the instrument to respond quickly to these changes, as well as the time over which this process occurs. Depending on the inertial properties, the instrument can either cope well with rapid changes or smooth out these changes, which is important to consider when choosing a measuring instrument for specific tasks.

Inertial properties are characterized by a time constant . Knowing τ , it is quite easy to determine the time required for the transient process to approach the static regime for any given accuracy.

Studying the dynamic characteristics of a gas concentration sensor is crucial for understanding how the sensor responds to changes in gas levels over time. These characteristics include parameters such as response time, recovery time, lag, settling time, and dynamic range. They determine how quickly and accurately the sensor can detect and adapt to fluctuations in gas concentrations in real-world environments.

One of the most critical dynamic parameters is the response time — how fast the sensor reacts to a sudden increase or decrease in gas concentration. A sensor with a slow response time may not detect hazardous conditions quickly enough, leading to delays in alarms or safety interventions. In fast-changing environments like industrial plants or confined spaces, quick detection is vital for protecting human health and preventing accidents.

Recovery time, or how long the sensor takes to return to its baseline after the gas is removed, is equally important. A slow recovery can reduce the sensor's ability to detect subsequent gas events accurately, especially in environments where concentrations vary rapidly.

Lag and delay in sensor output can result in inaccurate real-time monitoring. If the sensor doesn't reflect the actual concentration quickly enough, it may mislead operators or automated systems, leading to poor decisions or inappropriate responses.

Settling time describes how long it takes for the sensor to stabilize within an acceptable range after a step change in concentration. In applications requiring high precision, knowing this value is essential to determine when a measurement can be considered reliable.

Studying these dynamic behaviors also helps optimize the sensor's integration into control systems. For example, in automated ventilation or alarm systems, knowing the sensor's response and recovery characteristics ensures that the system reacts at the right moment and avoids false alarms or unnecessary actions.

In research and calibration procedures, dynamic characteristics must be well-understood to ensure valid comparisons and accurate modeling of sensor behavior under real operating conditions.

In summary, exploring the dynamic characteristics of a gas sensor is essential for ensuring accurate, timely, and reliable measurements in both safety-critical and data-sensitive applications.

The steady-state error is a static error. The presence of a transient process causes a dynamic error. The duration of the transient process at a given (allowable) dynamic error is determined from the equation

$$\Delta_{ДН} = k \cdot e^{-(\frac{t_{ПП}}{\tau})}, \qquad (3.12)$$

where t_{PP} – duration of the transition process.

From the last equation, the duration of the transient process for a given dynamic error is determined by the formula

$$t_{ПП} = \tau \cdot \ln(\frac{k}{\Delta_{ДН}}). \qquad (3.13)$$

Thus, in measuring instruments with an aperiodic transient process, which is described by a first-order transient, the duration of the transient process decreases with a decrease in the constant τ and an increase in the permissible dynamic error.

Let us take the initial value U (T) as a unit function (Heaviside function) and obtain an analytical dependence for the transient characteristic of the aperiodic link

$$U(T) = k \cdot (1 - e^{-(\frac{t}{\tau})}), \qquad (3.14)$$

where k is the transmission coefficient; τ is the time constant determined by the parameters of the measuring instrument.

The obtained results of modeling the response of the control device sensors to the input signal $1(t)$ are presented in Fig. 3.15-3.17 Transient characteristic $h(t)$ was constructed experimentally using a pulse timer in the WinPLC 7 package (the model for studying the transient process is presented in Fig. 3. 20) .

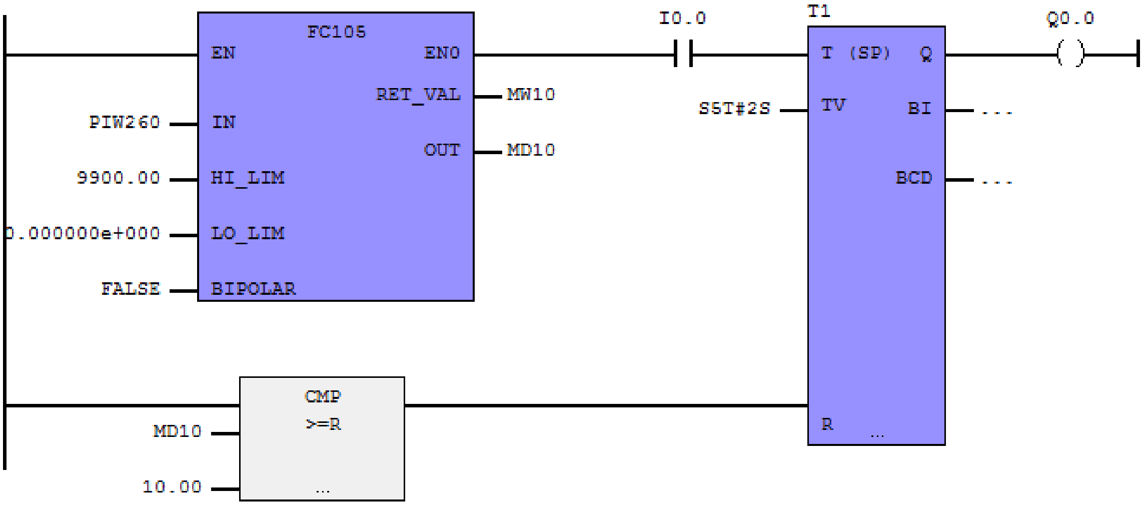

Fig . 3. 20. Model for studying the transient process

The course of the transition process in the VP after changing the concentration of the gas mixture (constructed in the Scilab package) based on experimental data is presented in Fig. 3.21 :

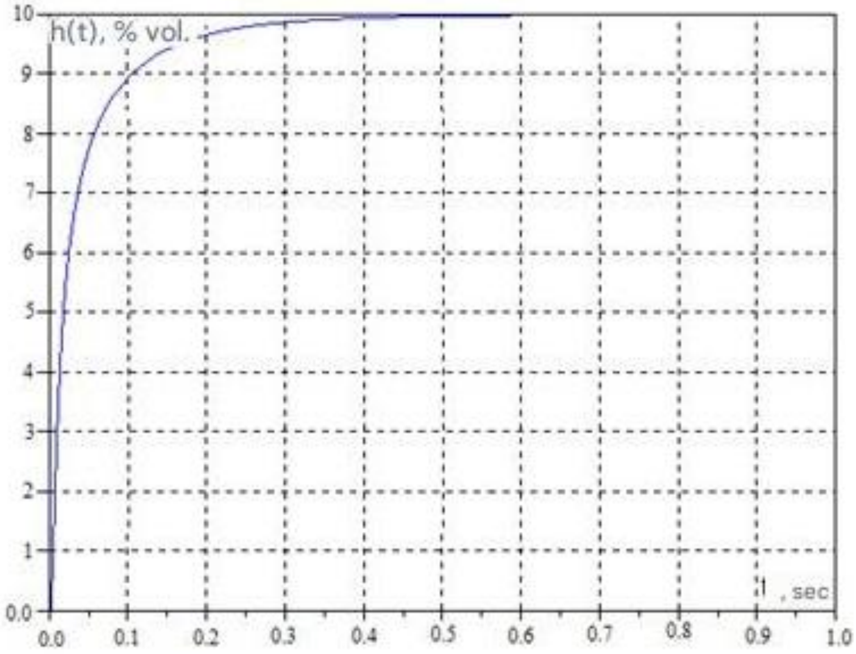

Fig. 3. 21. Transient process in the CO $_2$ measuring channel

The course of the transition process in the VP after a temperature change is presented in Fig. 3.22 :

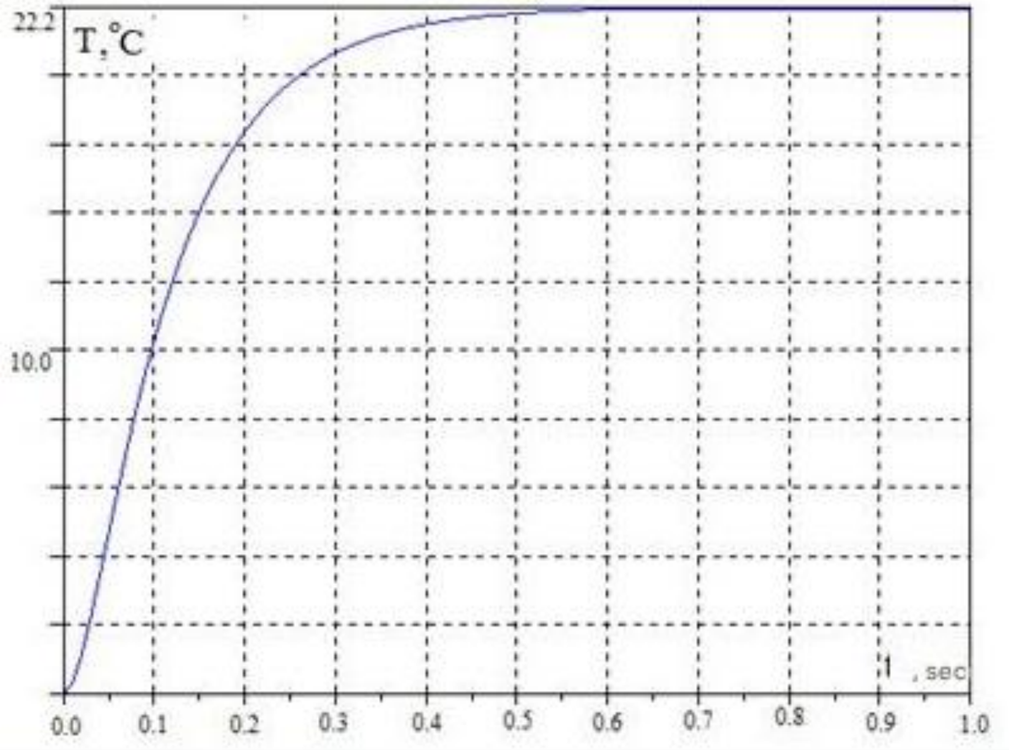

Fig. 3. 22. Transient process in the temperature measuring channel

The course of the transient process in the VP after a pressure change is presented in Fig. 3.23 :

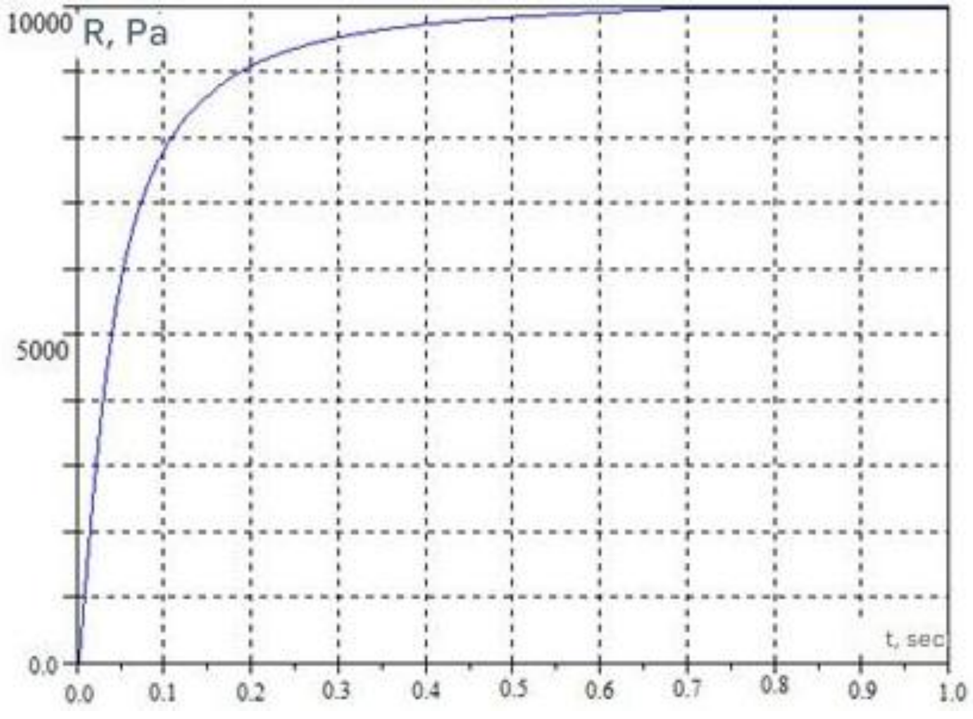

Fig. 3. 23. Transient process in the pressure measuring channel

At t ≈ from 0 to 0. 1 s – time from the moment of change in flue gas concentration at the inlet to the moment the output signal reaches a certain level. This is the sample transportation time and the inertia of the elements.

When t ≈ from 0.1 to 0.35 s – the time after which the instantaneous value of the output signal will be proportional to the value of the change in the concentration of carbon dioxide in the gases. The time depends on the dynamic processes of the gas mixture being analyzed.

From Fig. 3.21 we can conclude that the problem posed in subsection 3.3 ($\varDelta_{DN1} > \varDelta_{DN2}$, with $\varDelta_{ST1} < \varDelta_{ST2}$, and vice versa $\varDelta_{DN1} < \varDelta_{DN2}$, at $\varDelta_{ST1} > \varDelta_{CT2}$) – solved. Comparing the obtained data with the data in Fig. 3. 6 , it can be seen that the processing time of the instantaneous signal increased to ≈ 0.44 s (compared to the open optical channel) and decreased by ≈ 6 s (compared to the closed optical channel). The obtained results fully comply with the requirements of GOST R 50759-95 (clause 9.3) and it can be stated that the goal (with the required speed) has been achieved.

Analysis and evaluation of measurement errors. Accurately determining the metrological characteristics of a gas concentration sensor is essential for ensuring the precision, reliability, and consistency of measurements. Metrological characteristics include parameters such as accuracy, sensitivity, detection limit, response time, linearity, repeatability, and long-term stability. Each of these factors plays a key role in the quality and trustworthiness of the data provided by the sensor.

First and foremost, accurate knowledge of a sensor's accuracy and sensitivity allows users to interpret the measurement results correctly. Without understanding the potential error margin or the smallest detectable concentration, there is a risk of overestimating or underestimating gas levels, which can lead to incorrect conclusions or unsafe decisions.

Linearity ensures that the sensor's response remains proportional across the full range of measured concentrations. This is particularly important in applications where both low and high concentrations need to be monitored with the same device. A non-linear response can distort data and complicate calibration procedures.

Response time is another critical factor, especially in dynamic environments such as industrial safety monitoring, leak detection, or environmental surveillance. Knowing how quickly a sensor can react to changes in gas concentration is vital for real-time decision-making and timely responses.

Repeatability and reproducibility are key for comparing data across time and devices. If a sensor produces inconsistent results under the same conditions, it cannot be trusted for long-term monitoring or scientific research.

Understanding long-term stability and drift is important for maintenance planning and data reliability. Sensors may lose calibration over time, and if their behavior is not well-characterized, this degradation can go unnoticed, resulting in false readings and potentially dangerous situations.

Finally, in regulated industries and scientific research, proper documentation of metrological characteristics is often a legal or compliance requirement. Certification, calibration traceability, and validation reports all depend on clear knowledge of sensor specifications.

In conclusion, accurately determining the metrological characteristics of a gas sensor is fundamental to obtaining meaningful, accurate, and actionable data. It supports safety, regulatory compliance, scientific integrity, and operational efficiency.

For the developed means of controlling the concentration of carbon dioxide in gases, we will take into account the following components of the total error: instrumental and methodological components. For a complete metrological analysis of the control means, we will evaluate each of them.

Instrumental error occurs in the measuring channels (optical, temperature, pressure, humidity) at the place of their occurrence. The main components of the instrumental error in the developed control tool are :

- a radiation source (in the developed device, a laser diode), which is set to the appropriate wavelength with a certain error , which is determined by the quality of its manufacture. The size of this error is determined by the manufacturer and indicated in the DataSheet .

- error in the conversion of the radiation receiver This error component is inherent in spectral instruments and makes a significant contribution to the total error.

- errors that occur in the optical measuring transducer. One of the main ones is the quality of the coating of the inner surface of the optical transducer. This error may also include an error caused by a change in the reflection angle and path length of the radiation beam due to roughness on the applied coating.

- errors of additional temperature and pressure measuring channels , the values of which have an impact on the readings of the carbon dioxide concentration monitor in gases .

- ADC error . The main component of the ADC error is the quantization error, other errors, in comparison with it, can be neglected. The quantization error was studied in 3.21.

Therefore, the total instrumental error will be:

$$\bar{\Delta} = \sqrt{\overline{\Delta^2_{\text{Radiation source}}}} + \overline{\Delta^2_{\text{Cchannel}}} + \overline{\Delta^2_{\text{Radiation receiver}}} + \overline{\Delta^2_{\text{ADC}}} + \overline{\Delta^2_{\text{Optical path materials}y}} \,. \quad (3.15)$$

By substituting the approximate error values taken from the DataSheet of the structural blocks of the control and calculation tool, we will obtain an estimated instrumental error value of 1%.

Methodological errors arise due to the imperfection of the measurement method (do not depend on the quality of the control tool) and the approximations allowed when designing the control tool. The main component of the methodological error is the use of the relative measurement method. The main methodological errors include:

- error Δfun of the measurement transformation of the mathematical model (2. 29). In the operating range, the maximum deviation is 0.3%.

- additivity error $\Delta_{add.}$. This total error includes the error in choosing the characteristic wavelength at which the measurement will be made (estimated depending on the type of the absorption spectrum of the selected gas); the error that arises due to the failure to take into account the Doppler broadening of the absorption spectral lines of the studied gas in the calculations (calculated using the value of the radiation absorption coefficient, which takes into account the Doppler effect - the formula); the error that appears due to the deviation from the Bouguer-Lambert-Beer law, which underlies the absorption spectroscopy method; the error that arises due to the exclusion from the calculations of the radiation scattering index (associated with the phenomenon of fluorescence of gas molecules, and the path length of the radiation beam in the optical primary converter is also reduced);

- measurement conversion error $\overline{\Delta}^2_{в.п.}$. Determines the discrepancy between the theoretical and experimental models (is at the level of 0.27%)

Thus, the total methodological error is:

$$\overline{\Delta} = \sqrt{\overline{\Delta^2{}_{fun}} + \overline{\Delta^2}_{ad} + \overline{\Delta^2}_{Meas}}. \qquad (3.1\ 6)$$

By substituting the corresponding error values, we obtain the value of the methodological error – 0.9 % .

$$\overline{\Delta} = \overline{\Delta}_{instr.} + \overline{\Delta} metod. \qquad (3.1\ 7)$$

The total measurement error is equal to the sum of instrumental and methodological errors and is 1.9 % .

In the third chapter The monograph develops a structural and functional diagram of a means of controlling the concentration of carbon dioxide in gases and presents the transformation equation of the measuring channel.

The static and dynamic characteristics of a means of controlling the concentration of carbon dioxide in gases have been calculated.

An algorithmic organization has been developed for adapting a means of controlling the concentration of carbon dioxide in gases to real operating conditions, which takes into account not only external excitations but also the type of boiler unit.

An analysis of methods for filtering the measured gas concentration was conducted, which made it possible to avoid obtaining derivative values equal to ±∞ while maintaining the overall dynamics of the process.

methodological errors in gas concentration measurements using the developed tool were estimated. It was established that the total measurement error does not exceed 1.9 % .

CHAPTER 4

DETERMINATION OF THE CONTROL RELIABILITY AND ACCURACY OF EXPERIMENTAL RESEARCH RESULTS

Software implementation of a means of controlling the concentration of carbon dioxide in gases. The task that is set involves a solution on a programmable logic controller (PLC).

A programmable logic controller (PLC) is a specialized computer used to automate and control various processes in industry. From a technical point of view, a PLC is an embedded system consisting of a central processing unit, input and output modules, and configuration and control software.

A PLC is capable of performing logical operations, processing signals from sensors, and controlling actuators such as motors, valves, or other devices. Its primary purpose is to automate the control of machines, processes, production lines, and in the management of objects based on specified programs.

PLC programming is often done using specialized programming languages, such as Ladder Diagram (LD), Function Block Diagram (FBD), or Structured Text (ST), which allow you to create control logic for various processes, automating work with equipment.

Hardware. To implement the task, we will use the VIPA PLC of the System 200V series [30]. System 200V modules can be used to expand automation systems based on Siemens controllers and the PROFIBUS industrial bus, using a single development tool. The System 200V series is built on a modular principle. This means that the user has the opportunity to optimally select the composition of modules to solve his task and flexibly modify it when expanding or changing the requirements for the means. All input-output modules and interface modules have the property of universality, that is, they can be used together with any CPU of this series.

Software. To implement the task, we will use the WINPLC7 software package for configuring, programming, program tuning and diagnostics of VIPA controllers of all series. WINPLC7 contains all the necessary tools for creating a project: hardware configurator, symbol editor, PROFIBUS network configurator, program editor, controller emulator.

This software can be used to solve a wide range of automation problems [37] . The package contains a built-in Hardware configuration - an application for communication between the microcontroller and the computer.

Development of the algorithm and program. The program will be written in the WINPLC7 software package in the Statement List (STL) programming language.

Statement List (STL) is a programming language used to program programmable logic controllers (PLCs). STL is a low-level language that is very similar to assembly language, allowing direct interaction with PLC hardware. It is used to create complex software algorithms that require precise control of devices at the instruction level, close to machine code.

STL has a simple structure, consisting of instructions, each of which performs a specific operation or action. Programs in STL look like a set of operations, where each instruction consists of three main components: an operation, operands (or data), and conditions. These instructions are usually executed sequentially, but can have conditional execution or loops to repeat actions.

In STL, you can use standard operations and instructions, such as:

M — for controlling relay states or memory bits.

L — to load values into registers or variables.

S — to write values to variables or outputs.

T — for performing operations with time (for example, timers).

B — for performing bitwise operations such as AND, OR, XOR.

J — for performing conditional branches, such as jumping to other instructions.

In STL, the data used in the program is stored in the PLC memory as bits, bytes, words, or double words. You can directly work with the memory to write and read values, allowing you to precisely control the input and output signals.

STL is often used in complex industrial automation applications where fast and accurate execution of programs that interact directly with the equipment is required. This includes working with devices that require high data processing speed or where specific functions must be performed that cannot be easily implemented using higher-level programming languages. **Statement List (STL)** is a powerful and efficient programming language for PLCs that allows programmers to interact accurately and quickly with the hardware resources of the system. Although STL is more complex to program compared to other languages such as Ladder Diagram, it gives maximum control over program execution and is ideal for complex automated processes.

The algorithm of the program is as follows: from the means of controlling the concentration of carbon dioxide in gases, a variable electrical information signal about the composition of the flue gas is received. This signal will be received by the functional block FC 105 (Scaling analog value) and convert it into a variable of type ' real ' (MDx). MDx – corresponds to the value of the electrical signal (voltage), which lies within the range of 0-5 V. Next, the electrical signal is converted into the corresponding carbon dioxide concentration. The oxygen concentration is calculated analytically. The conversion is carried out according to the mathematical model presented in section 2 (equation 2.16). After obtaining the value of the amount of a specific gas, it is compared with the settings given in the first section (table 1. 2). If the concentration is within the permissible limits , then the frequency regulators continue to operate in the same mode at reduced speeds. If the concentration goes beyond the settings, a signal is sent to the contact, which is responsible for the speed of the motors that supply air to the boiler furnace. The control and management process takes place in real time. The program listing is presented in Appendix B.

The developed software package for controlling the concentration of carbon dioxide in gases [11] with its main subroutines is presented in Fig. 4.1.

Example of the program working on the first channel when applying a zero electrical signal to the PLC to check the operation of the algorithm and program is shown in Fig. 4.2.

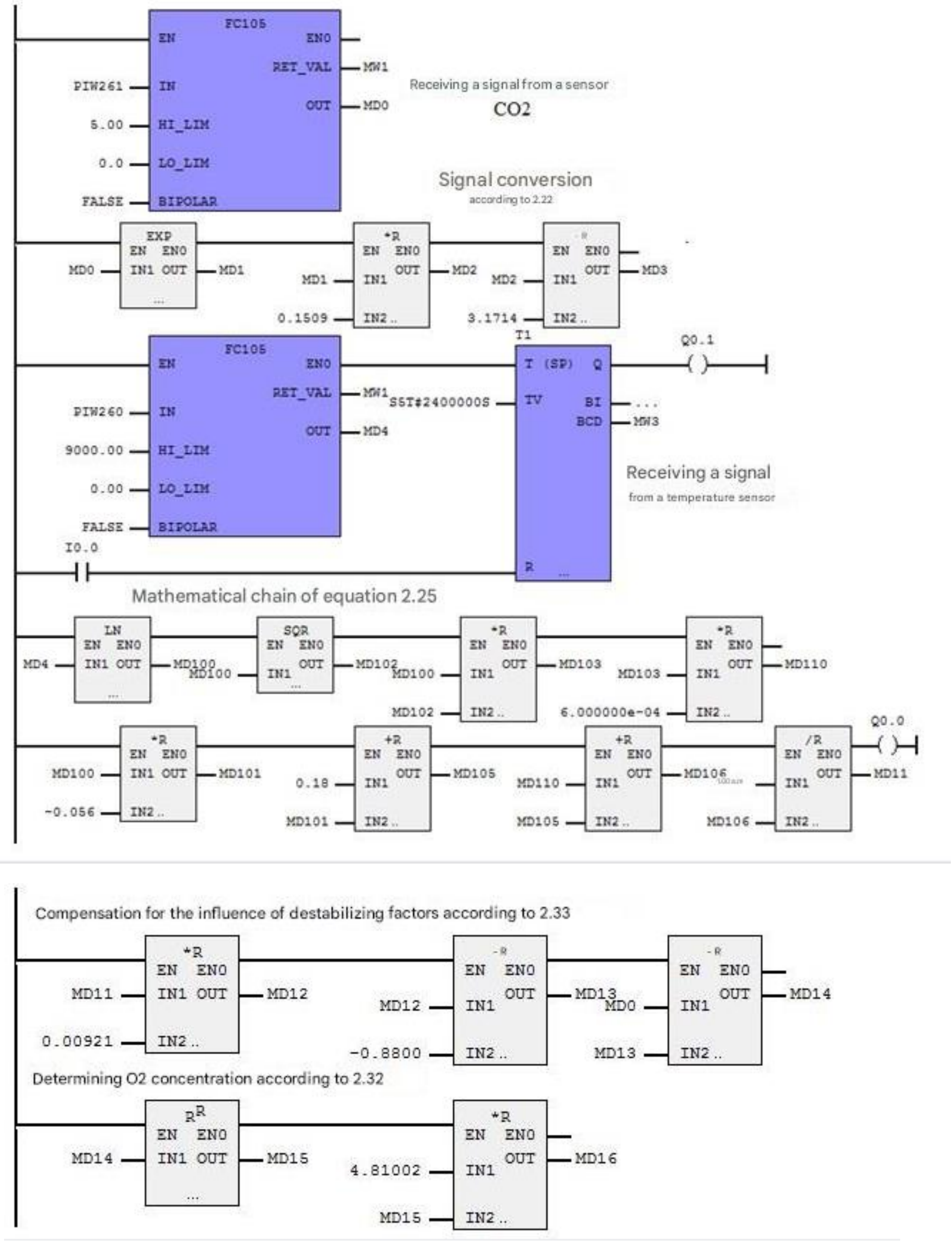

Fig. 4.1. CFG software complex

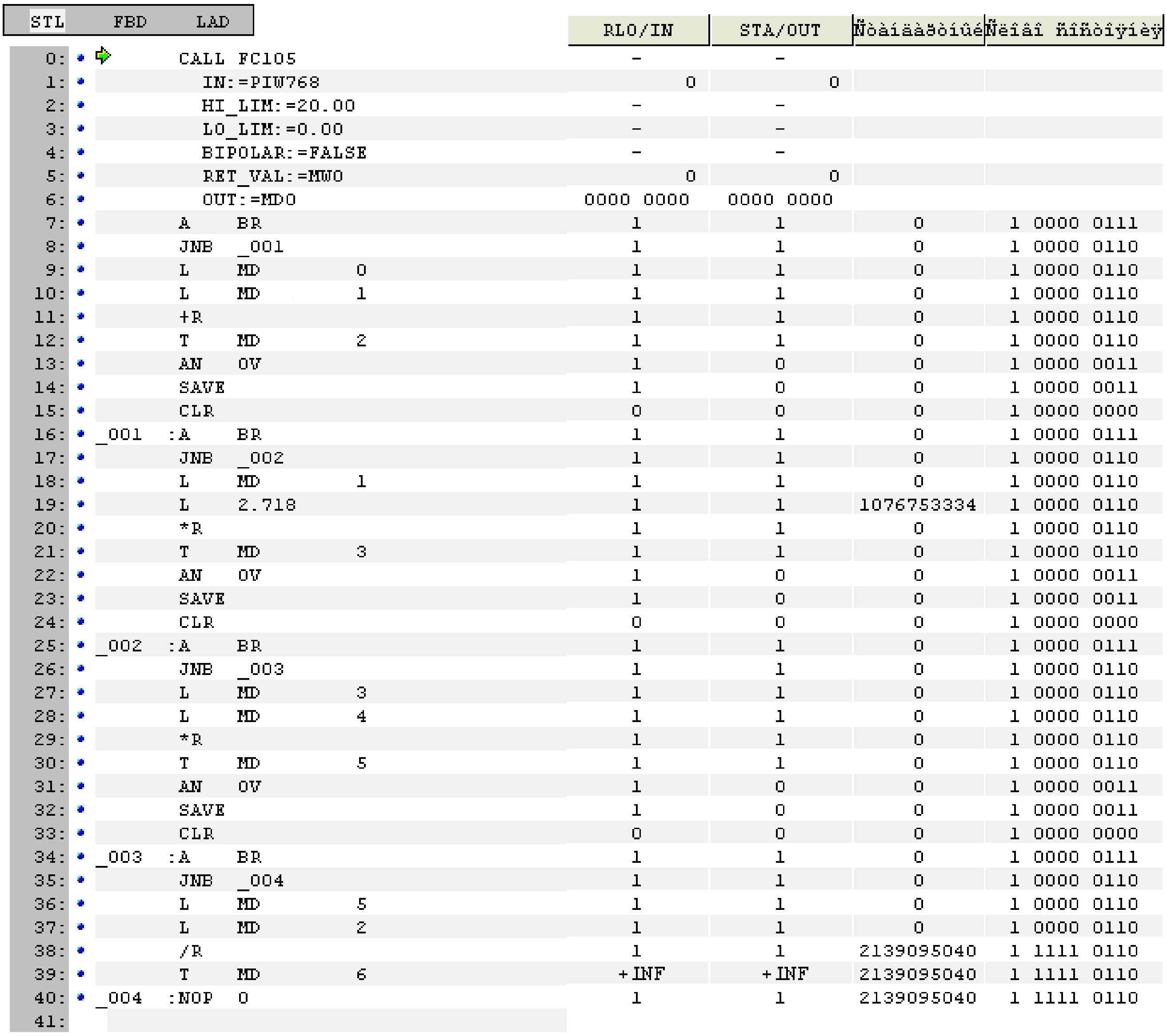

```
STL   FBD   LAD
                                          RLO/IN     STA/OUT    Ñòàíäàðòíûé Ñëîâî ñîñòîÿíèÿ
        CALL FC105                           -          -
          IN:=PIW768                             0          0
          HI_LIM:=20.00                      -          -
          LO_LIM:=0.00                       -          -
          BIPOLAR:=FALSE                     -          -
          RET_VAL:=MW0                           0          0
          OUT:=MD0                       0000 0000  0000 0000
        A    BR                              1          1          0        1 0000 0111
        JNB  _001                            1          1          0        1 0000 0110
        L    MD       0                      1          1          0        1 0000 0110
        L    MD       1                      1          1          0        1 0000 0110
        +R                                   1          1          0        1 0000 0110
        T    MD       2                      1          1          0        1 0000 0110
        AN   OV                              1          0          0        1 0000 0011
        SAVE                                 1          0          0        1 0000 0011
        CLR                                  0          0          0        1 0000 0000
_001   :A    BR                              1          1          0        1 0000 0111
        JNB  _002                            1          1          0        1 0000 0110
        L    MD       1                      1          1          0        1 0000 0110
        L    2.718                           1          1      1076753334   1 0000 0110
        *R                                   1          1          0        1 0000 0110
        T    MD       3                      1          1          0        1 0000 0110
        AN   OV                              1          0          0        1 0000 0011
        SAVE                                 1          0          0        1 0000 0011
        CLR                                  0          0          0        1 0000 0000
_002   :A    BR                              1          1          0        1 0000 0111
        JNB  _003                            1          1          0        1 0000 0110
        L    MD       3                      1          1          0        1 0000 0110
        L    MD       4                      1          1          0        1 0000 0110
        *R                                   1          1          0        1 0000 0110
        T    MD       5                      1          1          0        1 0000 0110
        AN   OV                              1          0          0        1 0000 0011
        SAVE                                 1          0          0        1 0000 0011
        CLR                                  0          0          0        1 0000 0000
_003   :A    BR                              1          1          0        1 0000 0111
        JNB  _004                            1          1          0        1 0000 0110
        L    MD       5                      1          1          0        1 0000 0110
        L    MD       2                      1          1          0        1 0000 0110
        /R                                   1          1      2139095040   1 1111 0110
        T    MD       6                     +INF       +INF    2139095040   1 1111 0110
_004   :NOP  0                               1          1      2139095040   1 1111 0110
```

Fig. 4.2. Example of the program working on the first channel

The algorithm of operation of the carbon dioxide concentration control device in gases with compensation of the main influencing factors is presented in Fig. 4.3.

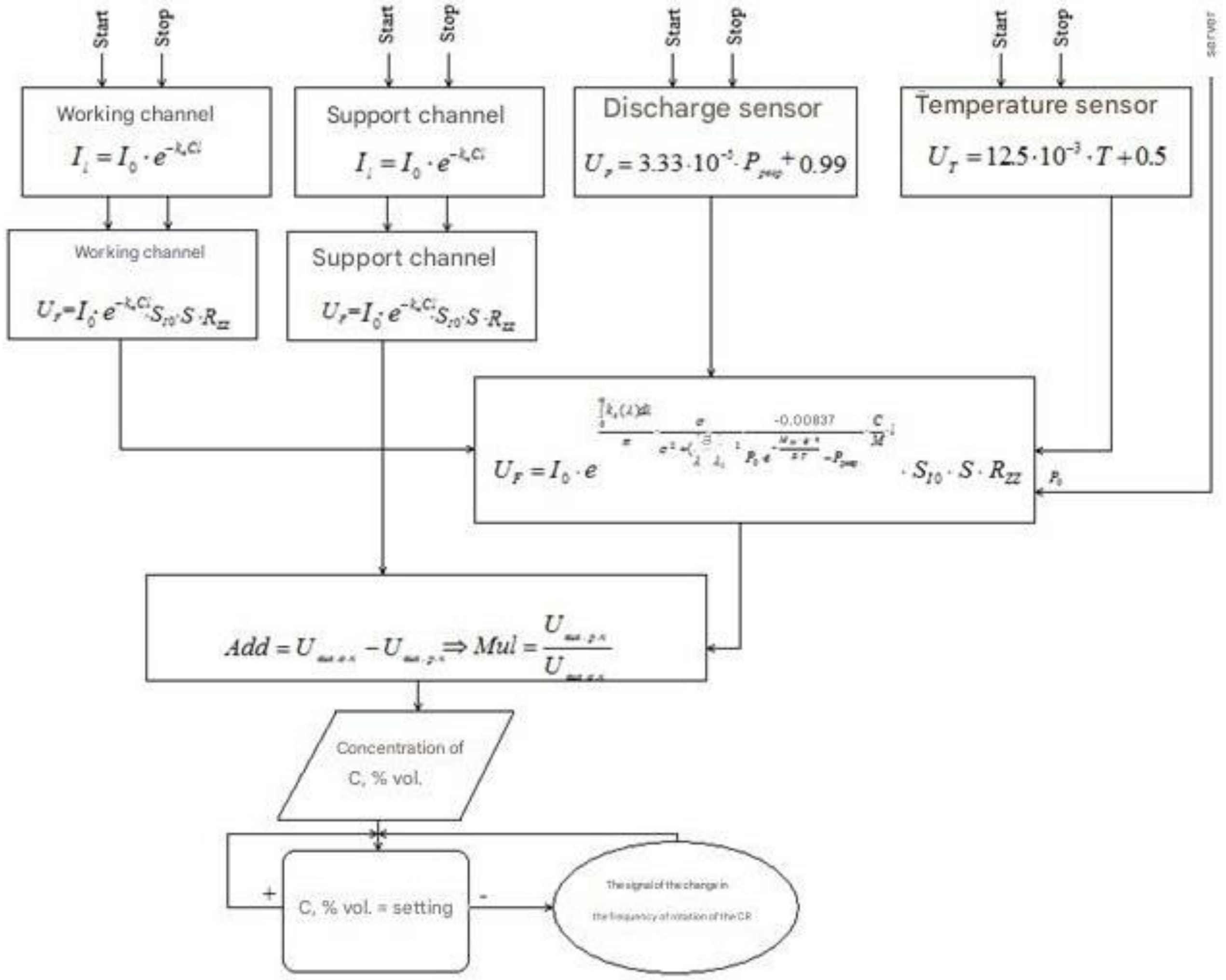

Fig. 4.3. Algorithm of operation of a means of controlling the concentration of carbon dioxide in gases

Also, by introducing an additional flue gas density measurement channel, the method of emergency control of boiler burner extinction has been improved, which, unlike existing methods, analyzes the sample not only for methane concentration, but also for flue gas density, which allowed to increase the probability of establishing a correct diagnosis and reduce false alarms during emergency control. Experimental studies are presented in Appendix A. The emergency control algorithm is implemented software (Appendix B).

An example of the program operation is demonstrated using the example of the temperature measurement channel. The measurement channel is implemented in the WINPLC 7 software package [37] in the Ladder programming language. Diagram (LAD) [38]. In the program, the function block FC 105 (Scaling analog value) receives the value from the turbocharger in the specified range (0–9000 Ohm) and displays it as a real value (variable MD 4). When the signal from the sensor begins to arrive, a programmable timer (T1) is started. The variable MD 4 at the next stage is transferred to the mathematical circuit that describes the functional dependence (2.24) and at the output of the circuit (variable MD 1) displays the value of the gas mixture temperature at ^{0}C. In the operating mode, the signaling devices Q 0.0 and Q 0.1 are in the state of a logical unit. Example of the program operation [39] with a resistance value of 1621.92 Ohm taken from the turbocharger and, accordingly, a temperature of 116.82 ^{0}C on $22\cdot10^{3}$ seconds after the start of the measurement is shown in Fig. 4.4.

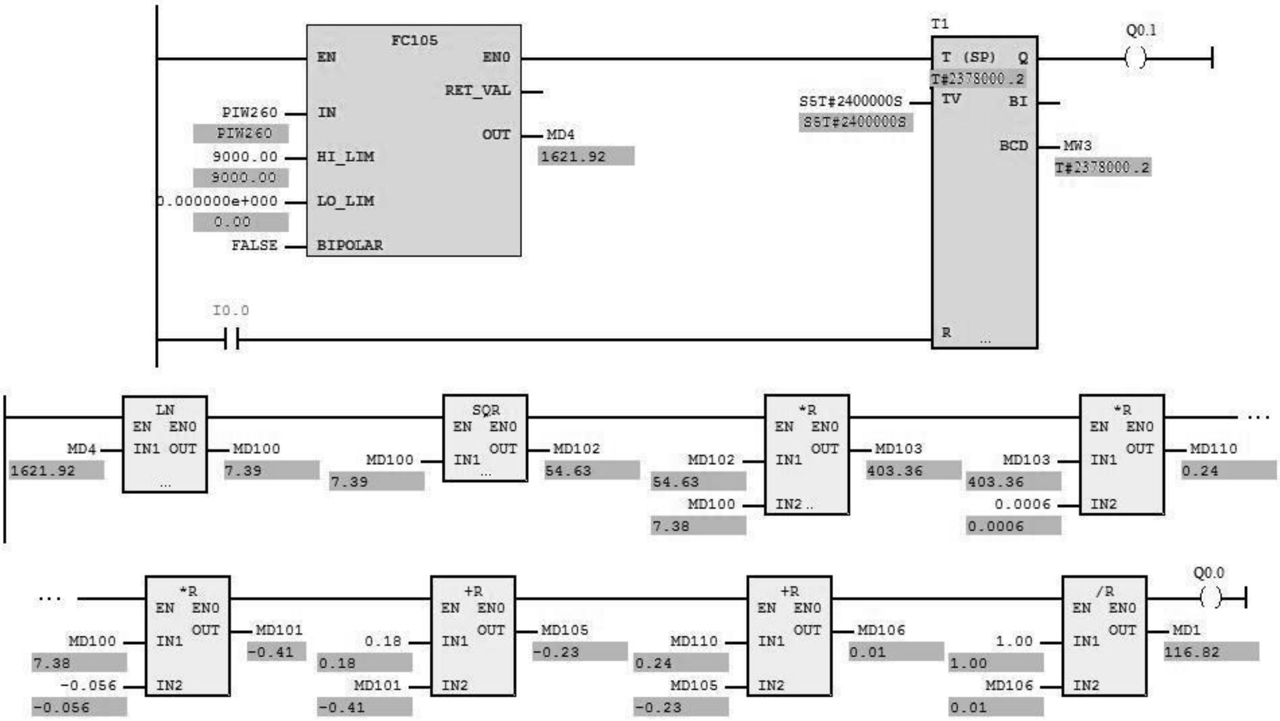

Fig. 4.4. Software implementation of the temperature measurement channel

An experimental sample of a means of controlling the concentration of carbon dioxide in gases has been developed. Its appearance is presented in the appendix.

Development of a laboratory sample and experimental studies. Verifying the adequacy of a developed mathematical model is a fundamental step in ensuring that the model accurately represents the real-world system or process it is intended to describe. Without this verification, the model’s predictions, conclusions, and practical applications may be misleading or even completely incorrect.

Adequacy means that the model not only fits the available experimental or observational data, but also reliably reflects the behavior of the actual system under a wide range of conditions. A model may mathematically "fit" the data, yet still be inadequate if it fails to capture the true underlying mechanisms or respond correctly outside the tested range.

Testing for adequacy typically involves statistical validation methods, such as analyzing residuals, checking for normality and independence of errors, comparing predicted vs. observed values, and evaluating the model’s performance on new or unseen data. These steps help ensure the model is not overfitted — that is, tailored too closely to a specific dataset without general applicability.

In engineering, environmental monitoring, or sensor development (such as gas concentration sensors), using an inadequate model can lead to false predictions, poor control decisions, and unsafe outcomes. For example, if a gas sensor model inaccurately represents dynamic behavior or environmental influences, it may trigger false alarms or fail to detect hazardous levels in time.

An adequate model also serves as a reliable tool for system optimization, forecasting, and automation. It can be confidently used to simulate different scenarios, test hypotheses, and guide decision-making processes in both scientific and industrial contexts.

Moreover, in academic or regulatory environments, demonstrating the adequacy of a model adds credibility to your work. Peer reviewers, clients, or oversight agencies often require proof that the model has been rigorously tested and validated.

In conclusion, verifying the adequacy of a mathematical model is essential to ensure its validity, reliability, and usefulness. It transforms a theoretical construct into a practical, trustworthy tool.

The scheme for conducting a laboratory study of the ZVC is presented in Fig. 4.5.

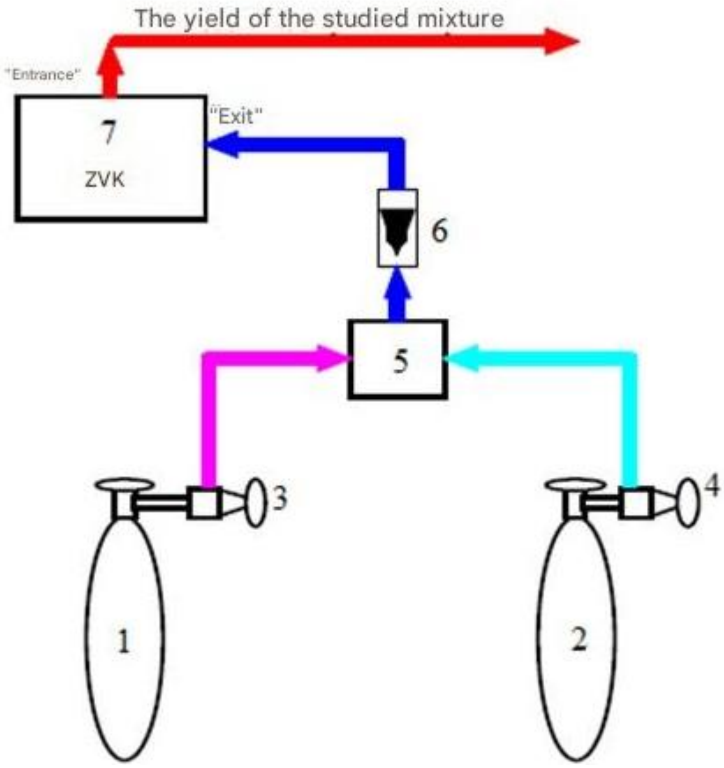

Fig. 4.5. Scheme of laboratory research of ZVK :
1, 2 – cylinders with test gas mixture, 3,4 – taps, 5 – mixer, 6 – rotometer, 7 – ZVK

A mixture of nitrogen and sulfur dioxide is used as an additional gas , as is found in cylinder 1. The measured gas mixtures of carbon dioxide are in the cylinder and 2. The gas mixture is taken alternately from the desired cylinder fed through a mixer 5 at the inlet of the gas supply system . Gas consumption The mixture is controlled using a rotameter 6 .

The test gas mixtures are under a pressure of 85 atm. and contain carbon dioxide and nitrogen in cylinders according to table. 4. 1 .

Table 4.1

Composition of cylinders with standardized gas mixture

Number 1 cylinders	Volume fraction of CO_2, % vol.	Volume fraction $N_2 + SO_2$, % vol.
No. 1	0	100
No. 2	10	90
No. 3	12	88
No. 4	14	86
No. 5	16	84

The experiment was conducted using the products of the company "Kriotechgaz KPK" LLC, namely : gaseous carbon dioxide , top grade, State Standards of Ukraine 8050-85 (99.99 % vol.); and the nitrogen is gaseous, of high purity, State Standards of Ukraine 9293-74 (99.9 % vol.) .

The procedure for performing the experimental study: connecting the hose from the gas junction and the rotometer to the "INPUT" fitting of the ZVK; connecting the hose from the "OUTPUT" fitting to the fitting for the outlet of the mixture under study; opening tap 3 on cylinder 1 and tap 4 on cylinder 2; checking the “zero” readings of the ZVK (according to Fig. 4.2) in the SFG program ; closing tap 3 on the nitrogen cylinder, and tap 4 with carbon dioxide; measuring the volume fraction of CO_2 in the gas mixture from cylinders No. 2 and No. 1; the measurement procedure was carried out 10 times; taking readings and further processing of measurements.

Adequacy study of the developed mathematical model . Adequacy study of a mathematical model is the process of checking how accurately a mathematical model reflects the real system or process that it is supposed to model. The purpose of this study is to determine whether the model is sufficiently accurate and correct for use in practice, and whether it produces acceptable results under appropriate conditions.

The process of studying the adequacy of a mathematical model includes several stages:

1. Checking the correspondence between the model and the real process. First, it is important to compare the model with the real process or system that it is supposed to describe. This means that it is necessary to find out whether all the key factors that affect the system are taken into account. For example, for physical processes, it is necessary to check whether the model accurately reflects the basic physical laws that operate in the real world.

2. Empirical testing and comparison with experimental data. To assess the adequacy of the model, it is necessary to compare its predictions with real experimental or observational data. If the model results coincide with the actual data within the limits of permissible errors, the model can be considered adequate for this type of problem. This comparison helps to assess how well the model predicts the behavior of the system.

3. Model sensitivity analysis. One important aspect of adequacy testing is assessing the sensitivity of the model to changes in input parameters. If small changes in input parameters lead to large changes in the simulation results, this may indicate that the model is inadequate or requires refinement. Ideally, the model should be robust to small fluctuations in the input data.

4. Assessing the predictive power of the model. A mathematical model should be able to predict future values or behavior of the system under conditions that were not included in its creation. If the model successfully predicts new outcomes that were not in the original data, this confirms its adequacy.

5. Checking assumptions and simplifications made in building the model. A mathematical model is often based on a number of assumptions or simplifications that make it easier to solve or reduce complexity. It is important to check whether these assumptions do not lead to significant errors in the results. For example, you can check whether assumptions about ideal conditions or linearity of the process are valid in real conditions.

6. Analysis of the existing limitations of the model. No model is perfect and each has its own limitations. These may be limitations on accuracy, on the range of values of variables that the model can describe, or on the specific conditions for which it was created. Evaluating these limitations allows us to understand in which situations the model works correctly and in which its use can give significant errors.

7. Statistical methods for assessing adequacy. To formalize the adequacy of a model, statistical methods are used, such as hypothesis testing, error estimation, analysis of variance, etc. For example, for regression models, the coefficient of determination (R^2) is often used, which shows how well the model explains the variations in the data.

8. Testing in real conditions. The final stage may be testing the model in real conditions in practice. This may involve applying the model to make decisions in real problems and verifying its results in real conditions. If the model shows good results in practice, it can be said that it is adequate.

Thus, the study of the adequacy of a mathematical model is a complex process that includes theoretical and practical verification of the model at various stages of its development and application. The main goal is to determine whether the model is sufficiently accurate and correct to solve the problems for which it was created.

To verify the mathematical model developed in section 2, on a prototype installation (appendix G) experimental studies were conducted to determine the concentration of carbon dioxide in gases with a known CO2 content (10-12-14-16 vol.%) at a wavelength of 4.267 μm. A laser diode based on InAsSb P with a power of 1.5 mW –was used as a radiation source , and a thin-film thermoelectric receiver (operating without cooling) was used as a radiation receiver. The results of measurements of the intensity of radiation that passed through the gas under study, as well as the influencing variables of pressure and temperature, are shown in Fig. 4.10–4.12 (in Fig. 4.12. (1) is the theoretical value of the voltage, (2) is the measured value). In this case, the experimental measurements were divided into 10 cycles (10 measurements in each cycle). The characteristics of the external microclimate during the adequacy study are presented in Table 4.2. The parameters were measured using a combined instrument testo 400 .

Table 4.2

Microclimate parameters during the experiment

Parameter \ Cycle No. measurement	Temperature, ^{0} °C	Humidity, %	Pressure m m . Hg. st..	Precipitation (rain, snow)
1	15.7	75	741	-
2	14.1	76	744	-
3	20.0	55	748	-
4	22.2	39	736	-
5	21.8	57	738	-
6	23.2	40	743	-
7	18.2	97	732	+
8	17.1	98	735	+
9	20.9	44	741	-
10	20.7	57	742	-

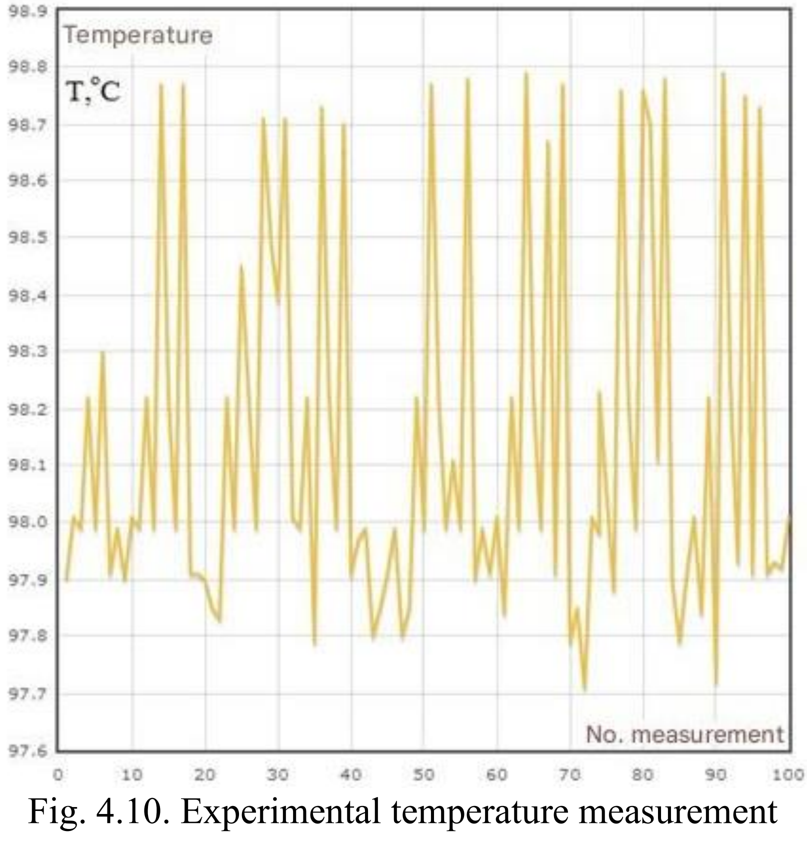

Fig. 4.10. Experimental temperature measurement

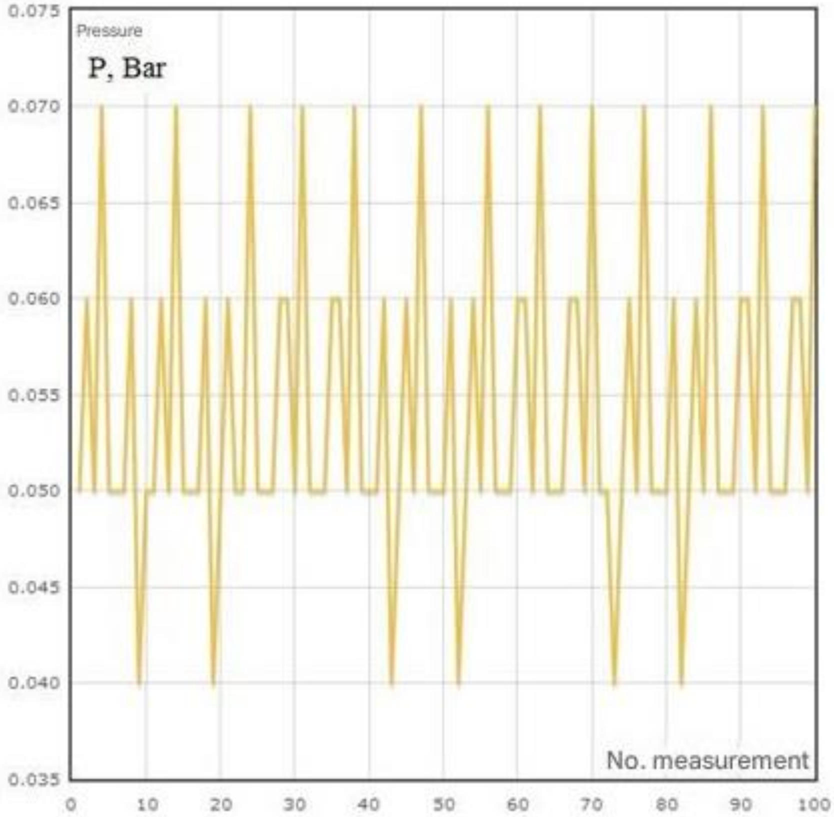

Fig. 4.11. Experimental pressure measurement

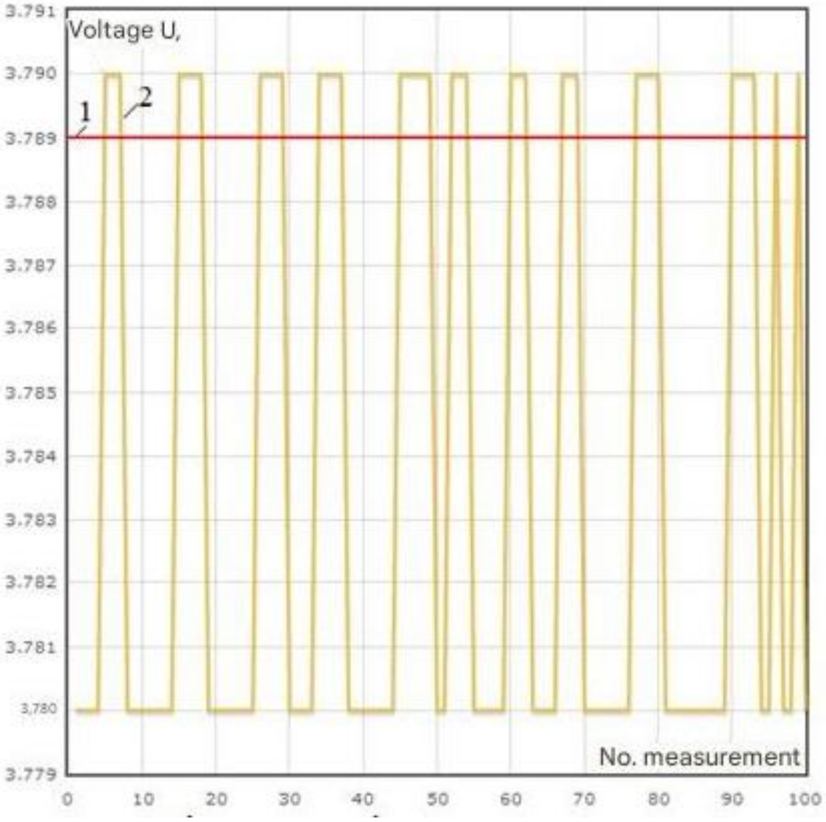

Fig. 4.12. Voltage measurement

CO_2 concentration according to the mathematical model developed in Section 2, which takes into account the influence of influencing factors. As a result, a number of carbon dioxide concentration values were obtained (Table 4.3).

Table 4.3

CO_2 concentration according to mathematical model 2.39

Cycle No. measurement\actual value	1	2	3	4	5	6	7	8	9	10
0	0.00 4	0.0 01	0.002	0.0 01	0.00 3	0.0 02	0.0 01	0.0 01	0.0 01	0.0 02
10	10.035	10.035	10.044	10,092	10,092	10,092	10,092	10,092	10.035	10.035
12	12.017	12.018	12.007	12.034	12.055	12.043	12.023	12.011	12.015	12.017
14	14.029	14.027	14.021	14.022	14.029	14.021	14.023	14.028	14.021	14.022
16	16.017	16.019	16.007	16.009	16.003	16.011	16.015	16.016	16.017	16.015

The structure of the model for estimating control error is presented in Fig. 4.13.

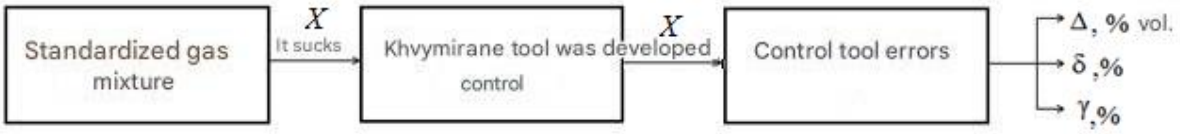

Fig. 4.13. Control errors

As shown by calculations, the value that differs the most from the actual value is 10.092%. Therefore, the maximum absolute, relative and combined error of determining the concentration using the control is

$$\Delta = X - X_D = 0.092\%. \tag{4.1}$$

$$\delta = \frac{\Delta}{X_D} = \frac{10.092 - 10.000}{10.000} \cdot 100\% = 0.92\%. \tag{4.2}$$

$$\gamma = \frac{\Delta}{X_N} \cdot 100\% = \frac{0.092}{20} \cdot 100\% = 0.46\%. \tag{4.3}$$

Then the limit value of the combined error is

$$-\gamma_{гр} < \gamma < +\gamma_{гр} \Rightarrow -0.1\% < \gamma < 0.1\% \tag{4.4}$$

From here, we can determine the permissible limits of absolute and relative errors.

$$\Delta_{\lim} = \pm \frac{\gamma_{\lim}}{100\%} \cdot X_N = \pm 0.1\%. \tag{4.5}$$

$$\delta_{\lim} = \pm \gamma_{\lim} \cdot \frac{X_N}{X_M} = \pm 0.99\% \tag{4.6}$$

Therefore, the absolute error limit is constant (does not depend on the measured value), and the relative error limit increases with a decrease in the measured value, i.e. the accuracy of the control means will decrease if the device readings are significantly less than the measurement limit.

After measuring according to the device display X_P, we get an estimate of the measurand, the true value of which X lies within

$$X_P - \Delta_{\lim} < X < X_P + \Delta_{\lim} \Rightarrow -9.9\% < X < 10.1\%. \quad (4.7)$$

Estimating measurement uncertainties. Measurement uncertainty in metrology is a characteristic that indicates the possible variations in measurement results when repeated under the same conditions. In other words, it is an indicator of how accurately a measured value can be estimated and what range of possible values may be true, taking into account the limitations of the equipment, measurement methods, and the influence of other factors.

Measurement uncertainty is inevitable, as even the best-tuned equipment cannot give a completely accurate result. This is due to various sources of error that can occur during the measurement process, such as temperature changes, instrument errors, human factors, and other external conditions.

In metrology, two main types of uncertainty are distinguished:

Systematic uncertainty — arises from the presence of constant but unaccounted for factors. It can be reduced or eliminated by adjusting measuring instruments or improving methods.

Random uncertainty — arises from random fluctuations, such as environmental influences or changes in measurement conditions. This uncertainty is usually described by statistical methods, and is often reduced by making a series of measurements and determining the average value.

To estimate the uncertainty of measurements, we will use the algorithm [3]. A series of measurements of the intensity of radiation that passed through the gas under study (air with a content of CO_2 10 %vol. – 10000 pm , the calculation in absolute terms is presented by software calculation according to GOST 2939-63 in Fig. 4.14), as well as influential variables - temperature and pressure.

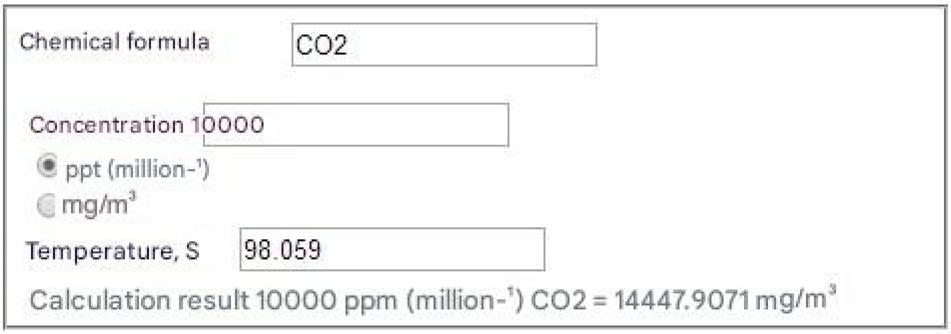

Chemical formula CO2

Concentration 10000

● ppt (million^{-1})

○ mg/m^3

Temperature, S 98.059

Calculation result 10000 ppm (million^{-1}) CO2 = 14447.9071 mg/m^3

Fig. 4.14. Window of the program for converting ppm to mg/ m^3

Having a set of statistical data on these parameters (A) , we calculate for them the standard uncertainty of the type AND:

$$u_A(\overline{I_l}) = \sqrt{\frac{\sum_{i=1}^{n}(U_{l_i} - \overline{U_l})^2}{n \cdot (n-1)}}, \quad (4.8)$$

$$u_A(\overline{T}) = \sqrt{\frac{\sum_{i=1}^{n}(T_i - \overline{T})^2}{n \cdot (n-1)}}\,, \tag{4.9 }$$

$$u_A(\overline{P}) = \sqrt{\frac{\sum_{i=1}^{n}(P_i - \overline{P})^2}{n \cdot (n-1)}}\,, \tag{4.10 }$$

where n is the number of measurements; $\overline{U}$, $\overline{T}$ and $\overline{P}$ –arithmetic averages of the measurement results for voltage, temperature and pressure, respectively.

The calculated values are $\overline{U}$ *=3.783 V*, $\overline{T}$ *= 98.059* ^oC, $\overline{P}$ *= 0.053 Pas.*

Substituting the obtained values into (4.29 – 4.31) we obtain: $u_A(U_l)$ *= 0.01 In,* $u_A(T)$ *= 0.2 ºC ,* $u_A(P)$ *= 0.01 Pa .*

Now we calculate the total standard uncertainty of the type A. To do this, we will determine whether the above-mentioned influencing quantities are correlated with each other. We will calculate the correlation coefficients for each pair of quantities:

$$r(T,P) = \frac{\frac{1}{n}\sum_{i=1}^{n}(T_i - \overline{T}) \cdot (P_i - \overline{P})}{\sqrt{\frac{1}{n}\sum_{i=1}^{n}(T_i - \overline{T})^2 \cdot \frac{1}{n}\sum_{i=1}^{n}(P_i - \overline{P})^2}}\,, \tag{4.11}$$

$$r(T,U_l) = \frac{\frac{1}{n}\sum_{i=1}^{n}(T_i - \overline{T}) \cdot (U_{l_i} - \overline{U_l})}{\sqrt{\frac{1}{n}\sum_{i=1}^{n}(T_i - \overline{T})^2 \cdot \frac{1}{n}\sum_{i=1}^{n}(U_{l_i} - \overline{U_l})^2}}\,. \tag{4.12}$$

$$r(P,U_l) = \frac{\frac{1}{n}\sum_{i=1}^{n}(P_i - \overline{P}) \cdot (U_{l_i} - \overline{U_l})}{\sqrt{\frac{1}{n}\sum_{i=1}^{n}(P_i - \overline{P})^2 \cdot \frac{1}{n}\sum_{i=1}^{n}(U_{l_i} - \overline{U_l})^2}}\,. \tag{4.13 }$$

Thus, $r(T,P)$ = 0.602 , $r(T,U_l)$ = 0.828 , $r(P,U_l)$ = 0.709. Therefore, the correlation between all influential quantities is present, therefore, to calculate the total standard uncertainty of type A, we use the formula

$$\begin{aligned} u_{cA}{}^2 = {} & (\frac{\partial f}{\partial U_l})^2 \cdot u_A^2(U_l) + (\frac{\partial f}{\partial T})^2 \cdot u_A^2(T) + (\frac{\partial f}{\partial P})^2 \cdot u_A^2(P) + \\ & + 2r(T,U_l) \cdot \frac{\partial f}{\partial T} \cdot \frac{\partial f}{\partial U_l} \cdot u_A(T) \cdot u_A(U_l) + 2r(P,U_l) \cdot \frac{\partial f}{\partial P} \cdot \frac{\partial f}{\partial U_l} \cdot u_A(P) \cdot u_A(U_l) + \\ & + 2r(T,P) \cdot \frac{\partial f}{\partial T} \cdot \frac{\partial f}{\partial P} \cdot u_A(T) \cdot u_A(P), \end{aligned} \tag{ 4.14 }$$

where f is a function that connects the measurement result and the influencing variables, i.e. the function (2.32).

That is, the problem is reduced to determining the sensitivity coefficients $\frac{\partial f}{\partial U_I}$, $\frac{\partial f}{\partial T}$ and $\frac{\partial f}{\partial P}$. We find the partial derivatives using the Mathcad mathematical package : $\frac{\partial f}{\partial U_I} = \text{-}904{,}00 \frac{mg}{m^3 \cdot B}$, $\frac{\partial f}{\partial T} = -6.02\ mg/(m^3 \cdot {}^o C)$, $\frac{\partial f}{\partial P} = 0.001\ mg/(m^3 \cdot Pa)$.

And the total standard uncertainty of type A, calculated according to equation (4.14) , is $u_{cA} = 7.91\ mg/m^3$.

For parameters S_{IO} , I_0 , R_{ZZ} , S , L there are no statistical measurement data and the distribution laws are not known. Therefore, according to international recommendations, we determine the standard uncertainty of type B for them, assuming that they have a uniform distribution law:

$$u_B = \frac{\Delta}{\sqrt{12}}, \tag{4.15}$$

where Δ is the limit of unextracted residual systematic effects .

The total standard uncertainty of type B is equal to:

$$u_{cB}^2 = \left(\frac{\partial f}{\partial S_{IO}}\right)^2 \cdot u_{B1}^2(S_{IO}) + \left(\frac{\partial f}{\partial I_0}\right)^2 \cdot u_{B2}^2(I_0) + \left(\frac{\partial f}{\partial R_{ZZ}}\right)^2 \cdot u_{B3}^2(R_{ZZ}) + \\ + \left(\frac{\partial f}{\partial S}\right)^2 \cdot u_{B4}^2(S) + \left(\frac{\partial f}{\partial L}\right)^2 \cdot u_{B5}^2(L). \tag{4.16}$$

Thus, $u_{cB} = 119.1$ mg /m3 .

The remaining parameters in the model are constants, so uncertainty is not estimated for them.

Total standard uncertainty:

$$u_c = \sqrt{u_{cA}^2 + u_{cB}^2} = 121{,}01 mg/м^3 \tag{4.17}$$

Next, we calculate the expanded uncertainty of the measurement result. To do this, we first obtain the value of the coverage factor, which creates an interval that corresponds to the confidence level $p = 0.95$. The coverage factor k is generally defined as:

$$k = t_p(b_{eff}), \tag{4.18}$$

where $t_p(b_{eff})$ is the coefficient from the Student distribution for the probability of coverage p with the effective number of degrees of freedom b_{eff}. $t_p(b_{eff})$ is selected from the table according to the calculated value of b_{eff}:

$$b_{eff} = \frac{u_c^4}{\frac{u_A^4(\overline{U_I})}{b} \cdot \left(\frac{\partial f}{\partial U_I}\right)^4 + \frac{u_A^4(\overline{T})}{b} \cdot \left(\frac{\partial f}{\partial T}\right)^4 + \frac{u_A^4(\overline{P})}{b} \cdot \left(\frac{\partial f}{\partial P}\right)^4}, \tag{4.19}$$

where b – the number of degrees of freedom. (for uncertainties of input quantities, which were determined by type A, $b = n - 1$. For uncertainties obtained by type B, the number of degrees of freedom is taken equal to infinity. Therefore, the terms containing uncertainties obtained by type B will be equal to zero and are not specified in formula (4.40).

Substituting the previously obtained values, we obtain $b_{eff} = 2 \cdot 10^6$. Given the large value of b_{eff} , from the table of Student's coefficients for a confidence probability of 0.95, taking $b_{eff} = \infty$, we choose $k = 1.96$.

Therefore, the expanded uncertainty of the measurement result at a confidence level of 0.9 7 :

$$U = k \cdot u_c = 237.18[mg/m^3] \qquad (4.20)$$

Assessment of the control probability and accuracy of gas concentration measurements. It is known that the control probability reflects the degree of objectivity of the obtained results in comparison with the normalized value of the measured quantity. The control probability consists of instrumental and methodological probabilities.

Let us first consider the instrumental probability of control. It is defined as follows

$$Д_i = 1 - \alpha - \beta, \qquad (4.21)$$

where α is the first type error (manufacturer's risk); β is the second type error (customer's risk).

The controlled parameter in this work is the gas concentration *C* (4). Its determination is carried out with a certain error *Δ* . Accordingly, errors of the 1st and 2nd kind are described by equations [11]:

$$\alpha = \int_{C_A}^{C_B} f(C) \left[\int_{C_{A-\Delta}}^{C_A} \varphi(\Delta) d\Delta + \int_{C_B}^{C_{B+\Delta}} \varphi(\Delta) d\Delta \right] dC, \qquad (4.22)$$

$$\beta = \int_{C_B}^{C_{B+\Delta}} f(C) \left[\int_{C_{B-\Delta}}^{C_B} \varphi(\Delta) d\Delta \right] dC + \int_{C_{A-\Delta}}^{C_A} f(C) \left[\int_{C_A}^{C_{A+\Delta}} \varphi(\Delta) d\Delta \right] dC, \qquad (4.23)$$

where $f(C)$ – probability distribution density of gas concentration; $\varphi(\Delta)$ – probability distribution density of gas concentration measurement errors; C_A, C_B – gas concentration tolerance limits.

the measurement error *Δ* is shown in Fig . 4.15 .

The gas concentration values and measurement error values are distributed according to a normal law (Fig. 4.16) and are described by equations (4.24-4.25).

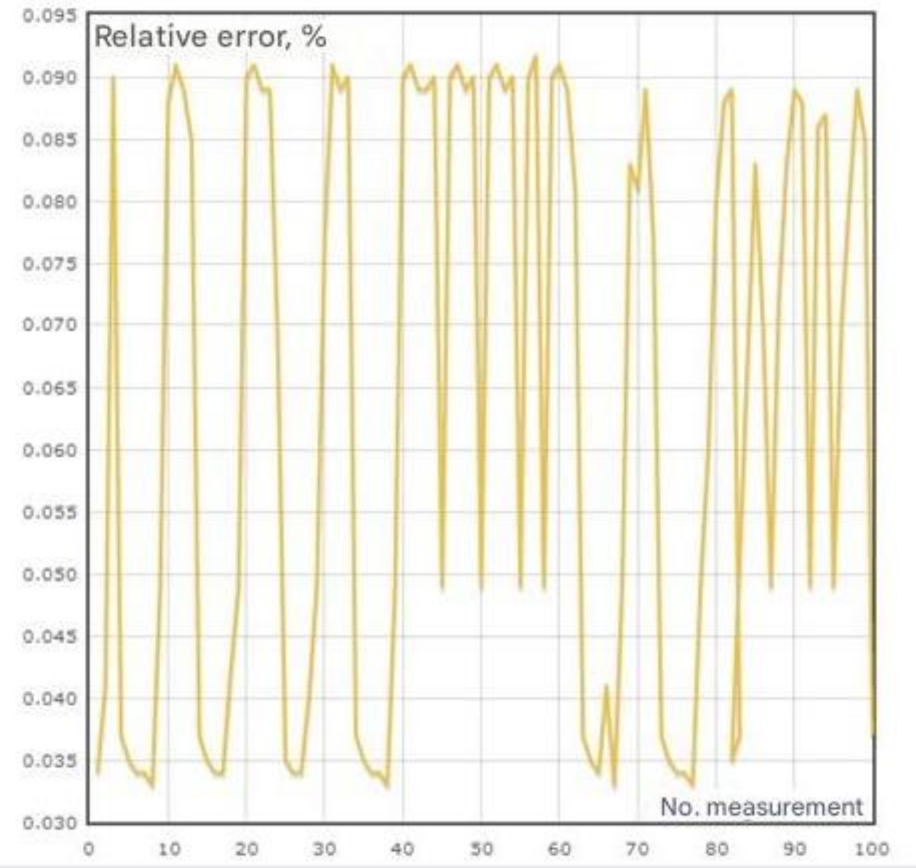

Fig . 4.15 . Graphical representation of measurement error *Δ*

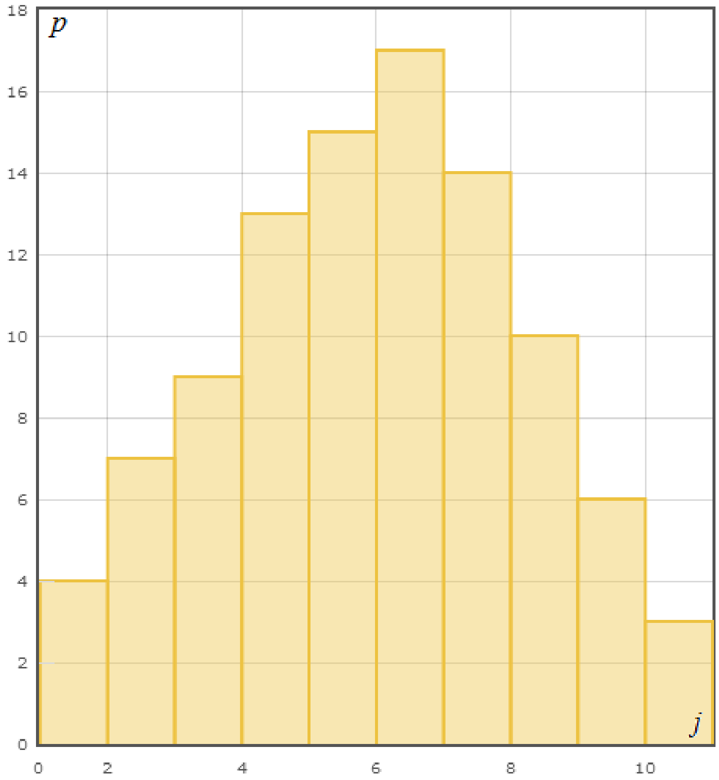

Fig . 4.16. Histogram of the probability frequency distribution of the values of the concentration of the studied gas and the probabilities of the values of measurement errors:

j – the interval number into which the ranges of gas concentration values and measurement errors are divided; *p* – the number of gas concentration values and measurement errors that fall into the specified interval

$$f(C) = \frac{1}{\sqrt{2\pi\delta}} \cdot e^{-\frac{(C-\bar{C})^2}{2\delta^2}}; \qquad (4.24)$$

$$\varphi(\Delta) = \frac{1}{\sqrt{2\pi\delta}} \cdot e^{-\frac{(\Delta-\bar{\Delta})^2}{2\delta^2}}, \qquad (4.25)$$

where σ is the standard deviation.

The graphical representation of the functions *f (C)* and *φ(Δ)* is shown in Fig. 4.17 – 4.18.

Verification that both the gas concentration values and the measurement error values are indeed normally distributed was carried out using the Pearson $\chi^{2\ \text{test}}$.

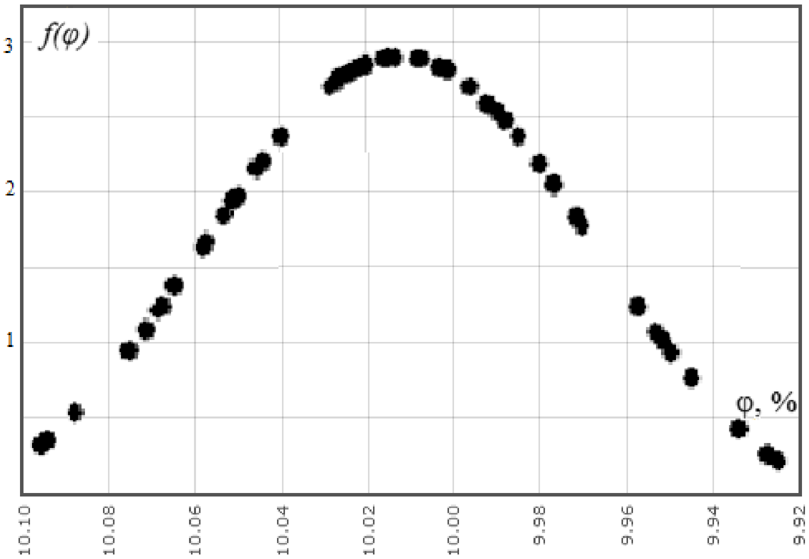

Fig. 4.17. Gas concentration probability distribution density function

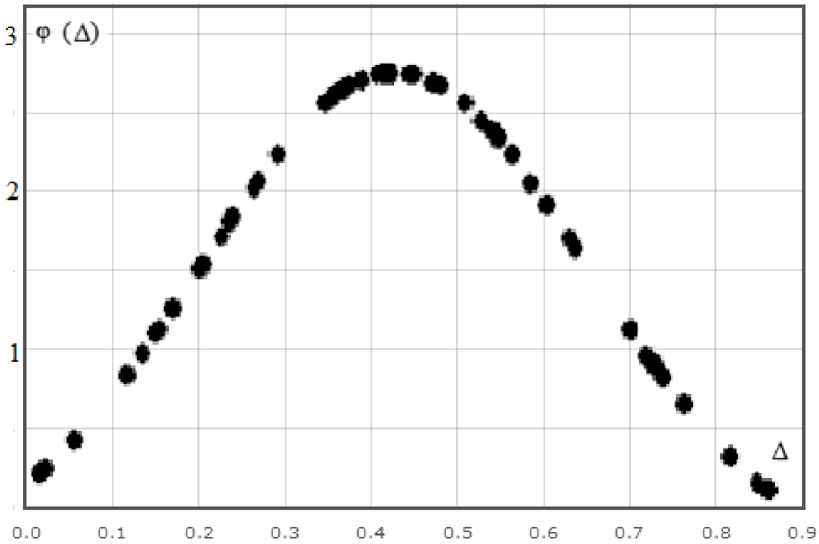

Fig. 4.18. Probability density function of gas concentration measurement error

The tolerance limits are set within 3% deviation from the actual value of the gas concentration (10% vol. or 14448 mg/m ^{3}): C_A = 9.7% vol., C_B = 10.3 %vol. or C_A = 14015 mg/m ^{3} , C_B = 14881 mg/m ^{3} .

Substituting the given and experimental values into the formulas (4.22- 4.23), we obtain the values $\alpha = 0.03\,12$, $\beta = 0.0010$. From (4 .21) the instrumental control probability $D_i = 0.96\,8$, it is higher in comparison with the control probability of known gas analysis devices (0.8–0.94), as presented in Table 1.3. Therefore, taking into account this result, we can consider the goal of the work achieved (the control reliability increased by 0.028).

The methodological reliability of gas concentration control using the developed tool increases compared to existing control tools due to the inclusion of a larger number of influential parameters (temperature, pressure, broadening of the spectral lines of the gas under study).

The accuracy of measurements is the inverse of the relative error, expressed in relative units. Considering that according to the results of experimental studies for a sample concentration of CO_2 14448 mg/m ^{3} (10% vol. in relative terms) the value of the total standard uncertainty is obtained as 1 21 mg/m ^{3} , then the relative measurement error is 0.92 %. Thus, we obtain the accuracy $T = 108$.

Determining the accuracy of a developed concentration control device is crucial because the accuracy directly influences the precision and reliability of the measurements, which are essential for the proper functioning of the control system. Accurate measurement is critical in ensuring that the concentration of specific substances is consistently maintained within the required range, whether it is for manufacturing processes, chemical reactions, or environmental monitoring.

Inaccuracies in concentration measurement can result in significant deviations from the desired operational parameters, leading to poor product quality, compromised safety, or non-compliance with regulatory standards. For instance, in chemical or pharmaceutical industries, even small inaccuracies in concentration control can lead to the production of faulty or unsafe products, which could have serious health or environmental consequences.

Moreover, accurate concentration control is fundamental for process optimization. It enables more efficient use of raw materials, minimizes waste, and ensures that the desired chemical reactions or processes occur in the most effective manner. In industrial applications, precise control also enhances the overall performance and lifespan of equipment, reducing the risk of malfunctions and minimizing operational downtime.

Therefore, the determination of accuracy is not just a matter of technical measurement; it is integral to maintaining the economic, safety, and regulatory integrity of the entire process. This is why the accuracy of concentration control devices is a critical factor in system design, calibration, and operational performance monitoring.

Measurement accuracy is a characteristic that determines how close the measured result is to the true value of the measurand. It is an important indicator of the quality of the measurement process, allowing you to assess whether the value of the parameter can be accurately reflected using a particular measuring instrument or device. Measurement accuracy is an important indicator that determines how accurately a measuring instrument or system reflects the true value of the measurand. To achieve high accuracy, various factors must be taken into account, such as calibration, measurement methods, instrument resolution, and error reduction.

Comparing this value with the accuracy values of the devices given in section 1 , we can conclude that the accuracy of measurements using the developed tool is increased compared to existing devices.

In the fourth section of the monograph, the choice of hardware and software for implementing a means of controlling the concentration of carbon dioxide in gases was justified. A program for controlling the concentration of carbon dioxide in gases was developed. The program is written in the WinPLC 7 software package in the STL programming language .

The adequacy of the developed mathematical model was assessed and the control reliability and accuracy of measurements of carbon dioxide concentration in gases were determined . The measurement uncertainties were assessed. The results of the assessments confirmed the adequacy of the developed model.

CONCLUSIONS

1. An analysis of existing systems and methods for controlling the concentration of carbon dioxide in gases was conducted. Based on the review of known methods and means of control, their main shortcomings were identified, and a direction for further research was chosen.
2. An improved mathematical model of radiation transfer in a flue gas medium was developed. Unlike existing models, it considers the characteristics of the controlled object, specifically representing pressure values as either atmospheric pressure or vacuum. Moreover, the model accounts for the altitude of the control device above sea level in atmospheric pressure calculations, which enhances measurement accuracy.
3. The method of measuring the carbon dioxide concentration in gases in the main infrared region was further developed. A structural scheme with open measurement and compensation channels was designed, reducing the number of controlled parameters (such as humidity and dust content). Unlike known methods, this approach determines the CO_2 concentration based on the ratio of light intensity indicators passing through the open measurement and compensation channels, considering both additive and multiplicative correction coefficients depending on the measurement range.
4. A mathematical model of the photoelectric measuring transducer of light intensity was improved. This model takes into account parasitic parameters of the photodetector’s components. The resulting transformation equation explicitly links the output value—the photodetector's output voltage—with the input value—the light intensity, thereby enhancing measurement reliability.
5. An analysis of the optical measuring transducer's transmission coefficient and the CO_2 absorption coefficient in gases was conducted. The impact of the infrared receiver's spectral bandwidth on the sensitivity of the gas sensor’s optical channel was also investigated.
6. The technical feasibility of implementing the carbon dioxide concentration control device was substantiated. The static and dynamic characteristics of the device, based on the optical absorption method, were calculated.
7. Structural and functional diagrams of the carbon dioxide concentration control device were developed, along with the transformation equation for the measurement channel.
8. Methods for compensating for the influence of external factors on carbon dioxide concentration measurements were designed. Experimental studies examined the dependence of the optical transducer’s output characteristics on temperature, both with and without thermal compensation. A methodology for temperature compensation of the optical transducer’s output characteristics was proposed. The influence of pressure, humidity, and dust content of the flue gas sample on measurement accuracy was also evaluated.
9. A software tool and an industrial prototype for automatic carbon dioxide concentration control in gases were developed. The hardware choice was justified—

utilizing a powerful VIPA 200V controller—while the control software was implemented using WinPLC7 in the STL programming language.

10. An algorithm for carbon dioxide concentration control in gases was developed, enabling the maintenance of an optimal fuel-to-air ratio in the boiler furnace throughout the operation period.

11. An algorithmic approach was designed to adapt the carbon dioxide concentration control device to real-world operating conditions, considering both external disturbances and the type of boiler unit.

12. Experimental studies were conducted to verify the adequacy of the developed mathematical model. The experimental results demonstrated a complete match between theoretical and practical (experimental) data. The developed device achieved a response time of 0.44 seconds with a maximum relative error of 0.92%.

13. The adequacy of the developed mathematical model was assessed, and the reliability of the control system and accuracy of CO_2 concentration measurements were determined. Measurement uncertainties were evaluated, confirming the validity of the proposed model.

LIST OF REFERENCES

1. Howell Y.R. Solution of Thermal Transfer through Radiant Media Betweer Gray Walls / Howell Y.R., Permutter M. Monte Carlo // Yourn. Heat Transfer. - 1964. – P. 116-122.
2. Zanelly S. On the cjlculation of spatical temperature and radiative transfer in industrial watertube boiler/ Zanelly S., Corsi R., Rieri Y. // Heat Transfer in Flames. – Washington: Scripta Book Company, 1973. – P. 18-24.
3. Rychkov A. D., Krasinskii D. V., Keino A. J., Salomatov V. V. Modeling the vortex furnace aero dynamics // Proc. 4th Europ. Conf. on Industrial Furnace and Boilers.Vol. 2. Portugal, Esphino-Porto. – 1997. – P.9.
4. Rychkov A. D., Filipov K. P. Numerical modeling of coal combustion processes in ecological clear circulating fluidized bed boiler units // Proc. of 4th Intern. Korean Nat.Symp. on Sci. and Technologies KORUS 2000, Ulsan, 2000. – Pt 1. – P.304–309.
5. Remennyi M.A., Zotova N.V., Karandashev S.A., Matveev B.A., Stus’ N.M., Talalakin G.N. // Sensors&ActuatoatorsB: Chemical. 2003. Vol. 91. N 1−3. P. 256−261.
6. Share S.W., Jonson T.J. et al. // Applied Spectroscopy. 2004.Vol. 58. N 12. - P. 1452−1460.
7. Matveev B.A. // Mid-infrared Semiconductor Optoelectronics. Springer, 2006. - P. 395−428.
8. Kucheruk V. Laboratory stand control composition smoke gases of caldron options / Kucheruk V., Dudatiev I. // VI International conference on optoelectronic information technologies “Photonics-ODS 2012”. - Vinnytsia, VNTU 2012. - P. 124
9. Kucheruk V. Optical-gas analysis absorption system with compensation of destabilizing factors / Kucheruk V. Yu., Dudatiev I. // VIII International salon of inventions and new technologies«New Time», september , 2012. – Sevastopol, 2012. – P.330-331.
10. Kucheruk V. Automatic control of concentration of flue gases / Kucheruk V., Dudatiev I. // Pomiary avtovatyka kontrola. - № 7. – 2013. - P.621-623.
11. Kucheruk V. Physical nature metrological select of range of infrared waves to optical absorption methods of control flue gas boilers / Kucheruk V. Yu., Dudatiev I. // II International Scientific Conference in memory of Professor Vladimir Podzharenko Measurement, control and diagnosis in technical systems (MCDTS -2013). – Vinnitsya, 2013. – P. 26-27.
12. Daniel J. On the climate forcing of carbonmonoxide / Daniel J. , Solomon S. - J. Geophys.: Res. Atmos 103. -1998. - 13249–13260 p.
13. Dils B. Ground-based CO observations atJungfraujoch // Comparison between FTIR and NDIR measurements / Dils B., Mahieu E., Demoulin P., Steinbacher M., Buchmann B., and De Maziere M. - 2009. - 154p.
14. Duncan B. N. Global budget of CO, 1988–1997 // Source estimates and validationwith a global model / Duncan B. N., Logan J. A., Bey I., Megretskaia I. A.,

Yantosca R. M., Novelli P. C., Jones N. B., and Rinsland C. P. - J. Geophys. Res. Atmos. 112, D22301,doi:10.1029/2007JD008459. - 2007.

15. Folini D. Lagrangian particle dispersionmodeling for the high Alpine site Jungfraujoch / Folini D., Ubl S., and Kaufmann P. - J. Geophys.Res. Atmos., 113, D18111, doi:10.1029/2007jd009558. - 2008.

16. Chevalier A., Gheusi F., Atti´e, J., Zbinden R., Athier G., and Cousin J.: Carbon monoxide observations from ground stations in France and Europe and long trends in the free troposphere, Atmos. Chem. Phys. Discuss., 8, 3313–3356. - 2008.

17. Daniel J. S. and Solomon S.: On the climate forcing of carbon monoxide, J. Geophys. Res. Atmos., 103, 13249–13260. - 1998.

18. Dils B., Mahieu E., Demoulin P., Steinbacher M., Buchmann B., and De Maziere M.: Ground-based CO observations at Jungfraujoch: Comparison between FTIR and NDIR measurements, in preparation. - 2009.

19. Duncan B. N., Logan J. A., Bey I., Megretskaia I. A., Yantosca R. M., Novelli P. C., Jones N. B., and Rinsland C. P.:Global budget of CO, 1988–1997: Source estimates and validation with a global model, J. Geophys. Res. Atmos., 112, D22301, doi:10.1029/2007JD008459. - 2007.

20. Ries L., Cemas D., and Jesenovec B.: Transport of nitrogen oxides, carbon monoxide and ozone to the Alpine Global AtmosphereWatch stations Jungfraujoch (Switzerland), Zugspitze andHohenpeissenberg (Germany), Sonnblick (Austria) and Mt. Krvavec (Slovenia), Atmos. Environ., 41, 9273–9287. - 2007.

21. Khalil M. A. K., Rasmussen R. A.: Carbon-Monoxide in the Earths Atmosphere – Indications of a Global Increase, Nature,332, 242–245. - 1988.

22. Khalil M. A. K., Rasmussen R. A.: Global Decrease in Atmospheric Carbon-Monoxide Concentration, Nature, 370, 639–641. - 1994.

23. Levy H., Kasibhatla P. S., Moxim W. J., Klonecki A. A., Hirsch A. I., Oltmans S. J., and Chameides W. L.: The global impact of human activity on tropospheric ozone, Geophys. Res. Lett., 24, 791–794. - 1997.

24. Luterbacher J., Dietrich D., Xoplaki E., Grosjean M., Wanner H.: European seasonal and annual temperature variability, trends, and extremes since 1500, Science, 303, 1499–1503. - 2004.

25. Meszaros T., Haszpra L., Gelencser A.: Tracking changes in carbon monoxide budget over Europe between 1995 and 2000, Atmos. Environ., 39, 7297–7306. - 2005.

26. Stemmler K., Zellweger C., Ridgeon P.: Two highspeed, portable GC systems designed for the measurement of non-methane hydrocarbons and PAN: Results from the Jungfraujoch High Altitude Observatory, J. Environ. Monit., 6, 234–241. - 2004.

27. Wild O., Prather M. J.: Excitation of the primary tropospheric chemical mode in a global three-dimensional model, J. Geophys. Res. Atmos., 105, 24647–24660. - 2000.

28. Rigby A. The most effective technology for NOx reduction in large combustion plants / A. Rigby, A. Klatt, T. Libuda, J. Zürbig – NOXCONF: International Conference on Industrial Atmospheric Pollution. - 2001.

29. S. Garavaglia. A Heuristic Self-Organizing Map Trained Using the Tanimoto Coefficient. // Proc. of International Joint Conference on Neural NetWorks. Washington, DC. - 1998.

30. Shaidurov V.V. Multigrid Method for Finite Elements // Mathematics and Its Applications. Kluwer Academic Publishers. - 1995.

31. T. Honkela, S.K. Lagus, T. Kohonen. Exploration of Full-Text Databases with Self-Organizing Map // Proc. of International Conference on Neural NetWorks. Washington, DC. - 1996. - Vol.1. - P. 56-62

32. Combustion. Michael Biarnes in collaboration with: Bill Freed and Jason Esteves.E. Instruments International LLC.– 40 p.

33. Lykov A.G. Analys is of gas analyzers of road transport exhaustand ways to improvetheir accuracy / Lykov, A.G., Vovna, A.V. // Naukovi praci Donec'kogo nacional'nogo tehnichnogouniversytetu: Serija “Obchysljuval'na tehnika ta avtomatyzacija”. – №. 2(25). – 2013. – p. 246-253.

34. Vovna A.V. Methods and means of the gas components concentration and dust analyticalmeasuring in the mine atmosphere of coal mines / Vovna A.V., Zori A.A., Korenev V.D. and Hlamov M.G. – Donetsk, DonNTU – №. 1. – 2013. – p. 47-54.

35. N. H. Ngo, D. Lisak, H. Tran, J.-M. Hartmann, "An isolated line-shape model to go beyond the Voigt profile in spectroscopic databases and radiative transfer codes", J. Quant. Spectrosc. Radiat. Transfer, 89-100 (2013).

36. H. Tran, N. H. Ngo, J.-M. Hartmann, "Efficient computation of some speed-dependent isolated line profiles", J. Quant. Spectrosc. Radiat. Transfer, 199-203 (2013).

37. H. Tran, N. H. Ngo, J.-M. Hartmann, Erratum to "Efficient computation of some speed-dependent isolated line profiles", J. Quant. Spectrosc. Radiat. Transfer**,** 104 (2014).

38. J. Tennyson, P. F. Bernath, A. Campargue et al., "Recommended isolated-line profile for representing high-resolution spectroscopic transitions (IUPAC Technical Report)", Pure Appl. Chem., 1931-1943 (2014).

39. A. L. Laraia, R. R. Gamache, J. Lamouroux, I. E. Gordon, L. S. Rothman, "Total internal partition sums to support planetary remote sensing", Icarus , 391-400 (2011).

40. L. S. Rothman, et al., "The HITRAN 2012 Molecular Spectroscopic Database", J.Quant. Spectrosc. Radiat. Transfer , 4-50 (2013).

41. L. S. Rothman, I. E. Gordon, R. J. Barber, H. Dothe, R. 2R. Gamache, A. Goldman, V. Perevalov, S. A. Tashkun, J. Tennyson, "HITEMP, the high-temperature molecular spectroscopic database", J. Quant. Spectrosc. Radiat. Transfer 111, 2139-2150 (2010).

42. L. S. Rothman, R. B. Wattson, R. R. Gamache, J. Schroeder, and A. McCann, "HITRAN, HAWKS and HITEMP High-Temperature Molecular Database", Proc. Soc. Photo Optical Instrumentation Engineers2471, 105-111 (1995).

43. Roman V. Kochanov HITRAN Application Programming Interface (HAPI) USA 2015, - 52 p.

44. Bernath P. F. Infrared fourier transform emission spectroscopy (англ.) // Chem. Soc. Rev. — 1996. — Vol. 25. — P. 111—115. — DOI:10.1039/CS9962500111.

45. Bernath P. F. Infrared emission spectroscopy (англ.) // Annu. Rep. Prog. Chem., Sect. C: Phys. Chem. — 2000. — Vol. 96. — P. 177—224. — DOI:10.1039/B001200I.

46. Encyclopedia of Spectroscopy and Spectrometry / Lindon J. — 2nd Ed. — Academic Press, 2010. — 3312 p.

47. Larkin P. J. Infrared and raman spectroscopy: principles and spectral interpretation. — Elsevier, 2011. — 230 p. — ISBN 978-0-12-386984-5.

48. Noda I. Two-Dimensional Infrared (2D IR) Spectroscopy: Theory and Applications (англ.) // Applied Spectroscopy. — 1990. — Т. 44. — № 4. — С. 550—561.

49. Stuart B. H. Infrared Spectroscopy: Fundamentals and Applications. — Wiley, 2004. — 242 p.

50. J. Hildenbrand. Micromachined mid-infrared emitter for fast transient temperature operation for optical gas sensing system /J. Hildenbrand, A. Kurzinger, C. Peter, E. Moretton, J. Wollenstein, F. Numann, M. Ebert, and J. Korvic. - in Proc. 7-th IEEEE SENSORS. - Lecce, Italy. - Oct. 2008. - p. 297–300.

APPENDICES

APPEARANCE OF THE LABORATORY SAMPLE

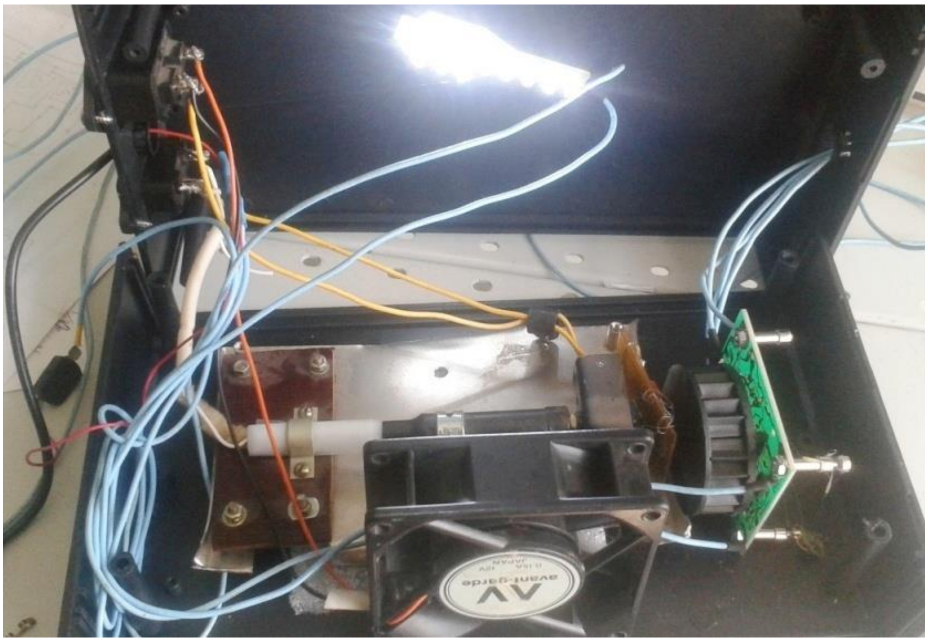

Laboratory sample of the carbon dioxide concentration control device in gases (internal unit)

Laboratory sample of the carbon dioxide concentration control device in gases (external unit)